EUROPEAN
JOURNAL OF
BIOLOGY

OFFICIAL JOURNAL OF ISTANBUL UNIVERSITY FACULTY OF SCIENCE

https://iupress.istanbul.edu.tr/en/journal/ejb/home

ISTANBUL
UNIVERSITY
PRESS

EUROPEAN
JOURNAL OF
BIOLOGY

EUROPEAN
JOURNAL OF
BIOLOGY

Authors bear responsibility for the content of their published articles.

The publication language of the journal is English.

This is a scholarly, international, peer-reviewed and open-access journal published biannually in June and December.

Publication Type: Periodical

EUROPEAN JOURNAL OF BIOLOGY

EUROPEAN JOURNAL OF BIOLOGY

EUROPEAN
JOURNAL OF
BIOLOGY

Aims and Scope

European Journal of Biology (Eur J Biol) is an international, scientific, open access periodical published in accordance with independent, unbiased, and double-blinded peer-review principles. The journal is the official publication of Istanbul University Faculty of Science and it is published biannually on June and December. The publication language of the journal is English. European Journal of Biology has been previously published as IUFS Journal of Biology. It has been published in continuous publication since 1940.

European Journal of Biology aims to contribute to the literature by publishing manuscripts at the highest scientific level on all fields of biology. The journal publishes original research and review articles, and short communications that are prepared in accordance with the ethical guidelines in all fields of biology and life sciences.

The scope of the journal includes but not limited to; animal biology and systematics, plant biology and systematics, hydrobiology, ecology and environmental biology, microbiology, cell and molecular biology, biochemistry, biotechnology and genetics, physiology, toxicology, cancer biology, developmental biology, and stem cell biology.

The target audience of the journal includes specialists and professionals working and interested in all disciplines of biology.

The editorial and publication processes of the journal are shaped in accordance with the guidelines of the International Committee of Medical Journal Editors (ICMJE), World Association of Medical Editors (WAME), Council of Science Editors (CSE), Committee on Publication Ethics (COPE), European Association of Science Editors (EASE), and National Information Standards Organization (NISO). The journal is in conformity with the Principles of Transparency and Best Practice in Scholarly Publishing (doaj.org/bestpractice).

European Journal of Biology is currently indexed by Web of Science Zoological Record, CAB Abstracts (CABI), Chemical Abstracts Service (CAS) and TUBITAK-ULAKBIM TR Index.

Processing and publication are free of charge with the journal. No fees are requested from the authors at any point throughout the evaluation and publication process. All manuscripts must be submitted via the online submission system, which is available at dergipark.gov.tr/iufsjb. The journal guidelines, technical information, and the required forms are available on the journal's web page.

All expenses of the journal are covered by the Istanbul University.

Statements or opinions expressed in the manuscripts published in the journal reflect the views of the author(s) and not the opinions of the Istanbul University Faculty of Science, editors, editorial board, and/or publisher; the editors, editorial board, and publisher disclaim any responsibility or liability for such materials.

All published content is available online, free of charge at https://dergipark.org.tr/tr/pub/iufsjb. Printed copies of the journal are distributed free of charge.

OPEN ACCESS

Address: Istanbul University, Faculty of Science, Department of Biology, 34134 Vezneciler, Fatih, Istanbul, TURKEY
Phone: +90 212 4555700 (Ext. 15079)
Fax: +90 212 5280527
E-mail: sbolkent@istanbul.edu.tr

Instructions to Authors

European Journal of Biology (Eur J Biol) is an international, scientific, open access periodical published in accordance with independent, unbiased, and double-blinded peer-review principles. The journal is the official publication of Istanbul University Faculty of Science and it is published biannually on June and December. The publication language of the journal is English. European Journal of Biology has been previously published as IUFS Journal of Biology. It has been published in continuous publication since 1940.

European Journal of Biology aims to contribute to the literature by publishing manuscripts at the highest scientific level on all fields of biology. The journal publishes original research and review articles, and short communications that are prepared in accordance with the ethical guidelines in all fields of biology and life sciences.

The scope of the journal includes but not limited to; animal biology and systematics, plant biology and systematics, hydrobiology, ecology and environmental biology, microbiology, cell and molecular biology, biochemistry, biotechnology and genetics, physiology, toxicology, cancer biology, developmental biology, and stem cell biology.

The editorial and publication processes of the journal are shaped in accordance with the guidelines of the International Council of Medical Journal Editors (ICMJE), the World Association of Medical Editors (WAME), the Council of Science Editors (CSE), the Committee on Publication Ethics (COPE), the European Association of Science Editors (EASE), and National Information Standards Organization (NISO). The journal conforms to the Principles of Transparency and Best Practice in Scholarly Publishing (doaj.org/bestpractice).

Originality, high scientific quality, and citation potential are the most important criteria for a manuscript to be accepted for publication. Manuscripts submitted for evaluation should not have been previously presented or already published in an electronic or printed medium. Manuscripts that have been presented in a meeting should be submitted with detailed information on the organization, including the name, date, and location of the organization.

Manuscripts submitted to European Journal of Biology will go through a double-blind peer-review process. Each submission will be reviewed by at least three external, independent peer reviewers who are experts in their fields in order to ensure an unbiased evaluation process. The editorial board will invite an external and independent editor to manage the evaluation processes of manuscripts submitted by editors or by the editorial board members of the journal. The Editor in Chief is the final authority in the decision-making process for all submissions.

An approval of research protocols by the Ethics Committee in accordance with international agreements (World Medical Association Declaration of Helsinki "Ethical Principles for Medical Research Involving Human Subjects," amended in October 2013, www.wma.net) is required for experimental, clinical, and drug studies. If required, ethics committee reports or an equivalent official document will be requested from the authors.

For manuscripts concerning experimental research on humans, a statement should be included that shows the written informed consent of patients and volunteers was obtained following a detailed explanation of the procedures that they may undergo. Information on patient consent, the name of the ethics committee, and the ethics committee approval number should also be stated in the Materials and Methods section of the manuscript. It is the authors' responsibility to carefully protect the patients' anonymity. For photographs that may reveal the identity of the patients, signed releases of the patient or of their legal representative should be enclosed.

European Journal of Biology requires experimental research studies on vertebrates or any regulated invertebrates to comply with relevant institutional, national and/or international guidelines. The journal supports the principles of Basel Declaration (basel-declaration.org) and the guidelines published by International Council for Laboratory Animal Science (ICLAS) (iclas.org). Authors are advised to clearly state their compliance with relevant guidelines.

European Journal of Biology advises authors to comply with IUCN Policy Statement on Research Involving Species at Risk of Extinction and the Convention on the Trade in Endangered Species of Wild IUCN Policy Statement on Research Involving Species at Risk of Extinction and the Convention on the Trade in Endangered Species of Wild Fauna and Flora.

All submissions are screened by a similarity detection software (iThenticate by CrossCheck).

In the event of alleged or suspected research misconduct, e.g., plagiarism, citation manipulation, and data falsification/fabrication, the Editorial Board will follow and act in accordance with COPE guidelines.

Each individual listed as an author should fulfil the authorship criteria recommended by the International Committee of Medical Journal Editors (ICMJE - www.icmje.org). The ICMJE recommends that authorship be based on the following 4 criteria:

1. Substantial contributions to the conception or design of the work; or the acquisition, analysis, or interpretation of data for the work; AND
2. Drafting the work or revising it critically for important intellectual content; AND
3. Final approval of the version to be published; AND
4. Agreement to be accountable for all aspects of the work in ensuring that questions related to the accuracy or integrity of any part of the work are appropriately investigated and resolved.

In addition to being accountable for the parts of the work he/she has done, an author should be able to identify which co-authors are responsible for specific other parts of the work. In addition, authors should have confidence in the integrity of the contributions of their co-authors.

All those designated as authors should meet all four criteria for authorship, and all who meet the four criteria should be identified as authors. Those who do not meet all four criteria should be acknowledged in the title page of the manuscript.

European Journal of Biology requires corresponding authors to submit a signed and scanned version of the authorship contribution form (available for download through the journal's web page) during the initial submission process in order to act appropriately on authorship rights and to prevent ghost or honorary authorship. If the editorial board suspects a case of "gift authorship," the submission will be rejected without further review. As part of the submission of the manuscript, the corresponding author should also send a short statement declaring that he/she accepts to undertake all the responsibility for authorship during the submission and review stages of the manuscript.

European Journal of Biology requires and encourages the authors and the individuals involved in the evaluation process of submitted manuscripts to disclose any existing or potential conflicts of interests, including financial, consultant, and institutional, that might lead to potential bias or a conflict of interest. Any financial grants or other supports received for a submitted study from individuals or institutions should be disclosed to the Editorial Board. To disclose a potential conflict of interest, the ICMJE Potential Conflict of Interest Disclosure Form should be filled and submitted by all contributing authors. Cases of a potential conflict of interest of the editors, authors, or reviewers are resolved by the journal's Editorial Board within the scope of COPE and ICMJE guidelines.

The Editorial Board of the journal handles all appeal and complaint cases within the scope of COPE guidelines. In such cases, authors should get in direct contact with the editorial office regarding their appeals and complaints. When needed, an ombudsperson may be assigned to resolve cases that cannot be resolved internally. The Editor in Chief is the final authority in the decision-making process for all appeals and complaints.

When submitting a manuscript to European Journal of Biology, authors accept to assign the copyright of their manuscript to Istanbul University Faculty of Science. If rejected for publication, the copyright of the manuscript will be assigned back to the authors. European Journal of Biology requires each submission to be accompanied by a Copyright Transfer Form (available for download at the journal's web page). When using previously published content, including figures, tables, or any other material in both print and electronic formats, authors must obtain permission from the copyright holder. Legal, financial and criminal liabilities in this regard belong to the author(s).

Statements or opinions expressed in the manuscripts published in European Journal of Biology reflect the views of the author(s) and not the opinions of the editors, the editorial board, or the publisher; the editors, the editorial board, and the publisher disclaim any responsibility or liability for such materials. The final responsibility in regard to the published content rests with the authors.

MANUSCRIPT SUBMISSION

European Journal of Biology endorses ICMJE-Recommendations for the Conduct, Reporting, Editing, and Publication of Scholarly Work in Medical Journals (updated in December 2015 - http://www.icmje.org/icmje-recommendations.pdf). Authors are required to prepare manuscripts in accordance with the CONSORT guidelines for randomized research studies, STROBE guidelines for observational original research studies, STARD guidelines for studies on diagnostic accuracy, PRISMA guidelines for systematic reviews and meta-analysis, ARRIVE guidelines for experimental animal studies, TREND guidelines for non-randomized public behaviour, and COREQ guidelines for qualitative research.

Manuscripts can only be submitted through the journal's online manuscript submission and evaluation system, available at the journal's web page. Manuscripts submitted via any other medium will not be evaluated.

Manuscripts submitted to the journal will first go through a technical evaluation process where the editorial office staff will ensure that the manuscript has been prepared and submitted in accordance with the journal's guidelines. Submissions that do not conform to the journal's guidelines will be returned to the submitting author with technical correction requests.

During the initial submission, authors are required to submit the following:

- Copyright Transfer Form,
- Author Contributions Form, and

ICMJE Potential Conflict of Interest Disclosure Form (should be filled in by all contributing authors). These forms are available for download at the journal's web page.

Preparation of the Manuscript

Title page: A separate title page should be submitted with all submissions and this page should include:

- The full title of the manuscript as well as a short title (running head) of no more than 50 characters,
- Name(s), affiliations, and highest academic degree(s) of the author(s),
- Grant information and detailed information on the other sources of support,
- Name, address, telephone (including the mobile phone number) and fax numbers, and email address of the corresponding author,
- Acknowledgment of the individuals who contributed to the preparation of the manuscript but who do not fulfil the authorship criteria.

Abstract: Abstract with subheadings should be written as structured abstract in submitted papers except for Review Articles and Letters to the Editor. Please check Table 1 below for word count specifications (250 words).

Keywords: Each submission must be accompanied by a minimum of three to a maximum of six keywords for subject indexing at the end of the abstract. The keywords should be listed in full without abbreviations.

Manuscript Types

Original Articles: This is the most important type of article since it provides new information based on original research. A structured abstract is required with original articles and it should include the following subheadings: Objective, Materials and Methods, Results and Conclusion. The main text of original articles should be structured with Introduction, Materials and Methods, Results, Discussion, and Conclusion subheadings. Please check Table 1 for the limitations of Original Articles.

Statistical analysis to support conclusions is usually necessary. Statistical analyses must be conducted in accordance with international statistical reporting standards. Information on statistical analyses should be provided with a separate subheading under the Materials and Methods section and the statistical software that was used during the process must be specified.

Units should be prepared in accordance with the International System of Units (SI).

Short Communications: Short communication is for a concise, but independent report representing a significant contribution to Biology. Short communication is not intended to publish preliminary results. But if these results are of exceptional interest and are particularly topical and relevant will be considered for publication.

Short Communications should include an abstract and should be structed with the following subheadings: "Introduction", "Materials and Methods", "Results and Discussion".

Editorial Comments: Editorial comments aim to provide a brief critical commentary by reviewers with expertise or with high reputation in the topic of the research article published in the journal. Authors are selected and invited by the journal to provide such comments. Abstract, Keywords, and Tables, Figures, Images, and other media are not included.

Review Articles: Reviews prepared by authors who have extensive knowledge on a particular field and whose scientific background has been translated into a high volume of publications with a high citation potential are welcomed. These authors may even be invited by the journal. Reviews should describe, discuss, and evaluate the current level of knowledge of a topic in clinical practice and should guide future studies. The main text should contain Introduction, Experimental and Clinical Research Consequences, and Conclusion sections. Please check Table 1 for the limitations for Review Articles.

Letters to the Editor: This type of manuscript discusses important parts, overlooked aspects, or lacking parts of a previously published article. Articles on subjects within the scope of the journal that might attract the readers' attention, particularly educative cases, may also be submitted in the form of a "Letter to the Editor." Readers can also present their comments on the published manuscripts in the form of a "Letter to the Editor." Abstract, Keywords, and Tables, Figures, Images, and other media should not be included. The text should be unstructured. The manuscript that is being commented on must be properly cited within this manuscript.

Tables

Tables should be included in the main document, presented after the reference list, and they should be numbered consecutively in the order they are referred to within the main text. A descriptive title must be placed above the tables. Abbreviations used in the tables should be defined below the tables by footnotes (even if they are defined within the main text). Tables should be created using the "insert table" command of the word processing software and they should be arranged clearly to provide easy reading. Data presented in the tables should not be a repetition of the data presented within the main text but should be supporting the main text.

Figures and Figure Legends

Figures, graphics, and photographs should be submitted as separate files (in TIFF or JPEG format with 1200 dpi for graphic and 600 dpi for colour images) through the submission system. The files should not be embedded in a Word document or the main document. When there are figure subunits, the subunits should be labeled merged to form a single image. Each subunit should be submitted separately through the submission system. Images

Table 1. Limitations for each manuscript type					
Type of manuscript	**Word limit**	**Abstract word limit**	**Reference limit**	**Table limit**	**Figure limit**
Original Article	4500	250 (Structured)	No limit	6	Maximum 10
Short Communication	2500	200	30	3	4
Review Article	5500	250	No limit	5	6
Letter to the Editor	500	No abstract	5	No tables	No media

should be labeled (a, b, c, etc.) to indicate figure subunits. Thick and thin arrows, arrowheads, stars, asterisks, and similar marks can be used on the images to support figure legends. Like the rest of the submission, the figures too should be blind. Any information within the images that may indicate an individual or institution should be blinded. The minimum resolution of each submitted figure should be 300 DPI. To prevent delays in the evaluation process, all submitted figures should be clear in resolution and large in size (minimum dimensions: 100 × 100 mm). Figure legends should be listed at the end of the main document.

All acronyms and abbreviations used in the manuscript should be defined at first use, both in the abstract and in the main text. The abbreviation should be provided in parentheses following the definition.

When a drug, chemical, product, hardware, or software program is mentioned within the main text, product information, including the name of the product, the producer of the product, and city and the country of the company (including the state if in USA), should be provided in parentheses in the following format: "Discovery St PET/CT scanner (General Electric, Milwaukee, WI, USA)".

All references, tables, and figures should be referred to within the main text, and they should be numbered consecutively in the order they are referred to within the main text.

Limitations, drawbacks, and the shortcomings of original articles should be mentioned in the Discussion section before the conclusion paragraph.

References

While citing publications, preference should be given to the latest, most up-to-date publications. If an ahead-of-print publication is cited, the DOI number should be provided. Authors are responsible for the accuracy of references. Journal titles should be abbreviated in accordance with the journal abbreviations in Index Medicus/ MEDLINE/PubMed. When there are six or fewer authors, all authors should be listed. If there are seven or more authors, the first six authors should be listed followed by "et al." In the main text of the manuscript, references should be cited using Arabic numbers in parentheses. The reference styles for different types of publications are presented in the following examples.

Journal Article: Rankovic A, Rancic N, Jovanovic M, Ivanović M, Gajović O, Lazić Z, et al. Impact of imaging diagnostics on the budget – Are we spending too much? Vojnosanit Pregl 2013; 70: 709-11.

Book Section: Suh KN, Keystone JS. Malaria and babesiosis. Gorbach SL, Barlett JG, Blacklow NR, editors. Infectious Diseases. Philadelphia: Lippincott Williams; 2004.p.2290-308.

Books with a Single Author: Sweetman SC. Martindale the Complete Drug Reference. 34th ed. London: Pharmaceutical Press; 2005.

Editor(s) as Author: Huizing EH, de Groot JAM, editors. Functional reconstructive nasal surgery. Stuttgart-New York: Thieme; 2003.

Conference Proceedings: Bengisson S. Sothemin BG. Enforcement of data protection, privacy and security in medical infor-

matics. In: Lun KC, Degoulet P, Piemme TE, Rienhoff O, editors. MEDINFO 92. Proceedings of the 7th World Congress on Medical Informatics; 1992 Sept 6-10; Geneva, Switzerland. Amsterdam: North-Holland; 1992. pp.1561-5.

Scientific or Technical Report: Cusick M, Chew EY, Hoogwerf B, Agrón E, Wu L, Lindley A, et al. Early Treatment Diabetic Retinopathy Study Research Group. Risk factors for renal replacement therapy in the Early Treatment Diabetic Retinopathy Study (ETDRS), Kidney Int: 2004. Report No: 26.

Thesis: Yılmaz B. Ankara Üniversitesindeki Öğrencilerin Beslenme Durumları, Fiziksel Aktiviteleri ve Beden Kitle İndeksleri Kan Lipidleri Arasındaki Ilişkiler. H.Ü. Sağlık Bilimleri Enstitüsü, Doktora Tezi. 2007.

Epub Ahead of Print Articles: Cai L, Yeh BM, Westphalen AC, Roberts JP, Wang ZJ. Adult living donor liver imaging. Diagn Interv Radiol. 2016 Feb 24. doi: 10.5152/dir.2016.15323. [Epub ahead of print].

Manuscripts Published in Electronic Format: Morse SS. Factors in the emergence of infectious diseases. Emerg Infect Dis (serial online) 1995 Jan-Mar (cited 1996 June 5): 1(1): (24 screens). Available from: URL: http:/ www.cdc.gov/ncidodlElD/cid.htm.

REVISIONS

When submitting a revised version of a paper, the author must submit a detailed "Response to the reviewers" that states point by point how each issue raised by the reviewers has been covered and where it can be found (each reviewer's comment, followed by the author's reply and line numbers where the changes have been made) as well as an annotated copy of the main document. Revised manuscripts must be submitted within 30 days from the date of the decision letter. If the revised version of the manuscript is not submitted within the allocated time, the revision option may be cancelled. If the submitting author(s) believe that additional time is required, they should request this extension before the initial 30-day period is over.

Accepted manuscripts are copy-edited for grammar, punctuation, and format. Once the publication process of a manuscript is completed, it is published online on the journal's webpage as an ahead-of-print publication before it is included in its scheduled issue. A PDF proof of the accepted manuscript is sent to the corresponding author and their publication approval is requested within 2 days of their receipt of the proof.

EUROPEAN
JOURNAL OF
BIOLOGY

Contents

Anatomy and Histology of Digestive Tract in *Melanophila (Trachypteris) picta decastigma* (Fabricius, 1787) (Coleoptera: Buprestidae)

Nurcan Ozyurt Kocakoglu[1] , Uzeyir Caglar[2] , Selami Candan[1]

[1]Gazi University, Science Faculty, Department of Biology, Ankara, Turkey
[2]Gazi University, Vocational School of Health Services, Ankara, Turkey

ORCID IDs of the authors: N.O.K. 0000-0001-7137-8631; U.C. 0000-0002-8401-0155; S.C. 0000-0002-7402-1360

ABSTRACT

Objective: The aim of this study is to investigate the anatomy and histology of *Melanophila picta decastigma* (Fabricius) (Coleoptera: Buprestidae).

Materials and Methods: Some of the samples were fixed in 10% formaldehyde for light microscopy, others were fixed with 2.5% glutaraldehyde for scanning electron microscopy (SEM). Then the samples were examined by using stereo, light, and SEM.

Results: The digestive tract in *M. picta decastigma* consists of foregut, midgut, and hindgut. The foregut is composed of the pharynx, esophagus, crop and proventriculus. The foregut showed muscle layers followed by intima and epithelium. There is a long, tubular pair of gastric caeca in the anterior part of the midgut. In cross-sections, a single-layered cylindrical epithelium with a short striated border. The midgut showed that the epithelial lining was substantially folded, giving its lumen a curved profile. These monolayered columnar epithelial cells had their nuclei located medially, and apically they have a striated border. The midgut surface was covered by rounded structures called regenerative crypts. The main sections of hindgut (pyloric valve, ileum, colon and rectum) were clearly observed. In the hindgut sections, there appeared to be a highly folded cuticular lining, a monolayer cubic epithelium and a very muscular wall.

Conclusions: Studies on the digestive tract histo-anatomy of *M. picta decastigma* will add more information to assist in experimental, taxonomical, histological, and anatomical studies about insect tissues and will serve as a basis for control studies.

Keywords: Foregut, midgut, hindgut, Malpighian tubules, light microscope, electron microscope

INTRODUCTION

Buprestidae is a family of insects known as gem beetles or metallic wood boring insects because of their bright iridescent color. The Buprestidae has 5,000 known species in 450 genera and it is the eighth largest family of Coleoptera with many extant common buprestids (1-3). Buprestidae (4% of Coleoptera) are all widespread terrestrial groups (4). There are many dangerous pests of fruit trees, forest trees, shrubs and herbaceous plants among the Buprestidae (5). Most Buprestidae family species are in the secondary pest status, but when they reproduce in large quantities and cannot find enough food sources to suit their wishes, they become primary pests and cause a lot of damage to the trees. Therefore, the Buprestidae family is considered to be an important family in forestry, covering many harmful species (6). *Melanophila* is a genus of buprestid beetles commonly known as fire beetles (7). Most of them are found in the Mediterranean environment, the Middle East and Europe (8). The majority of the adult buprestid beetles

including *Melanophila* beetles are diurnal, sun-loving, and oligophagous (9). The damage status of *Melanophila decastigma* on poplars has been reported to have a positive correlation between disease and pests (10). These pests attack many poplars in physiologically weakened conditions and cause considerable damage in nurseries, plantations and wood-lots (11).

The digestive tract of all insects is an epithelial tube that follows a straight or curved path from mouth to anus and consists of three separate parts: the foregut and hindgut arising as the ectodermal, but the midgut is endodermal in origin (12-16). The gut epithelium is a single cell-layer thick throughout the length of the alimentary canal and rests on a basement membrane surrounded by a variably developed muscle layer (17). In Coleopteran insects including Buprestidae, the foregut is usually short and subdivided into four distinct regions including a pharynx, an esophagus, a crop (food storage region) and the proventriculus (a grinding organ). The midgut is covered with small, regenerative crypts. There is a pair of caeca between the foregut and the midgut. The hindgut is equal to or greater than the length of the midgut. The hindgut has narrow small and larger intestines. The digestive tract ends in a rectum. The six cryptonephric Malpighian tubules join with the pyloric valve, between the midgut and hindgut (18). The foregut is responsible for the ingestion, storage, grinding and transport of nutrient to the midgut. Digestive enzymes are produced and secreted in the midgut, and digestion products are absorbed. Material remaining in the intestinal lumen along with urine from the Malpighian tubules then enters the posterior intestine, where the absorption of water, salts and other valuable molecules occurs before the feces are expelled from the anus. Coleoptera has a cryptonephric system in which the distal ends of the Malpighian tubules are held in contact with the rectal wall by the perinephric membrane. Such an arrangement allows some beetles that live on a very dry diet, such as stored grain, to be extraordinarily efficient in their conservation of water (17).

The digestive system of *Melanophila picta decastigma*, which is an important pest species, was examined anatomically and histologically since there have been no previous studies of the digestive tract of *Melanophila* genus. With this study, it is thought that the Buprestidae family including *Melanophila* genus and other Coleopterans will contribute to the digestive system histology and anatomy, and thus, basic information will be provided for studies to combat these harmful species.

MATERIALS AND METHODS

Insects
Adult specimens of *M. picta decastigma* (n=20) were collected at 39.255940E, 32.961942N in the Kömüşini, Kulu, Konya, Turkey in May 2019.

Preparation of Gut
For light microscope examinations, adult insects were anesthetized with ethyl acetate and dissected in 0.1 M sodium phosphate buffer solution (pH 7.2) under the stereomicroscope (Olympus SZX7). Any surrounding fat was removed. The specimens were fixed in 10% formaldehyde, and then they were dehydrated with graduated ethanol series. Then, specimens were cleaned by xylene and embedded in pure paraffin and sectioned (6-7 µm thick) via a Microm microtome. They were stained with hematoxylin and eosin (H&E). These sections were photographed under a light microscope (Olympus BX51).

Scanning Electron Microscopy (SEM)
For SEM examinations, the dissected guts were fixed with 2.5% glutaraldehyde (pH 7.2, sodium phosphate buffered), washed three times with phosphate buffer (pH 7.2) for 15 minutes, and then dehydrated in ethanol series (70-100% for 15 min each). Then tissues were dried with Hexamethyldisilazane (HMDS), and they were mounted by double-sided tape on SEM stubs, and then coated with gold for 2 minutes with a Polaron SC 502 sputter coater. The samples were examined with a JEOL (JSM 6060 LV) SEM operated at 10 kV, and photographed in an electron microscope laboratory in the faculty of science at Gazi University.

RESULTS

In *M. picta decastigma* adults, the digestive tract is a long tube (Figure 1a). The digestion starts from the mouth (Figure 1b). The mouth parts generally consist of a pair of maxillary palps, a pair of labial palps, a mentrum, a submentum, and a gula (Figure 1b). Muscle bundles were seen in the lower part of the head, anterior to the esophagus (Figure 1c). The digestive tract consisted of three basic regions, that is, fore, mid, and hindgut. The foregut and hindgut were almost equal in length, but the midgut was shorter than the other parts (Figure 1a). The foregut is composed of the pharynx, esophagus, crop and proventriculus (Figures 1a, d). The pharynx is the first part of the foregut, which connects the mouth with the esophagus. The esophagus was a simple, long tube connecting the pharynx with the crop (Figures 1a, d). Anatomically, the esophagus was surrounded by transverse and longitudinal muscle layers, and trachea and tracheoles were found on the muscle layer (Figure 1e). Histologically, the esophagus was composed of the lumen, intima, a single layer epithelium and muscle layer from the inside out (Figure 2a). On the inner surface of the intima of the esophagus, there were sometimes protrusions in the form of spines, sometimes in the form of blunt-tipped teeth (Figures 2b-d). The crop was located just behind the esophagus. The crop contains a series of longitudinal and transverse muscle layer bundles just outside the epithelium (Figure 3a). The epithelial cells, which are mono-layered and cubic, formed the tissue just outside the intima in the crop. There were oval nuclei of epithelial cells medially (Figure 3a). Food particles were distinguished in the lumen. Spiny protrusions in groups were observed on the inner surface of the intima layer. Food particles were found among these spiny protrusions (Figure 3b).

The proventriculus is a thick-walled region lying just posterior to the crop, called a grinding organ. Histologically, the proventriculus was from the inside out, the lumen was filled with food particles, the intima with sharp protrusions, the single-layered
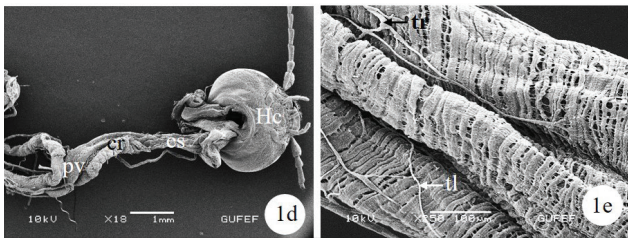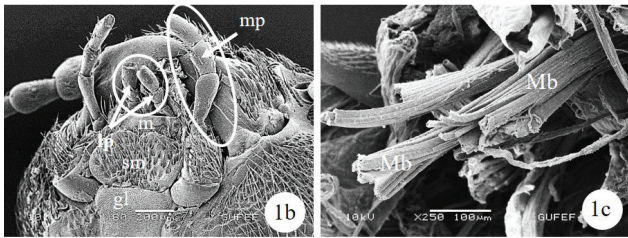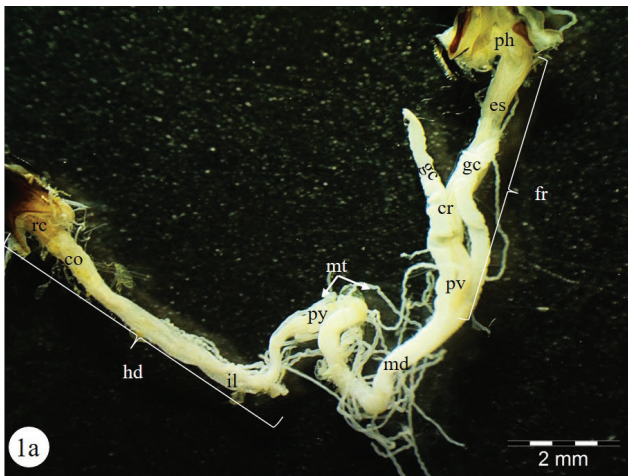
Figure 1. **a.** The general view of digestive tract in *M. picta decastigma* (SEM). **b.** SEM photograph of the general view of mouth structure. **c.** The muscle bundles around the esophagus (SEM). **d.** SEM photograph of the foregut parts. **e.** Longitudinal and transverse muscles surrounding the esophagus. Abbreviations: co-colon, cr-crop, es-esophagus, fr-foregut, gc-gastric caecum, gl-gula, Hc-head capsule, hd-hindgut, il-ileum, lp-labial palp, Mb-muscle bundle, md-midgut, m-mentrum, mp-maxillary palp, mt-Malpighian tubules, ph-pharynx, pv-proventriculus, py-pyloric valve, rc-rectum, sm-submentrum, tl-tracheole tr-trachea.

Figure 2. Light microscopy and SEM photographs of the esophagus in *M. picta decastigma*. a. Longitudinal section of the esophagus (H&E) (LM). b. The protrusions in the spines and blunt-tipped teeth form in the esophagus intima (SEM). c. SEM photograph of food particles on blunt-tipped teeth groups. d. Spine groups in the intima of the esophagus (SEM). Abbreviations: ep-epithelium, in-intima, lu-lumen, ml-muscle layer, nu-nucleus, sp-spine.
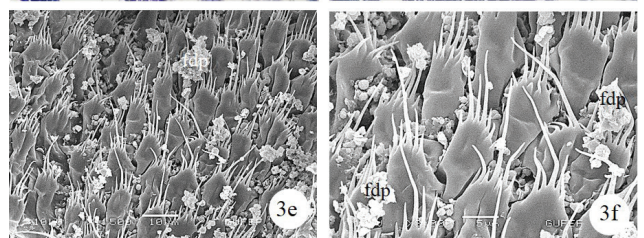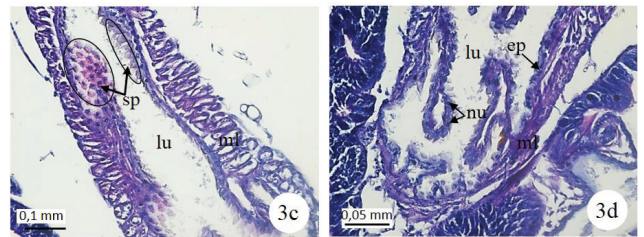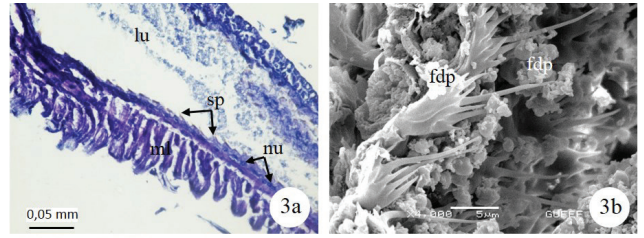
Figure 3. Light microscopy and SEM photographs of the crop and proventriculus in *M. picta decastigma*. **a.** Longitudinal section of the crop (H&E) (LM). **b.** Spiny protrusions on the inner surface of the crop intima layer (SEM). **c.** Longitudinal section of proventriculus (H&E) (LM). **d.** SEM photograph of spiny structures with very long protrusions in the proventriculus intima layer. **e.** Muscle layer, intima and epithelium surrounding the proventriculus (H&E) (LM). **f.** High magnification of the food particles around the spiny structures (SEM). Abbreviations: ep-epithelium, fdp-food particles, lu-lumen, ml-muscle layer, nu-nucleus, sp-spiny protrusions.

cubic epithelium with spherical nuclei medially, surrounded by a longitudinal and transverse muscle layer (Figures 3c and d). There were spiny structures with very long protrusions in the intima layer. Food particles of different sizes were seen between these spiny protrusions (Figures 3e and f).

There was a long, tubular pair of gastric caeca in the anterior part of the midgut, which is the second part of the digestive tract. Anatomically, the gastric caecum surface was seen as round protrusions resembling corn grains (Figures 4a and b). Trachea and tracheoles in the form of thin threads were found on these structures (Figure 4a). In cross-sections, a single-layered cylindrical epithelium with a short striated border at its apex was distinguished. The epithelium layers were convoluted

Figure 4. Light microscopy and SEM photographs of the gastric caecum in *M. picta decastigma*. **a.** Histological section of the gastric caecum (H&E) (LM). **b.** SEM photograph of protrusions resembling corn grains on the gastric caecum surface. **c.** The epithelial layer surrounding the gastric caecum (SEM). **d.** SEM micrograph showing microvilli in the apex of the epithelial cells of the gastric caecum. Abbreviations: ep-epithelium, lu-lumen, mv-microvilli, nu-nucleus, tl-tracheole, tr-tracheoles.

Figure 5. Light microscopy and SEM photographs of the midgut in *M. picta decastigma*. **a.** Longitudinal section of the midgut (H&E) (LM). **b.** The monolayered columnar epithelial cells surrounding the midgut (SEM). **c.** The cross section of some regenerative crypts, which are seen in direct contact with the midgut epithelium (H&E) (LM). **d.** SEM photograph of the outer surface of the midgut covered with regularly spaced rounded structures, which are called regenerative crypts. **e, f.** SEM photograph of a single layered columnar epithelial cells which have their nuclei located medially, and apically they have microvilli. Abbreviations: cry-crypt, ep-epithelium, lu-lumen, mt-Malpighian tubule, ml-muscle layer, mv-microvilli, nu-nucleus, sb-striated border.

in shaped (Figure 4c). SEM micrographs showed microvilli in the apex of the epithelial cells of the gastric caecum (Figure 4d).

The midgut was a slightly tortuous tube, and it was shorter than the foregut and hindgut. LM and SEM images of the transverse sections of the midgut indicated that the epithelial lining was greatly folded giving its lumen a convoluted profile (Figures 5a and b). These mono-layered columnar epithelial cells had their nuclei located medially, and apically they had a striated border (Figures 5a and c). The outer surface of the midgut was covered with regularly spaced rounded structures, which are called regenerative crypts and responsible for providing a continuous supply of new cells for the epithelial lining of the midgut (Figure 5d). Some of the regenerative crypts surrounding the midgut were seen in direct contact with the epithelium lining the lumen of the midgut (Figure 5c). The outer wall consisted of a thin muscle layer beneath which is a convoluted line that completely encircled the midgut (Figure 5c). The microvilli were seen in the apex of the epithelial cells at high magnifications (Figures 5e and f). The microvilli were grouped in threads, and they are responsible for absorption.

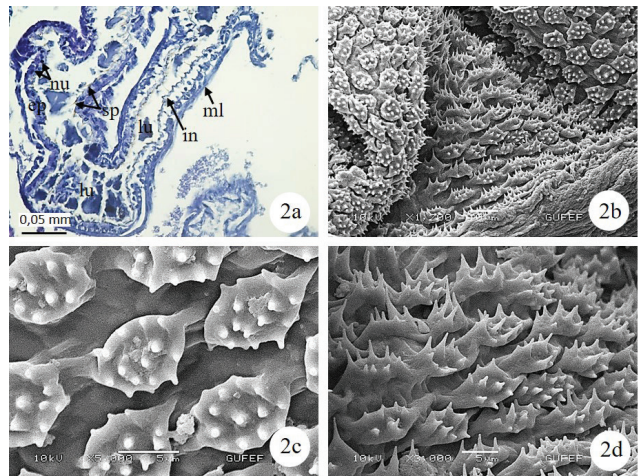Anatomically, the proximal ends of the six Malpighian tubules were located between the mid and hindgut. They were divisible into two groups; the first group consisted of four tubules and the second consisted of two tubules (Figures 6a and b). They were highly tortuous tubes, and they had smooth surfaces (Figures 6a-c). The tracheae and tracheoles were seen between the Malpighian tubules (Figures 6c). These tubules were made up of 5-6 cells with large oval nuclei, and the epithelial layer had microvilli. A thin layer of connective tissue surrounded these cells (Figures 6c and d).

The hindgut comprised slightly more than one-third of the total length of the gut. The main sections of the hindgut (pyloric valve, ileum, colon and rectum) were clearly observed. In sections of the ileum, a highly folded cuticular lining, a monolayer cubic epithelium and a very muscular wall were seen (Figure 6d). In the epithelial cells, the nucleus was round and located in the center of the cell (Figure 6d). The intima in this region had spines in groups (Figures 6e and f). The epithelial layer of the ileum was thicker than those surrounding the other parts of the hindgut (Figures 6d, 7c and 8b).

The colon linked the distal end of the ileum with the proximal end of the rectum (Figure 7a). The distal ends of the Malpighian tubules in *M. picta decastigma* were in contact with the colon surface constituting its excretory or cryptonephric system (Figures 7b and c). The colon had a star-shaped lumen. In cross sections of the colon, the lumen, intima, convoluted single-layered cubic epithelium, Malpighian tubules and sheath were distinguished from inside to outside, respectively (Figures 7c and d).
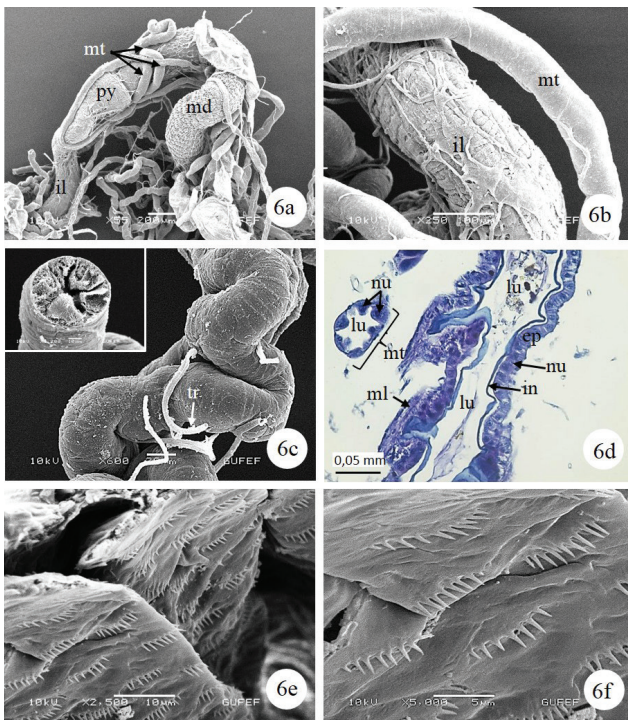
Figure 6. Light microscopy and SEM photographs of the ileum and Malpighian tubules in *M. picta decastigma*. **a.** Malpighian tubules, which are located between the mid and hindgut. **b.** The cubic epithelial cells and sheath surrounding Malpighian tubules, which are smooth surfaced and tortuous tube shaped (SEM). **c.** Longitudinal section of the ileum (X400) (H&E) (LM). **d.** Surface view of the ileum and Malpighian tubules (SEM). **e, f.** SEM photographs of spine groups in the intima layer. Abbreviations: ep-epithelium, il-ileum, in-intima, lu-lumen, md-midgut, ml-muscle layer, mt-Malpighian tubule, nu-nucleus, py-pylorus, tr-trachea.

Figure 7. Light and SEM photographs of the colon in *M. picta decastigma*. **a.** The general view of the colon, rectum and aedeagus (SM). **b.** Malpighian tubules, which are in contact with the colon surface (SEM). **c, d.** The colon wall which is surrounded by the lumen, intima, convoluted single-layered cubic epithelium, Malpighian tubules and sheath (H&E) (LM). Abbreviations: ae-aedeagus, cl-colon, ep-epithelium, tr-trachea, in-intima, lu-lumen, mt-Malpighian tubules, nu-nucleus, rc-rectum, sh-sheath, tl-tracheole.

Figure 8. Light microscopy and SEM photographs of the rectum in *M. picta decastigma*. **a.** The general view of the six rectal pads located on the inner surface of the wall of the rectum (H&E) (LM). **b, c.** Intima, monolayer cubic epithelium and muscle layer which are surrounding the rectum wall (H&E) (LM). **d.** SEM photograph of spines in groups of two or three in the intima. Abbreviations: 1-6-rectal pads, ep-epithelium, in-intima, lu-lumen, ml-muscle layer, sp-spine.

The colon connected the ileum with the rectum. In the cross section, the rectum lumen consisted of intima, a single layer of cubic epithelium and a muscle layer (Figures 8a and b). There were six rectal pads located on the inner surface of the wall of the rectum (Figure 8a). These pads were composed of cubic cells with round nuclei (Figures 8b and c). The intima had protrusions in the form of spines in groups of two or three (Figure 8d). The muscle layers lay immediately outside the epithelial layer. When comparing the rectum, ileum and colon, the first had a convoluted cuticular lining and a thick muscular wall, but its lumen was larger than the others (Figures 6d, 7c and 8b).

DISCUSSION

Insects use many different food sources. Therefore, the structure and function of insect guts is bewilderingly diverse (14). The gut is the most universally conspicuous internal organ of insects and is considerably longer than the body. Its structure varies greatly with different foods and different eating habits of insects (17).

The digestive system in general, is similar to that found in other coleopterous insects, and it consists of 3 parts in insects; foregut, midgut and hindgut, and the lengths of these 3 regions vary according to the species (19-24). In *M. picta decastigma* adults, the foregut and hindgut are almost equal in length, but the midgut is shorter than the other parts. In *Adalia bipunctata* (Linnaeus) (Coccinellidae), the foregut is the shortest region of the gut (12). The foregut of *Asaphes memnonius Hbst.* (Elateridae) comprises about one-thirteenth of the total length of the alimentary canal and the length of each midgut and hindgut is approximately one-half the entire length (25). The hind-intestine is approximately two-thirds as long as the body in *Penthe*

pimelia (Fabricius, 1801) (Tetratomidae) (20). The midgut of *Epicauta cinerea marginata* Fab. (Meloidae) occupies about one-fourth the entire canal (9).

The foregut of *M. picta decastigma* distinguishes a pharynx, esophagus, crop and proventriculus. In *Phanaeus vindex* Macleay (Scarabaeidae), no crop or gizzard is present (19). In *A. memnonius* (Elateridae), the foregut consists of pharynx and crop (25). The foregut in *Phyllophaga gracilis* (Burmeister, 1855) (Scarabaeidae) and *Crioceris asparagi* (L.) (Chrysomelidae) consists of the following regions: pharynx, esophagus, crop, and esophageal valve (22,23). The foregut in *P. pimelia* (Dacnidae) consists of the mouth, the pharynx, the esophagus, and terminates at the esophageal valve (20).

In the esophagus intima, there are no spines in some species while in other species, different protrusions were seen. On the inner surface of the intima of the esophagus in *M. picta decastigma*, there were sometimes protrusions in the form of spines, sometimes in the form of blunt-tipped teeth. The spines have been observed within the esophageal intima in *Alphitobius diaperinus* Panzer, 1797 (Tenebrionidae), *Dendroctonus micans* (Kugelann, 1794), *D. ponderosae* (Hopkins, 1902), *D. pseudotsugae pseudotsugae* Hopk., *D. rufipennis* (Kirby, 1837) and *D. terebrans* (Olivier) (Scolytidae) (10,26).There are no spines in the esophagus intima of *P. vindex* (Scarabaeidae) and *Platynotus belli* Fairmere (Tenebrionidae) (19,27).

Trachelizus bisulcatus (Fabricius) (Brentidae), *Allaeometrus breviceps* Senna (Brentidae) and *Calendyma chilensis* (Spinola 1849) (Cleridae), *Tanymecus dilaticollis* Gyllenhal, 1834 (Curculionidae) have a well-developed proventriculus, but it is weakly developed in *M. picta decastigma* (Buprestidae), *Aporhina australis* (Heller) (Brentidae), *Mecysolobus bubo* (Fabricius) (Curculionidae), *Tillus elongatus* (Linnaeus) (Cleridae) and *Onychotillus vittatus* Chapin (Cleridae) (28-30).

In *M. picta decastigma*, teeth lined up in groups were seen on the inner surface of proventriculus intima, like in *Capnodis tenebrionis* (L. 1758) (Buprestidae) (3). In *Dendroctonus armandi* Tsai and Li (Curculionidae), *Sitophilus zeamais* Motschulsky, 1855 (Curculionidae), *Epiphaneus malachiticus* Boheman, 1842 (Coleoptera: Curculionidae) and *T. dilaticollis* (Curculionidae), the proventriculus consists of eight heavily sclerotized chitinous basal plates (29,31-33).

The gastric caeca position, number, and arrangement vary among coleopteran species (28,34). In *M. picta decastigma,* the midgut has a pair of tubular gastric caeca at the anterior end, as in *Capnodis tenebrionis* (L. 1758) (Buprestidae) (3). In the posterior midgut of *Hypothenemus hampei* (Ferrari) (Curculionidae) and in the anterior portion of the midgut in *A. bipunctata*, two gastric caeca are seen (12,34). *D. armandi* (Curculionidae) has approximately 160 gastric caeca in the middle of the midgut (32). In the middle of the posterior midgut of *E. malachiticus* (Curculionidae), there are a lot of gastric caeca (31). However, unlike these species, there is no clear intestinal caeca in the midgut of *A. diaperinus* (Tenebrionidae) and *Epilachna chrysomelina*
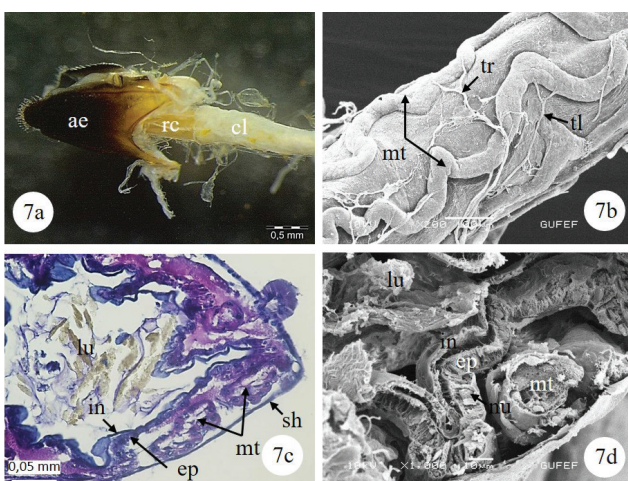
(Fabricius) (Coleoptera: Coccinellidae) (35,36). They are responsible for secretion and absorption (37). The midgut of *Calosoma sycophanta* Linnaeus, 1758 (Carabidae) has numerous closely packed small villus-like caeca (37).

There are regenerative crypts surrounding the midgut of *M. picta decastigma*. They are suppliers of new cells to the midgut epithelial lining. Similar structures are seen in *P. vindex* (Scarabaeidae), *P. pimelia* (Dacnidae) and *Prostephanus truncatus* (Horn) (Bostrichidae) (19,20,17). In *M. picta decastigma*, the midgut epithelium is monolayered columnar cells, as in other species (32,38).

The proximal ends of the six Malpighian tubules are located between mid and hindgut in *M. picta decastigma,* and they are divisible into two groups: the first group consisting of four tubules and the second consisting of two tubules. Similarly, in *C. asparagi* (Chrysomelidae) and *P. pimelia* (Dacnidae), the Malpighian tubules are six in number and are attached to the canal at the pyloric valve (20,22). However, the four Malpighian tubules arise at the posterior end of the foregut in *P. vindex* (Scarabaeidae) (19). The Malpighian tubules of *A. memnonius* (Coleoptera: Elateridae) are four in number and are attached at four different points around the circumference of the gut (25). In *M. picta decastigma*, histologically they are composed of large cells with large and oval nuclei. Similar structures have been observed in other Coleopteran species (26,31,32,34-36,38-40).

The hindgut in *M. picta decastigma* is made up of the following regions, pyloric valve, ileum, colon, and rectum as with most other species (20-22,31,35,40). In *A. diaperinus* (Tenebrionidae), the hindgut is divided into two distinct sections, the anterior small intestine and the posterior large intestine (36). The hindgut in *A. bipunctata* consists of the ileum, rectum and rectal canal (12).

Ileum epithelial cells in *M. picta decastigma* are cubic. However, columnar cells constitute the epithelial layer in the ileum of *P. vindex* (Scarabaeidae) (19). In *M. picta decastigma*, the intima in the ileum has spines. There are spines in the ileum intima of *C. sycophanta* (37).

In *M. picta decastigma*, the distal ends of the Malpighian tubules also form a layer around the colon as in *C. asparagi* (Chrysomelidae) (22). However, in *P. truncatus*, the distal ends of the Malpighian tubules are located in the rectum. They have the same cryptonephric system (17).

There are six rectal pads located on the inner surface of the wall of the rectum of *M. picta decastigma*. A similar structure is also seen in *C. sycophanta* (37).

CONCLUSION

In the present study, the anatomy and histology of the alimentary tract of *M. picta decastigma* were examined. These results were compared with those of other species of Coleoptera. It is

hoped that this study will contribute to the knowledge of the digestive system of other Coleopteran species and other insect species. Furthermore, it is hoped that the characteristics revealed may provide information for future research into the ecology and biological control of noxious Coleoptera.

REFERENCES

1. Bellamy CL. A catalogue of the higher taxa of the family Buprestidae (Coleoptera). Navorsinge van die Nasionale Museum, Bloemfontein 1985;4(15):405-72.

2. Bíly S. Summary of the bionomy of the buprestid beetles of central Europe (Coleoptera: Buprestidae). Acta Entomologica Musaei Nationalis Pragae, Supplement 2002;10:1-104.

3. Özyurt Koçakoğlu N, Candan S, Çağlar Ü. Histomorphology of the adult digestive tract of *Capnodis tenebrionis* (L. 1758) (Coleoptera, Buprestidae). Microsc Microanal 2020;26(6):1245-54. doi:10.1017/S1431927620024472

4. Foottit RG, Adler, PH. Insect biodiversity: Science and society, Blackwell Publishing, West Sussex, UK, 2009.

5. Sakalian V, Langourov M. Color trap a method for distributional and ecological investigations of Buprestidae (Coleoptera). Acta Soc Zool Bohem 2004;68:53-9.

6. Çanakçıoğlu H. Orman Entomolojisi. İ.Ü. Orman Fakültesi Yayınları, İ.Ü. Yay. No: 3152, Orman Fak. Yay. No: 349, İstanbul, Birinci baskı, Matbaa Teknisyenleri Basımevi; 1983.

7. Schmitz H, Bousack H. Modelling a historic oil-tank fire allows an estimation of the sensitivity of the infrared receptors in Pyrophilous melanophila beetles. Plos One 2012;7(5):e37627.

8. Bily S. The Buprestidae (Coleoptera) of Fennoscandia and Denmark. Fauna Entomol Scand 1982;110:1-109.

9. Evans HF, Moraal LG, Pajares JA. Biology, ecology and economic importance of Buprestidae and Cerambycidae. Lieutier KRD F, Battisti A, Grégoire J-C, Evans HF, editors. Bark and wood boring insects in living trees in europe, a synthesis. Dordrecht: Springer; 2007. pp. 447-74.

10. Liu XD, Jia XZ. A grey related analysis Cytospora chrysosperma with Melanophila decastigma of poplar. Forest Pest and Disease 1988;4:26-7.

11. Khabir ZH & Sadeghi SE. Determination of Melanophila picta Pall. (Coleoptera: Buprestidae) damage rate in Populus alba/Medicago sativa agroforestry system. Mun Ent Zool 2012;7(2):920-5.

12. Borges I, Nóia M, Camarinho R, Rodrigues AS, Soares AO. Characterization of the alimentary canal of the aphidophagous ladybird, Adalia bipunctata (Coleoptera: Coccinellidae): anatomical and histological approaches. Entomol Sci 2015;18(1):66-73.

13. Chapman RF. Comprehensive and insect physiology. Kerkut GA, Gilbert LI editors. Biochemistry and Pharmacology. Oxford Pergamon, 1985.

14. Dow JA. Insect midgut function. Adv In Insect Phys 1986;19;187-328.

15. Gullan DJ, Cranston PS. The Insects: An outline of entomology, 3rd edn, Blackwell Publishing Ltd, Melbourne, 2005.

16. Wigglesworth VB. The Principles of insect physiology. Chapman and Hall Ltd, London, 1977.

17. Vazquez-Arista M. Anatomical, enzymatic, and microbiological studies on the digestive system of *Prostephanus truncatus* (Horn), Doctoral thesis, University of Leicester, England, 1997.

18. Gardner JA. Revision of the higher categories of Stigmoderini (Coleoptera: Buprestidae), The University of Adelaide, South Australia, Doctoral thesis, 1986.

19. Bection Jr, EM. The alimentary tract of *Phanaeus vindex* Macl. (Scarabaeidæ). Ohio J Sci 1930;30(5):315-23.

20. Brubaker RW. The alimentary tract of Penthe *Pimelia*, Fabr. (Coleoptera: Dacnidae). Ohio J Sci 1934;34(1):46-56.

21. Everly RT. The alimentary tract of the margined blister beetle, *Epicauta cinerea marginata* Fab. (Coleoptera-Meloidae). Ohio J Sci 1936;36(4):204-16.

22. Davidson RH. The alimentary canal of *Criocerus asparagi* Linn. Ohio J Sci 1931;31(5):396-405.

23. Fletcher FW. The alimentary canal of *Phyllophaga gracilis* Burm. Ohio J Sci 1930;30(2):109-19.

24. Lewis HC. The alimentary canal of *Passalus*. Ohio J Sci 1926;26(1):11-24.

25. Bigham JT. The alimentary canal of *Asaphes memnonius* Hbst. Ohio J Sci 1931;31(5):386-95.

26. Díaz E, Arciniega O, Sánchez L, Cisneros R, Zúñiga G. Anatomical and histological comparison of the alimentary canal of *Dendroctonus micans*, *D. ponderosae*, *D. pseudotsugae pseudotsugae*, *D. rufipennis*, and *D. terebrans* (Coleoptera: Scolytidae). Ann Entomol Soc Am 2003;96(2):144-52.

27. Sarwade AB, Bhawane GP. Anatomical and histological structure of alimentary canal of adult Platynotus belli (Coleoptera: Tenebrionidae). BFAIJ 2013;5:47-55.

28. Calder AA. The alimentary canal and nervous system of Curculionoidea (Coleoptera): Gross morphology and systematic significance. J Nat Hist 1989;23(6):1205-65.

29. Candan S, Özyurt Koçakoğlu N, Güllü M, Çağlar Ü. Anatomical and histological studies of the alimentary canal of adult maize leaf weevil, Tanymecusdilaticollis Gyllenhal, 1834 (Coleoptera: Curculionidae). Microsc Res Tech 2020;83:1153-62.

30. Opitz W. Morphologic studies of the alimentary canal and internal reproductive organs of the Chaetosomatidae and the Cleridae (Coleoptera: Cleroidea) with comparative morphology and taxonomic analyses. Insecta Mundi 2014;0342:1-40.

31. Candan S, Özyurt Koçakoğlu N, Erbey M. Morphology and histology of the alimentary canal of Epiphaneus malachiticus Boheman, 1842 (Coleoptera, Curculionidae). Entomol Rev 2019;99(3):326-36.

32. Bu SH, Chen H. The alimentary canal of *Dendroctonus armandi* Tsai and Li (Coleoptera: Curculionidae: Scolytinae). Coleopts Bull 2009;63(4):485-96.

33. De Sousa G, Scudeler EL, Abrahão J, Conte H. Functional morphology of the crop and proventriculus of *Sitophilus zeamais* (Coleoptera: Curculionidae). Ann Entomol Soc Am 2013;106(6):846-52.

Eur J Biol 2021; 80(1): 1-8

Ozyurt Kocakoglu et al. Anatomy and Histology of Digestive Tract in *M. picta decastigma*

34. Rubio JDG, Bustillo PAE, Vallejo ELF, Acuña ZJR, Benavides MP Alimentary canal and reproductive tract of *Hypothenemus hampei* (Ferrari) (Coleoptera: Curculionidae, Scolytinae). Neotrop Entomol 2008;37(2):143-51.

35. Aldigail SA, Alsaggaff AI, Al-Azab AM. Anatomical and histological study on the digestive tract of *Epilachna chrysomelina* (Coleoptera: Coccinellidae). Biosci Biotechnol Res 2013;10(1):183-92.

36. McAllister JC, Steelman CD, Carlton CE. Histomorphology of the larval and adult digestive systems of *Alphitobius diaperinus* (Coleoptera: Tenebrionidae). J Kansas Entomol Soc 1995;195-205.

37. Bess HA. The alimentary canal of *Calosoma sycophanta* Linnaeus. Ohio J Sci 1935;35:54-61.

38. Díaz E, Cisneros R, Zúñiga G. Comparative anatomical and histological Study of the alimentary canal of the *Dendroctonus frontalis* (Coleoptera: Scolytidae) Comp Ann Entomol Soc Am 2000;93(2): 303-11.

39. Singh OL, Prasad B. Histomorphology of the alimentary tract of adult, Odoiporus longicollis (Oliv.) (Coleoptera: Curculionidae). J Entomol Res Soc 2013;1:109-15.

40. Sinha RN. The alimentary canal of the adult of Tribolium castaneum Herbst (Coleoptera, Tenebrionidae). J Kansas Entomol Soc, 1958;31(2);118-25.

ISTANBUL
UNIVERSITY
PRESS

Tumor Necrosis Factor-α Induced Cellular Stress on Trophoblastic Cells: NF-κB Signaling Could be a Potential Therapeutic Target

Erengul Tokay Varolli[1] , **Serbay Ozkan[1]** , **Burcu Biltekin[1]** , **Meral Koyuturk[1]**

[1]Istanbul University-Cerrahpasa, Cerrahpasa Medical Faculty, Histology and Embryology Department, Turkey

ORCID IDs of the authors: E.T.V. 0000-0002-0270-5069; S.O. 0000-0001-7854-4735; B.B. 0000-0002-8435-6797; M.K. 0000-0002-0270-5069

ABSTRACT

Objective: The development of the human placenta depends on proliferation and differentiation of trophoblastic cells. Deficiencies in trophoblastic functions are known to have a critical role in the progression of placental pathologies such as preeclampsia. Therefore, in this research, it was aimed to evaluate the responses of trophoblastic cells to tumor necrosis factor-α (TNF-α) mediated cellular stress.

Materials and Methods: In this study, the cellular stress model was set up by treating JAR cells with 100ng/ml TNF-α for 1, 6, 12 and 24 hour long periods. In this model, the effects of TNF-α on the proliferation capacity and apoptotic activity of JAR trophoblastic cells were investigated by immunocytochemistry. The nuclear and total expression levels of nuclear factor-κB (NF-κB) was evaluated with immunocytochemistry and Western blot, respectively.

Results: It was shown that 100 ng/ml TNF-α treated cells had a reduced proliferative capacity and increased apoptotic activity by immunocytochemical staining of PCNA and caspase-8 proteins respectively. In this respect, the NF-κB signaling pathway plays a critical role in TNF-α induced processes. So that, it was shown that the TNF-α treated group had increased nuclear and total NF-κB expressions compared to the untreated one.

Conclusion: Our findings showed that TNF-α has a significant role as a cellular stress source in JAR cells. TNF-α stimulated cellular response could be defined as decreased proliferative capacity, increased apoptotic activity and NF-κB signaling in JAR syncytiotrohoblastic cell lines. Therefore, investigation of TNF-α related cellular responses especially NF-κB signaling is further required for the understanding of the mechanism of placental pathologies which is crucial for the development of therapeutic approaches.

Keywords: Cellular stress, NF-κB signaling pathway, placenta, TNF- α, trophoblastic cells

INTRODUCTION

The development of the human placenta depends on the proliferation and differentiation of trophoblastic cells. In this respect, dysfunction of trophoblasts plays an important role in the development of placental pathologies (1). Therefore, an aberrant development and differentiation of the villous syncytiotrophoblast risks the integrity of the placental barrier and causes the release of necrotic and aponecrotic trophoblast frag-

ments (2). Histological evidences suggest a role for trophoblasts in remodeling of the uterine spiral arteries. The disruption of trophoblastic invasion and incomplete remodeling result in reduction of uteroplacental perfusion, which in turn could cause ischemia of the placenta. The alterations resulted from ischemic placenta lead to increased production of oxidative stress and stimulation of proinflammatory cytokine secretion. In this connection, it was found that production of proinflammatory cytokines such as tumor necrosis fac-

tor alpha (TNF-α) was increased in placental pathologies including preeclampsia (3,4). TNF-α regulates the expression of genes associated with inflammation, cell survival, proliferation and differentiation mainly through the activation of the nuclear factor κB (NF-κB) signaling pathway (5,6). TNF-α is associated with apoptotic cell death via two distinct caspase-8 activation pathways. One of the pathways is regulated by cIAP1 (cellular inhibitor of apoptosis protein1) and cIAP2, the two of which join to form the signaling complex referred to as complex I that leads to the activation of the NF-κB pathway (7). On the other hand, pentoxifylline (PTX), which is a pharmacologic agent used for improving the circulation, has been reported to have various effects at the cellular level including inhibition of TNF-α (8,9).

TNF-α gene expression was demonstrated at endometrial cells, decidual cells and trophoblastic cells during the trimesters of pregnancy (10). Moreover a group of pregnancy pathologies was associated with increased maternal TNF-α, which was suggested to influence fetal-maternal crosstalk during pregnancy. In this respect, because it is difficult to elucidate the role of TNF-α in such a complex process in *in vivo, in vitro* experiments with cell lines treated with recombinant TNF-α could be illuminating. Therefore, in this research, it was aimed to examine the response of trophoblasts to TNF-α mediated cellular stress in the JAR cell line by the evaluation of proliferative, apoptotic indexes and expression levels of NF-κB which is a key signaling molecule and to assess the therapeutic potential of PTX in TNF-α induced interactions.

MATERIALS AND METHODS

Cell Culture
JAR human choriocarcinoma cell line was purchased from the American Type Culture Collection. The cells were cultured in Dulbecco's modified Eagle's medium/F12 medium with 10% heat inactivated fetal bovine serum under the humidified atmosphere with 5% CO_2 at 37 ºC. First of all, the cells grown on coverslips were cultured with experimental doses of TNF-α (PI-RP-10921, Thermo Fisher, MA, USA) ranging from 0.1 to 1000 ng/ml; the optimal dose of TNF-α was determined in accordance with evaluation of NF-κB expressions preliminarily. Then experimental groups were organized at 1, 6, 12 and 24 h-long 100 ng/ml TNF-α treatment. Afterwards, experimental groups were set up, treating the cells with 1, 10 and 20 mM doses of PTX (prepared from 100 mg per injection ampule) in the presence of TNF-α or not for 1h.

Immunocytochemistry
JAR cells were fixed with cold methanol. Following the incubation with blocking serum at room temperature, primary antibodies against proliferating cell nuclear antigen (PCNA) (MA1-16827, Thermo Fisher, MA, USA), caspase-8 (PI-MA1-91442, Thermo Fisher, MA, USA) and NF-κB p65 (Sc-109, Santa Cruz, CA, USA) were applied overnight at 4°C. After washing with phosphate buffered saline (PBS), biotinylated secondary antibodies and horseradish peroxidase (HRP) conjugated streptavidin were applied in order. Finally, after treatment with aminoethyl carba-

zole, the cells were investigated with an Olympus BX-61 bright field microscope. Proliferation indexes were calculated by taking the averages of the values obtained by dividing the number of PCNA positive cells by the total number of cells in each one of the 5 different areas. The intensities of immunocytochemical stainings for caspase-8 and NF-κB were semi-quantitatively scored in accordance with the following grading system: 0 (no staining), 1+ (weak, but detectable staining), 2+ (moderate or distinct staining), and 3+ (intense staining). Experiments were repeated three times and histological scores (HSCORE) were obtained for each slide. HSCORE = Σ Pi (i + 1), where i represents the intensity score, and Pi is the corresponding percentage of the cells (11).

DAPI Staining
The cells cultured on lamellas were treated with 100 ng/ml TNF-α for 24 h and then fixed with 4% of paraformaldehyde. After two times of washing with phosphate buffered saline (PBS) for 5 min, 4',6-diamidino-2-phenylindole dihydrochloride (DAPI) stain was applied to detect apoptotic cells with their characteristic nucleus morphologies (nuclear compaction, fragmentation or semilunar appearance). The samples were investigated under an Olympus BX-61 florescence microscopy and apoptotic indexes were calculated by dividing the number of apoptotic cells by the total cell number.

Western Blot Analysis
JAR cells grown in different experimental conditions were washed with ice-cold PBS and scraped from culture flasks and then lysed with the cell lysis buffer containing a protease inhibitor cocktail to extract the total protein. The collected samples were subjected to electrophoresis on SDS-PAGE gels and transferred to nitrocellulose membranes. The membranes were blocked with 5% non-fat dried milk and then incubated with anti-NF-κB (Sc-109, Santa Cruz, CA, USA) primary antibodies overnight at 4°C. After washing the membranes with tris-buffered saline containing 0.1% Tween 20 for 15 min, they were incubated with goat HRP-conjugated anti-rabbit secondary antibody (PI-31460 Thermo Fisher, USA) for 1 h at room temperature. Then, following a second washing step, the membranes were also incubated with HRP-conjugated β-actin primary antibody (Sc-47778, Santa Cruz, CA, USA) as a loading control. The protein bands were visualized by using 3,3'-diaminobenzidine. Experiments were repeated three times and band intensities were quantified by densitometric analysis (Adobe Photoshop CS5) and normalized to β-actin readings.

Statistical Analyses
Statistical analyses were performed with Sigma Plot 12.0 software packages for the immunocytochemical and Western blot analyses. The data were presented as mean ± standard error (SE). Analysis between the groups were performed with One Way ANOVA test followed by Student t-test and non-parametric Kruskal Wallis-H tests for the immunocytochemistry and Western blot scores respectively. A value of $p < 0.05$ was considered statistically significant.

RESULTS

In accordance with our preliminary studies, 100 ng/ml TNF-α was determined as an optimal dose for cellular stress induction in JAR cells. In this respect, the effects of cellular stress over the proliferation capacity of JAR cells were evaluated at the end of the 6, 12 and 24 h long incubations with TNF-α through the
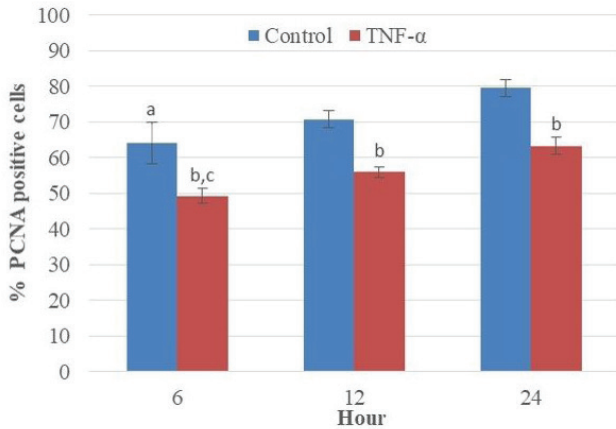
Figure 1. Proliferation indexes expressed with percentages (%) of PCNA positive cells for the control and TNF-α treated cell groups with different time intervals. [a]P<0.05 vs 12- and 24-hour control groups. [b]P<0.05 vs control groups. [c]P<0.05 vs 12- and 24-hour of TNF-α treated cell groups.

PCNA immunocytochemical analysis. The percentages of PCNA expressing cells after TNF-α treatment were statistically lower than the control and PCNA expression tended to increase with higher incubation time from 6th hr (Figure 1).

Second of all, cellular stress related apoptotic activity in JAR cells was investigated by evaluation of the immune reactivity of caspase-8 at the end of the 1, 6, 12 and 24 h of treatment with TNF-α. The caspase-8 immune reactivities of all the TNF-α applied groups were significantly higher than the control group and 1 h of TNF-α treatment brought about the highest caspase-8 immune reactivity (Figure 2A). Furthermore, cells treated with TNF-α for 24 h were compared with the non-treated ones by DAPI staining which is specific for DNA in order to show apoptosis related morphologic changes (Figure 2B-D). The number of cells having characteristic apoptotic nuclear morphology in the TNF-α treated group was significantly higher than the ones in the control (Figure 2B).

NF-κB signaling is one of the key pathways for the regulation of expressions of genes related to cell survival and proliferation, and activated by TNF-α (5,6). Therefore, nuclear NF-κB expression levels of the JAR cells were evaluated at the end of the 1-, 6-, 12- and 24 h long incubation with TNF-α through the immunocytochemical (Figure 3A-E and Table 1) and Western blot analysis (Figure 3F). It was found that 1 h long induction with TNF-α was effective to induce NF-κB expression significantly (Table 1). At this point, we assessed the effects of dif-
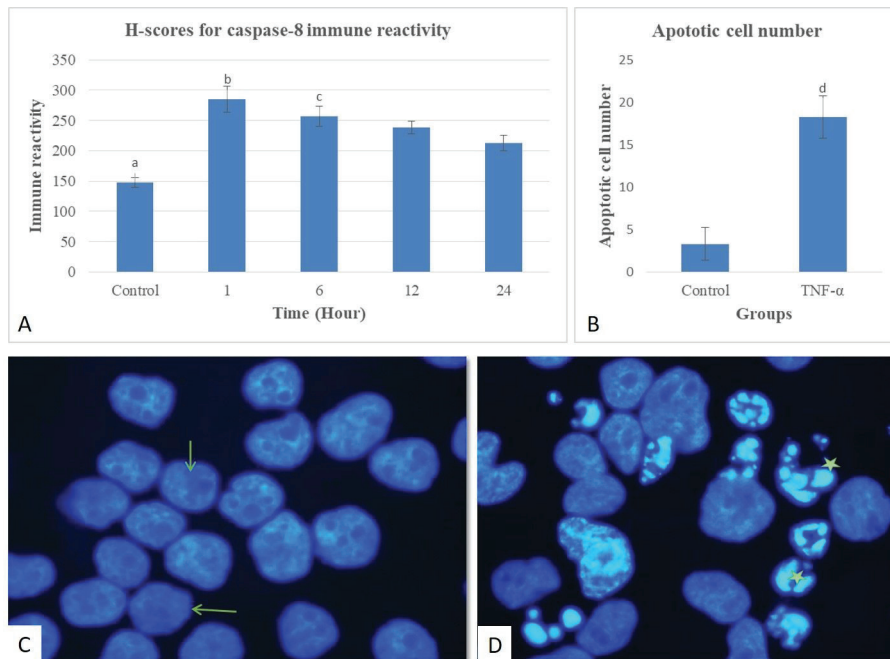
Figure 2. Caspase-8 immune reactivities of control and TNF-α treated cell groups with different time intervals (A). Apoptotic cell rates for the control and 24-hour TNF-α treated cell groups (B). Representative photomicrographs of control (C) and 24-hour long TNF-α treated cells (D) (arrow: normal nucleus morphology; star: apoptotic nucleus morphology, 100X). [a]P<0.05 vs TNF-α treated cell groups. [b]P<0.05 vs 6-, 12- and 24-hour of TNF-α treated cell groups. [c]P<0.05 vs 12- and 24-hour of TNF-α treated cell groups. [d]P<0.05 vs control group.
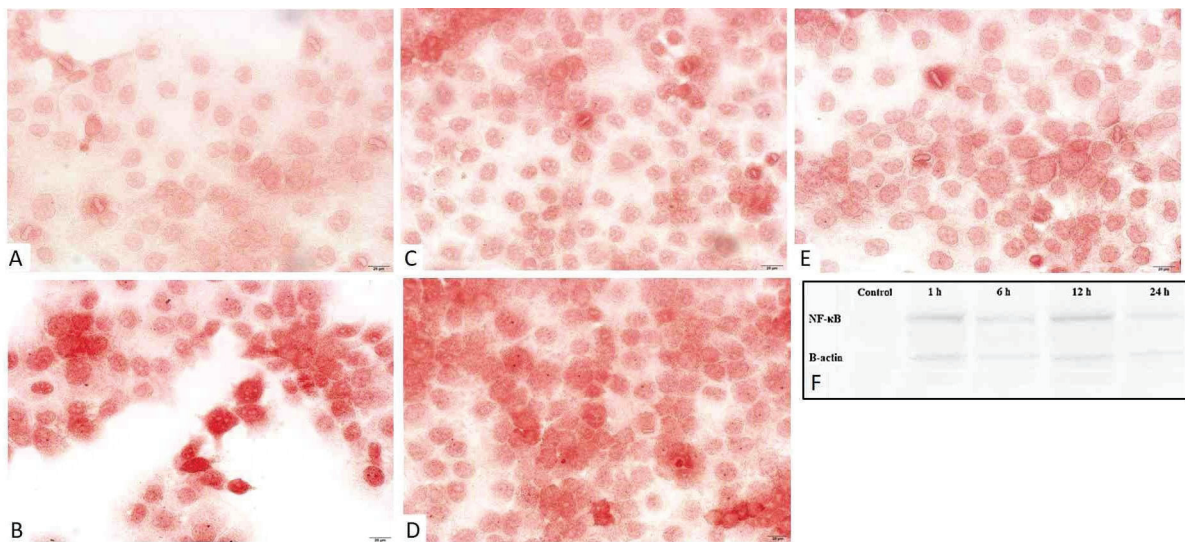
Figure 3. Representative photomicrographs of nuclear NF-κB immune reactivities in control (A), and 1 h- (B), 6 h- (C), 12 h- (D) and 24 h long (E) 100ng/ml TNF-α treated groups. Total NF-κB and β-actin protein levels (F).

Table 1. H scores for nuclear expressions of NF-κB average±SD in the control and TNF-α groups with different time intervals

Groups	Average±SD
Ctrl	169±7
TNF-α (1h)	329±7[a][b]
TNF-α (6h)	219±9[a]
TNF-α (12h)	302±11[a][b]
TNF-α(24h)	224±7[a]

SD: standard deviation, [a]P<0.05 vs. control (ctrl) group, [b]P<0.05 vs. 6 h and 24 h long TNF-α treated groups.

ferent doses of PTX, which has been reported as an inhibitory molecule for TNF-α on NF-κB expression levels. NF-κB immunoreactivities disappeared in all of the nuclei of cells treated with only 1 mM, 10 mM and 20 mM PTX. However, it was found that only 10 mM PTX was able to completely abolish the basal level of nuclear NF-κB expression, and significantly reduced the nuclear NF-κB expression induced by 1-h long incubation with 100 ng/ml TNF-α (Figure 4, Table 2).

Table 2. H scores for nuclear expressions of NF-κB average±SD in the control, TNF-α (1h) and PTX groups.

Groups	Average±SD
Ctrl	169±7
TNF-α (1h)	329±7
10 mM PTX	0
10 mM PTX + TNF-α (1h)	180±10[a]

SD: standard deviation, [a]P<0.05 vs. TNF-α (1h) treated group.
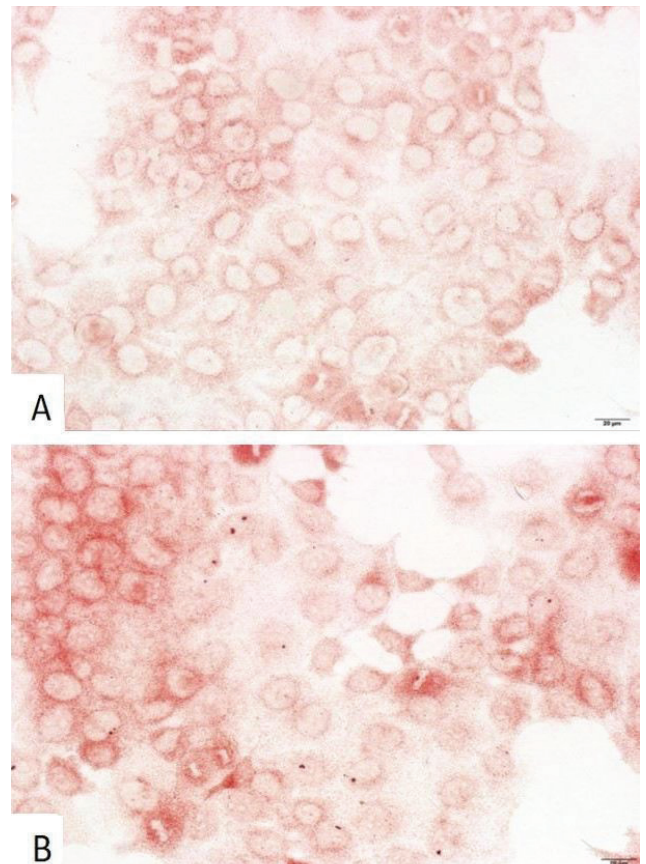
Figure 4. Representative photomicrographs of nuclear NF-κB immune reactivities in 10 mM PTX (A) and 10 mM PTX + TNF-α (B) treated groups.

Furthermore, Western blot analysis showed that total NF-κB expression was slightly increased with the TNF-α treatment and PTX application reduced total NF-κB expressions significantly compared to the control and only TNF-α treated ones (Figure 5).
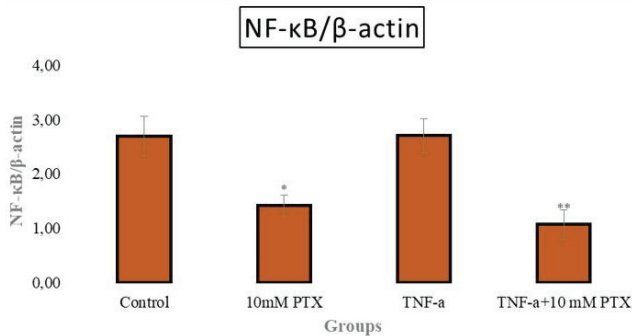
Figure 5. Graphical representation of average densitometric ratios of NF-κB to β-actin. *$P<0.05$ vs control group, **$P<0.01$ vs TNF-α group.

DISCUSSION

Invasiveness of syncytiotrophoblasts is required for remodeling of spiral arteries during pregnancy. Inadequate invasion of trophoblasts leads to a deficient rupture of spiral arteries in the muscular layer, which in turn leads to disruption of utero-placental circulation (12,13). Interrupted arterial blood supply results in an increased generation of inflammatory cytokines like TNF-α (14,15). In this respect, determination of increased level of TNF-α in the plasma of preeclamptic pregnant women has shown that TNF-α could be used as an inducing agent for the establishment of experimental models (16). TNF-α takes part in induction of rapid transcription of genes associated with the regulation of proliferation, cell survival, inflammation and differentiation mainly through activation of the NF-κB pathway (6). For those reasons, it was aimed to evaluate the effects of TNF-α as a potential cellular inducer on JAR trophoblastic cells in our research. First of all, the proliferation indexes of JAR cells were evaluated and it was found that following 6 h of incubation with TNF-α, proliferating cell numbers was significantly reduced which could be interpreted as TNF-α having an anti-proliferative effect on trophoblastic cells. Caspase-8 is an initiator caspase, and is predominantly located in mitochondria as a pro-enzyme and released upon apoptotic stimulation like TNF-α (17). Caspase-8 is a prototypic caspase of apoptotic death receptor pathways and activates its ligand by binding to members of the TNF-α receptor superfamily (18,19). In this respect, at the end of the 1 h, cells treated with 100 ng/ml TNF-α had significantly higher caspase-8 immune reactivity. As an initiator caspase, caspase-8 plays an important role in TNF-α induced cellular stress, which could lead to apoptosis in the end. In this respect, morphologic changes like nuclear fragmentation are a late stage event for apoptosis (20). Therefore, the long-term effects have been showed by DAPI staining at the end of the 24 h long incubation with TNF-α. Those results

support that TNF-α could be one of the main cytokine factors taking part in the placental pathologies, which are associated with trophoblast apoptosis such as preeclampsia. In addition, 100 nm/ml TNF-α treatment is quite effective for setting up an in vitro preeclamptic experimental model in trophoblastic JAR cells. Therefore, we wanted to know the role of the NF-κB signaling pathway in those processes. In the absence of inducing stimuli, NF-κB molecules are in an inactive state in the cytoplasm. Upon activation by TNF-α, NF-κB is transferred to the nucleus, and regulates the associated genes (21,22). In this respect, the effects of TNF-α treatment on the nuclear NF-kB expression levels in different time intervals were evaluated. In our experiments, we showed that a 1 h long induction with TNF-α brought about a significant increase in the total and nuclear expression of NF-κB. Even though the nuclear expression of NF-κB was fluctuating with increasing time of TNF-α stimulation, the decrease in proliferative capacity and increase in apoptotic activity are quite consistent with longer incubation time. Similarly, increased NF-κB expression induced with TNF-α was demonstrated in ED27 cells, which are immortalized trophoblast-like cells (23). Furthermore, increased NF-κB expression was also shown for syncytiotrophoblastic cells of preeclamptic placental tissues (24). As a result, we could define a positive feedback loop between TNF-α and NF-κB expressions in JAR trophoblastic cells which possibly participates in progressive aggravation of inflammation in the placenta. PTX, which is a methylxanthine derivative and a non-specific inhibitor of cAMP phosphodiesterase, is generally applied as a pharmacologic agent for improvement of circulation in peripheral vascular disorders (8,25). Moreover, possible therapeutic effects of PTX as an inhibitor of TNF-α synthesis have been investigated in various diseases (26,27). Importantly, it was noted that PTX treatment has a reducing effect on plasma levels of proinflammatory cytokines including TNF in addition to its antioxidant effects (9). In our study, we investigated the optimal dose of PTX for inhibition of TNF-α induced NF-κB expression and it was found that 10 mM PTX application was quite effective in the reduction of TNF-α stimulated nuclear expression of NF-κB. It was reported that NF-κB translocation to nuclei was blocked by PTX application in TNF-α stimulated vascular smooth muscle cells (28). Therefore, PTX could be a potential therapeutic agent for the treatment of TNF-α related placental pathologies.

CONCLUSION

In summary, the present study showed that incubation with TNF-α leads to a decrease in proliferation capacity and an increase in apoptotic activity and NF-κB signaling in JAR syncytiotrophoblastic cell lines. In addition to all of this, PTX could be a potential regulatory agent for TNF-α induced cellular stress by down regulating the nuclear translocation of NF-κB. Further in vitro and in vivo experiments are required to clarify the effects of PTX which has the potential to be used as a pharmacologic therapeutic in TNF-α associated cellular stress of placental pathologies.

REFERENCES

1. Knöfler M, Haider S, Saleh L, Pollheimer J, Gamage TKJB, James J. Human placenta and trophoblast development: key molecular mechanisms and model systems. Cell Mol Life Sci 2019;76:3479–96.

2. Schoots MH, Gordijn SJ, Scherjon SA, van Goor H, Hillebrands J-L. Oxidative stress in placental pathology. Placenta 2018;69:153–61.

3. Otun HA, Lash GE, Innes BA, Bulmer JN, Naruse K, Hannon T, et al. Effect of tumour necrosis factor-α in combination with interferon-γ on first trimester extravillous trophoblast invasion. J Reprod Immunol 2011;88:1–11.

4. Aouache R, Biquard L, Vaiman D, Miralles F. Oxidative stress in preeclampsia and placental diseases. Int J Mol Sci 2018;19:1496.

5. Schütze S, Wiegmann K, Machleidt T, Krönke M. TNF-induced activation of NF-κB. Immunobiology 1995;193:193–203.

6. Hayden MS, Ghosh S. Regulation of NF-κB by TNF family cytokines. Semin Immunol 2014;26:253–66.

7. Wang L, Du F, Wang X. TNF-α induces two distinct caspase-8 activation pathways. Cell 2008;133(4):693-703.

8. McCarty MF, O'Keefe JH, DiNicolantonio JJ. Pentoxifylline for vascular health: a brief review of the literature. Open Hear 2016;3:e000365.

9. Samlaska CP, Winfield EA. Pentoxifylline. J Am Acad Dermatol 1994;30:603–21.

10. Chen HL, Yang Y, Hu XL, Yelavarthi KK, Fishback JL, Hunt JS. Tumor necrosis factor alpha mRNA and protein are present in human placental and uterine cells at early and late stages of gestation. Am J Pathol 1991;139(2):327-35.

11. Guzel E, Basar M, Ocak N, Arici A, Kayisli UA. Bidirectional interaction between unfolded-protein-response key protein HSPA5 and estrogen signaling in human endometrium. Biol Reprod 2011;85:121–7.

12. Cetin I, Huppertz B, Burton G, Cuckle H, Gonen R, Lapaire O, et al. Pregenesys pre-eclampsia markers consensus meeting: What do we require from markers, risk assessment and model systems to tailor preventive strategies? Placenta 2011;32:S4–16.

13. Roberts JM, Gammill HS. Preeclampsia. Hypertension 2005;46:1243–9.

14. Uzun M, Gencer M, Turkon H, Oztopuz RO, Demir U, Ovali MA. Effects of melatonin on blood pressure, oxidative stress and placental expressions of TNFα, IL-6, VEGF and sFlt-1 in RUPP rat model of preeclampsia. Arch Med Res 2017;48:592–8.

15. Raghupathy R. Cytokines as key players in the pathophysiology of preeclampsia. Med Princ Pract 2013;22:8–19.

16. Weel IC, Baergen RN, Romão-Veiga M, Borges VT, Ribeiro VR, Witkin SS, et al. Association between placental lesions, cytokines and angiogenic factors in pregnant women with preeclampsia. PLoS One 2016;11:e0157584.

17. Qin ZH, Wang Y, Kikly KK, Sapp E, Kegel KB, Aronin N, et al. Procaspase-8 is predominantly localized in mitochondria and released into cytoplasm upon apoptotic stimulation. J Biol Chem 2001;276(11):8079-86.

18. Boldin MP, Goncharov TM, Goltsev V V., Wallach D. Involvement of MACH, a novel MORT1/FADD-interacting protease, in Fas/APO-1- and TNF receptor-induced cell death. Cell 1996;85:803–15.

19. Muzio M, Chinnaiyan AM, Kischkel FC, O'Rourke K, Shevchenko A, Ni J, et al. FLICE, a novel FADD-homologous ICE/CED-3-like protease, is recruited to the CD95 (Fas/APO-1) death-inducing signaling complex. Cell 1996;85:817–27.

20. Collins JA, Schandl CA, Young KK, Vesely J, Willingham MC. Major DNA fragmentation is a late event in apoptosis. J Histochem Cytochem 1997;45(7):923-34.

21. Albensi BC. What is nuclear factor kappa B (NF-κB) doing in and to the mitochondrion? Front Cell Dev Biol 2019;7.

22. Durand JK, Baldwin AS. Targeting IKK and NF-κB for therapy. Adv Protein Chem Struct Biol 2017, p. 77–115.

23. Kniss DA, Rovin B, Fertel RH, Zimmerman PD. Blockade NF-κB activation prohibits TNF-α-induced cyclooxygenase-2 gene expression in ED27 trophoblast-like cells. Placenta 2001;22(1):80-9.

24. Armistead B, Kadam L, Drewlo S, Kohan-Ghadr HR. The role of NFκB in healthy and preeclamptic placenta: Trophoblasts in the spotlight. Int J Mol Sci 2020;21(5):1775.

25. Ciuffetti G, Mercuri M, Ott C, Lombardini R, Paltriccia R, Lupattelli G, et al. Use of pentoxifylline as an inhibitor of free radical generation in peripheral vascular disease. Eur J Clin Pharmacol 1991;41:511–5.

26. Hendawy N. Pentoxifylline attenuates cytokine stress and Fas system in syngeneic liver proteins induced experimental autoimmune hepatitis. Biomed Pharmacother 2017;92:316–23.

27. Muchhala SK, Benzeroual KE. Pentoxifylline suppressed LPS-induced inflammatory and apoptotic signaling in neuronal cells. Adv Biosci Biotechnol 2012;03:731–9.

28. Chen YM, Tu CJ, Hung KY, Wu KD, Tsai TJ, Hsieh BS. Inhibition by pentoxifylline of TNF-α-stimulated fractalkine production in vascular smooth muscle cells: Evidence for mediation by NF-κB down-regulation. Br J Pharmacol 2003;138(5):950-8.

Exercise and Caloric Restriction Improves Liver Damage in Metabolic Syndrome Model

Nevin Genc-Kahraman[1] ⓘ **, Burcin Alev Tuzuner[2]** ⓘ **, Hazal Ipekci[3]** ⓘ **,
Unsal Veli Ustundag[3]** ⓘ **, Tugba Tunali-Akbay[3]** ⓘ **, Ebru Emekli-Alturfan[3]** ⓘ **,
Goksel Sener[4]** ⓘ **, Aysen Yarat[3]** ⓘ

[1]Bursa Public Health Laboratory, Medical Biochemistry, Bursa, Turkey
[2]Department of Basic Medical Sciences, Faculty of Dentistry, Istanbul Gelisim University, Istanbul, Turkey
[3]Department of Basic Medical Sciences, Faculty of Dentistry, Marmara University, Istanbul, Turkey
[4]Department of Pharmacology, Faculty of Pharmacy, Marmara University, Istanbul, Turkey

ORCID IDs of the authors: N.G.K. 0000-0003-2143-0088; B.A.T. 0000-0001-5122-4977; H.I. 0000-0003-1193-168X;
U.V.U. 0000-0003-0804-1475; T.T.A. 0000-0002-2091-9298; E.E.A. 0000-0003-2419-8587; G.S. 0000-0001-7444-6193; A.Y. 0000-0002-8258-6118

ABSTRACT

Objective: Detecting the level of antioxidant and tissue damage that can occur in liver tissue induced metabolic syndrome by a high fructose diet in rats and the changes after exercise and/or caloric restriction.

Materials and Methods: Sprague-Dawley male rats were divided into five groups: control (C), metabolic syndrome (M), metabolic syndrome with exercise (ME), metabolic syndrome with caloric restriction (MCR), and metabolic syndrome with exercise and caloric restriction (MECR). To induce metabolic syndrome, a 10% fructose solution was given to rats in drinking water for 3 months. Exercise and caloric restriction were applied to the related groups for 6 weeks after the induction of metabolic syndrome. Glucose in the blood, lipid peroxidation (LPO), sialic acid (SA), hexosamine, mucin, fucose, glutathione (GSH) levels, alkaline phosphatase (ALP), tissue factor (TF), superoxide dismutase (SOD), catalase (CAT), and glutathione-S-transferase (GST) activities were measured in rat liver homogenates.

Results: In the liver, LPO levels increased and TF activities decreased in the M group compared to the C group and increased in the MCR and MECR groups compared to M group. GSH levels, SOD, and CAT activities decreased in M compared to C group and increased more significantly in MECR group compared to M group. SA levels increased in MCR and MECR groups compared with M group. Fucose levels also increased in MECR compared with the all others.

Conclusion: Liver tissue damage that occurs after a fructose diet and decreased antioxidant levels was shown to improve best in combined exercise and caloric restriction treatment (MECR group).

Keywords: Metabolic syndrome, exercise, caloric restriction, antioxidant-oxidant parameters

INTRODUCTION

Metabolic syndrome is characterized by a group of risk factors including abdominal obesity and/or body mass index, dyslipidemia, elevated blood pressure, insulin resistance, and increased markers of proinflammatory proteins in plasma (1-3). In the European Union, the epidemics of overweight and obesity are associated with sedentary lifestyle and physical inactivity (4). The etiology of metabolic syndrome is unclear but is associated with a variety of factors such as a modern lifestyle, environmental and hereditary factors, insulin resistance, low-grade inflammation, and oxidative stress (4-6).

The liver is the major tissue of fructose metabolism occurrence. Therefore, most toxic effects are observed

there after a high-fructose diet. The liver is the initial affected tissue in Type II diabetes by oxidative stress due to metabolic disorder and hepatic insulin resistance (7, 8).

Exercise is an effective method to improve insulin sensitivity. Glucose transport is increased to insulin sensitive tissues through exercise (9). The result of weight loss in the diet was also made with the restriction; a fatal illness that will cause obesity can be seen to decrease 10-40%. Many studies have shown that obese individuals can extend their lives as a result of food restriction or caloric restriction (10-14). When rats only being allowed less than 40% of the average food intake was determined, the average and maximum lifespan increased by 25-40% (15).

The aim of this study is to examine the effects of exercise and/or caloric restriction on rat liver tissue in a metabolic syndrome model induced by a high fructose diet.

MATERIALS AND METHODS

Chemicals
All chemical reagents used in this study were of analytical grade and supplied from Merck, Sigma-Aldrich, and Fluka.

Animals
Male Sprague-Dawley rats were obtained from the Experimental Animal Research Center of Marmara University in Istanbul, Turkey. The animal facilities and protocol were approved by the Laboratory Animal Care and Use Committee of Marmara University in Turkey (101.2013.mar). Fifty-six Sprague-Dawley male rats were kept in cages in a room maintained at 25±1⁰C on a 12 h light/dark cycle and allowed free access to food and water throughout the study. Normal pellet type rat feed produced in Istanbul Çobançeşme Feed Industry Factories was used for feeding. It contained 24% protein, 7% cellulose, 8% crude ash, 2% HCl insoluble ash, 1- 2.8% calcium, 0.9% phosphorus, 0.5-0.7% sodium, and 1% sodium chloride. Drinking water containing 0.6% methionine and 1% lysine and standard rat feed were administered ad libitum. Provided metabolic energy was 2650 kcal/kg.

Experimental Design
Animals were randomly divided into five groups; control (C), metabolic syndrome (M), metabolic syndrome with exercise (ME), metabolic syndrome with caloric restriction (MCR), and metabolic syndrome with exercise and caloric restriction (MECR). To induce metabolic syndrome, 10% fructose solution was given to rats in drinking water for 3 months. Exercise (swimming for 30 min 3 times/week) and caloric restriction (40% restriction of daily food) were applied to the related groups for 6 weeks after the induction of metabolic syndrome (1). At the end of the 18 weeks, the rats were sacrificed. Blood samples and liver tissue were taken and examined.

Blood Glucose Analysis
At the beginning of the experiment (Day 0), in the 3rd month (Week 12), and end of the experiment (Week 18), blood samples were taken from the orbital veins of rats under light ether anesthesia, and blood glucose levels were measured by glucometer (Accu-Chek, F. Hoffman-La Roche Ltd, Basel, Switzerland).

Biochemical Analysis
Liver tissue homogenates at 10% (w/v) were prepared. Glutathione (GSH) (16), lipid peroxidation (LPO) (17), sialic acid (SA) (18), hexosamine (19), mucin (19) and fucose (20,21) levels, superoxide dismutase (SOD) (22), catalase (CAT) (23), glutathione-S-transferase (GST) (24), alkaline phosphatase (ALP) (25), and tissue factor (TF) (26) activity in supernatants were measured by spectrophotometric methods.

Statistics
Statistical analysis was performed using GraphPad Prism 5.0 (GraphPad Software, San Diego, California, USA). All data were expressed as means ± standard deviation. An ANOVA analysis of variance was used for comparison of multiple groups; a Tukey test was used for binary comparisons between groups. A p value <0.05 was regarded as significant.

RESULTS

The blood glucose values at the beginning of the experiment (Day 0) was found at similar levels in all groups. There was no statistically significant difference between them. In Week 12, the blood glucose levels of the M, ME, MCR, and MECR groups, which were given 10% fructose, increased significantly compared with those at the beginning of the experiment (Day 0). In Week 18, blood glucose levels in the ME, MCR and MECR groups decreased significantly compared with those of Week 12 (Figure 1).
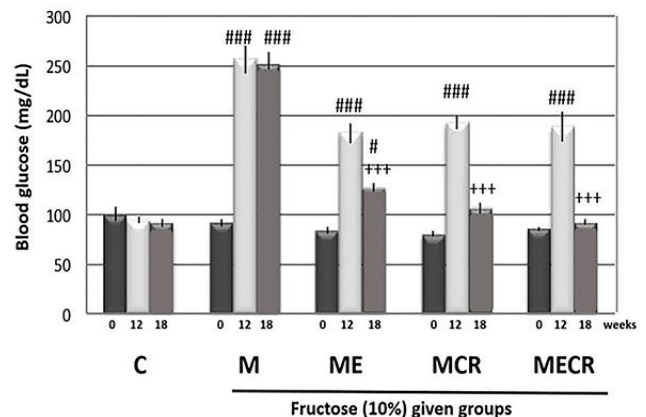
Figure 1. Blood glucose values.
Values were given as mean±SD. C: Control group, M: Metabolic Syndrome, ME: Metabolic syndrome with exercise, MCR: Metabolic syndrome with caloric restriction, MECR: Metabolic syndrome with exercise and caloric restriction. SD: Standard deviation. Dark gray bar: At day 0, White bar: At 12st week, Light gray bar: At 18th week. #p<0.05, ###p<0.001: significantly different from at day 0; +++p<0.001: significantly different from at 12st week.

In liver tissue, LPO levels increased and TF activities decreased in the M group compared with the C group. Other tissue damage parameters had no significant difference between the C group and the M group. LPO levels decreased in the ME, MCR, and MECR groups compared with the M group. TF activities decreased in the ME group compared with the C group; it increased in the MCR and MECR groups compared with the M and ME groups. Because the clotting time is inversely proportional to the TF activity, the prolonged clotting time is due to lower TF activity. SA levels increased in the MCR and MECR groups compared with the M group. Fucose levels also increased in the MECR group compared to the others (Figure 2).

In liver tissue, GSH levels decreased in the M group compared to the C group and increased in the ME, MCR, and MECR groups compared to the M group. SOD activities decreased in the M, ME, and MCR groups compared to the C group and increased in MECR compared to the M, ME, and MCR groups. CAT activities decreased in the M and ME groups compare to the C group and increased in the MCR and MECR groups compared to the M and ME groups. GST activities decreased in the MECR group compared to the C, M, and ME groups (Figure 3).
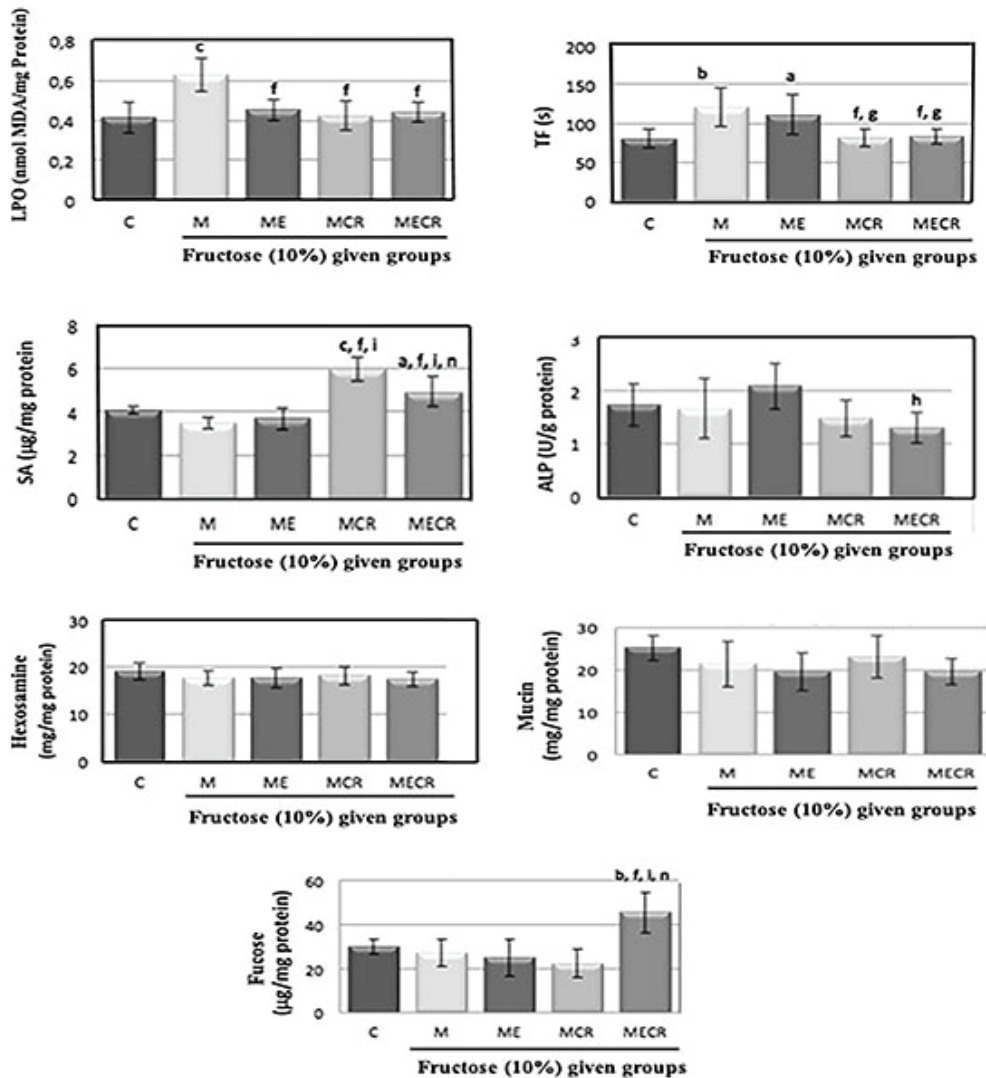
Figure 2. Liver tissue damage parameters.
Values were given as mean±SD. LPO: Lipidperoxidation, MDA: Malondialdehyde, TF: Tissue factor, SA: Sialic acid, ALP: Alkalen phosphatase, C: Control group, M: Metabolic Syndrome, ME: Metabolic syndrome with exercise, MCR: Metabolic syndrome with caloric restriction, MECR: Metabolic syndrome with exercise and caloric restriction. s: Second. SD: Standard deviation. [a]$p<0.05$, [b]$p<0.01$, [c]$p<0.001$ significantly different from group C; [d]$p<0.05$, [e]$p<0.01$, [f]$p<0.001$ significantly different from group M; [g]$p<0.05$, [h]$p<0.01$, [i]$p<0.001$ significantly different from group ME; [k]$p<0.05$, [m]$p<0.01$, [n]$p<0.001$ significantly different from group MECR.
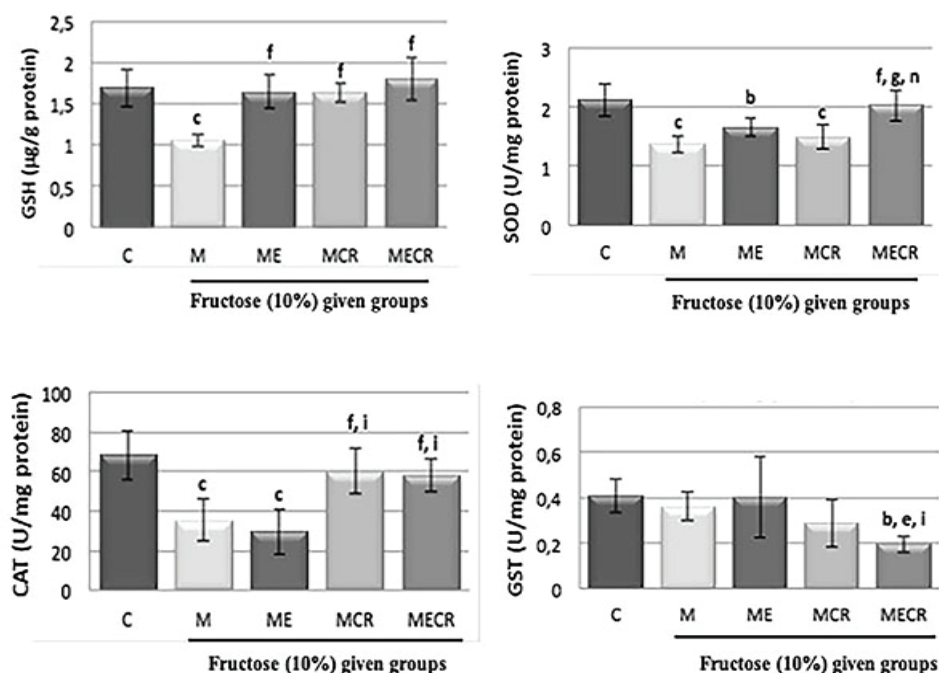
Figure 3. Liver antioxidant parameters.

Values were given as mean ± SD. GSH: Glutathione, SOD: Superoxide dismutase, CAT: Catalase, GST: Glutathione-S-transferase, C: Control group, M: Metabolic Syndrome, ME: Metabolic syndrome with exercise, MCR: Metabolic syndrome with caloric restriction, MECR: Metabolic syndrome with exercise and caloric restriction. SD: Standard deviation. [a]$p<0.05$, [b]$p<0.01$, [c]$p<0.001$ *significantly different from group C;* [d]$p<0.05$, [e]$p<0.01$, [f]$p<0.001$ *significantly different from group M;* [g]$p<0.05$, [h]$p<0.01$, [i]$p<0.001$ *significantly different from group ME;* [k]$p<0.05$, [m]$p<0.01$, [n]$p<0.001$ *significantly different from group MECR.*

DISCUSSION

Metabolic syndrome is an endocrinopathy characterized by insulin resistance, abdominal obesity, hyperinsulinemia, hypertension, and dyslipidemia (1). This disease emerges with a modern lifestyle, characterized with overeating and physical inactivity. Specifically, fructose rich diets are known to trigger other diseases with obesity (27).

Either a high fructose containing diet or drinking water is the most commonly used method to create a metabolic syndrome model with experimental animals (28-31). Fructose, depending on the dose and duration of use, is associated with a broad spectrum of pathologies such as glucose intolerance, insulin resistance, dyslipidemia, hypertension, and fatty liver, as well as indirectly clogging of heart and brain vessels (31, 32).

Recent studies have shown that being fed water containing 10% fructose for 6 or 8 weeks has led to an increase of triglyceride (TG), insulin, and glucose levels in plasma/serum (33-35). There was a study where a fructose diet caused an increase of a homeostatic model assessment (HOMA) value, endothelial dysfunction, and smooth muscle proliferation (36). It has also been shown that high fructose increased oxidative stress in the serum in rats (8, 29, 37,38). In agreement with these studies, we reported that after being fed 10% fructose for 18 weeks, Week 12 and 18 blood glucose values were found to be significantly

higher compared to the beginning of the experiment. The end of the experiment blood glucose of the rats in the MECR group decreased compared with Week 12 blood glucose.

Reactive oxygen species (ROS) cause oxidative stress and lead to oxidative damage in various tissues. This case leads to the depletion of the antioxidant system elements (SOD, CAT, vitamins C and E, reduced GSH), the development of cell injury induced by various inflammatory mediator molecules, organ dysfunction, and death. Kannappan et al. reported an increase in plasma glucose, insulin levels, and HOMA values as well as an increase in MDA, LPO, and PCO levels of livers and a decrease in GSH, SOD and vitamin E and C levels, CAT, GPx (glutathione peroxidase), glutathione reductase, and GST activity in rats fed with a diet containing 60% fructose for 2 months (8). In our study, in accordance with these studies, we found an increase in LPO levels and a decrease in GSH levels and CAT and SOD activity in the livers of rats given drinking water containing 10% fructose. We found no significant difference in GST activity.

There have been several studies that have examined the beneficial effects of exercise on human health (39-41). Energy production and consumption increase parallel to muscle activity. Oxygen consumption increases directly proportional to the intensity of exercise. Also, during exercise, production of ROS increases because of increased oxygen consumption. It has been pointed out that acute heavy exercise may cause tissue damage

and the rise of LPO, but regular physical activity can increase antioxidant capacity and can decrease LPO (40-42).

Alipour et al. have designed a running exercise for 8 weeks in a group of rats in which they had induced diabetes. They found increased values of LPO in the hippocampus zone of the rats for the diabetes and diabetes+exercise groups compared to the control group of rats. SOD, CAT, and GPx activities were detected to have decreased in the diabetic group and to have increased in the exercise group compared with the control. SOD and GPx activities increased significantly in the diabetes + exercise group compared with the diabetic group (43). In our study, the blood glucose levels of the exercise group of Week 18 decreased compared to those of Week 12. Although this decrease with exercise was significant, blood glucose levels remained significantly higher in the exercise group compared with the control group.

Lima et al. have designed a running exercise for 9 weeks in one group of rats, which they have created a model of diabetes. Increased TG levels in the livers of diabetic rats decreased in the diabetic rats that exercised. It was reported that SOD and CAT activities increased in the exercise group compared with the control and also in the diabetes+exercise group compared with the diabetic group (44). In our study, only increased significantly compared with the level of GSH in the ME group while the LPO levels were significantly decreased in the liver. Our study has shown that in liver tissue, the levels of GSH of the exercise group increased significantly and that the levels of LPO decreased significantly compared to the M group. There is no significant difference in the SOD, CAT, and GST activities. Moreover, SOD and CAT activities decreased compared to the control. Exercise was not enough to improve the activities of antioxidant enzymes in the livers of rats with metabolic syndrome. The exercise protocol may be heavy to rats with metabolic syndrome, and antioxidant enzymes in the liver may be caused by the loss of activity.

Caloric restriction is the reduction of food intake lower than the level of ad libitum, without becoming malnutrition. The generation of free radicals and oxidative damage is reduced by caloric restriction (45). Therefore, caloric restriction is a method used in research in order to prevent or delay the onset of diseases such as diabetes, cancer, and cardiovascular disease (46). Caloric restriction preserves β-cell function, prevents the onset of diabetes caused by the excessive production of free radicals, and provides treatment, all of which makes it clinically important (47). It is suggested that caloric restriction can improve the inflammatory state of the liver in mice with mild fibrotic livers and that of aged mice (48).

Mohammadi et al. reported that SOD and GPx activity increased significantly and LPO levels decreased in the livers of rats to which caloric restriction was applied (49). In this study we found an increase in GSH levels and CAT activities and a decrease in LPO levels of the MCR group compared with the M group in liver tissues. However, we found no difference in SOD and GST

activities. Caloric restriction and exercise applied separately is not enough to increase liver antioxidant enzyme levels of rats with metabolic syndrome.

TF is a transmembrane receptor and cellular initiator of coagulation extrinsic pathways (50). TF plays a main role in thrombosis and thrombogenesis (51). TF is known to have different activities in various tissues and bodily fluids and is affected by diet and systemic diseases (52-55). In the method of determination of TF activity, it should be noted that the clotting time is inversely proportional to the TF activity (52-55). Otherwise, it may cause a misunderstanding of the results. In the liver, the TF activity of the M and ME groups decreased compared with the C group. The TF activity increased in the MCR and MECR groups compared with the M and ME groups.

Another parameter studied in the liver tissue is ALP. There was no significant difference between the M and C group. ALP is one of the tests used as indicators of cholestasis rather than the destruction of liver cells (56). We found an increase in the livers of the ME group, but it was not significant. The reason for this could be a physiologic increase of ALP activity after exercise (57). ALP values decreased in the MECR group compared to the ME group. Exercise with caloric restriction seems to be the most effective way to reduce the level of ALP.

SA is a nine-carbon sugar derived from neuraminic acid, and it forms the terminal sugar component of glycoproteins and glycolipids. Sialidase activity increases as a result of oxidative stress, and it cleaves SA from end portions of glycoproteins and glycolipids and leads to the increase in free SA in body fluids (58). Serum SA levels were found to be increased in many other diseases associated with inflammation, such as Behcet's disease, central nervous system diseases, cardiovascular diseases, bacterial infections, and rheumatoid arthritis (59). The SA concentrations in the blood of patients with metabolic syndrome have been reported to be significantly higher (60). In this study, in liver tissue, there was no significant difference between the C and M groups in the levels of SA. Liver tissue SA values were detected to be significantly increased in the MCR and MECR groups compared with the M and ME groups.

Carbohydrates play a central role in the development of chronic diabetic complications. Glycoproteins, which are carbohydrate-linked protein macromolecules found on the cell surface, are one of the principal components of animal cells. Hexose, hexosamine, fucose, and sialic acid are the basic sugar components found in glycoproteins and glycosaminoglycans. Glycoprotein metabolism plays a major role in the pathogenesis of diabetes mellitus. Glycoproteins have multiple and complex functions and are found as hormones, enzymes, and blood group substances and as constituents of extracellular membranes (61, 62). They play an important role in functions such as cell differentiation and recognition, membrane transport, and the absorption of macromolecules (63). In a hyperglycemic state, high blood glucose levels accelerate the synthesis of basement membrane components, such as glycoproteins (64). In the liver,

we found no differences in hexosamine and mucin parameters, but fucose increased significantly in the MECR group compared with all other groups. Exercise plus caloric restriction did not reduce the fucose value, rather it increased even further.

CONCLUSION

Liver tissue damage that occurs after a fructose diet and decreased antioxidant levels were shown to be improved best in combined exercise and caloric restriction treatment (MECR group).

Peer-review: Externally peer-reviewed.

Conflict of Interest: The authors declare that they have no conflicts of interest to disclose.

Author Contributions: Conception/Design of study: A.Y., G.S.; Data Acquisition: N.G.K., B.A.T.,H.I., U.V.U.; Data Analysis/Interpretation: A.Y., G.S., T.T.A., E.E.A.; Drafting Manuscript: N.G.K., B.A.T., A.Y.; Critical Revision of Manuscript: A.Y., G.S., T.T.A., E.E.A.; Final Approval and Accountability: A.Y.

REFERENCES

1. Sener TE, Cevik O, Çetinel Ş, Şener G. Oxidative stress and urinary system damage in fructose-induced rat model of metabolic syndrome: Effect of calorie restriction and exercise. J Res Pharm 2020; 24 (3): 318-25.

2. Bouzas C, Bibiloni MDM, Garcia S, Mateos D, Martínez-González M.Á, Salas-Salvadó J, et al. Dietary quality changes according to the preceding maximum weight: A longitudinal analysis in the predimed-plus randomized trial. Nutrients 2020; 12(10): 3023.

3. Yilmaz Demirtas C, Bircan FS, Pasaoglu OT, Turkozkan N. The effects of resveratrol on hepatic oxidative stress in metabolic syndrome model induced by high fructose diet. Bratisl Lek Listy 2018; 119(1):36-40.

4. Martinez-Gonzalez MA, Martinez JA, Hu FB, Gibney MJ, Kearney J. Physical inactivity, sedentary lifestyle and obesity in the European Union. Int J Obes Relat Metab Disord 1999; 23: 1192-201.

5. Balton VH, Korita I, Bulo A. How is metabolic syndrome related to dyslipidemia? Biochem Med 2008; 18: 14-24.

6. Panickar KS. Beneficial effects of herbs, spices and medicinal plants on the metabolic syndrome, brain and cognitive function. Cent Nerv Syst Agents Med Chem 2013; 13: 13-29.

7. Basciano H, Federico L, Adeli K. Fructose, insulin resistance and metabolic dyslipidemia. Nutr Metab 2005; 2(1): 5.

8. Kannappan S, Palanisamy N, Anuradha CV. Suppression of hepatic oxidative events and regulation of eNOS expression in the liver by naringenin in fructose-administered rats. Eur J Pharmacol 2010; 645: 177-84.

9. Caponi PW, Lehnen AM, Pinto GH, Borges J, Markoski M, Machado UF, et al. Aerobic exercise training inducesmetabolic benefits in rats with metabolic syndrome independent of dietary changes. Clinics 2013; 68(7): 1010-7.

10. Williamson DF, Pamuk E, Thun M, Flanders D, Byers T, Heath C. Prospective study of intentional weight loss and mortality in never-smoking overweight US white women aged 40–64 years. Am J Epidemiol 1995; 141(12): 1128-41.

11. Williamson DF, Thompson JT, Thun M, Flanders D, Pamuk E, Byers E. Intentional weight loss and mortality among overweight individuals with diabetes. Diabetes Care 2000; 23(10): 1499-504.

12. Kurosaka Y, Machida S, Shiroya Y, Yamauchi H, & Minato K. Protective effects of voluntary exercise on hepatic fat accumulation induced by dietary restriction in Zucker fatty rats. Int J Mol Sci 2021; 22(4): 2014.

13. Pereira RM, Botezelli JD, da Cruz Rodrigues KC, Mekary RA, Cintra DE, Pauli JR, et al. Fructose consumption in the development of obesity and the effects of different protocols of physical exercise on the hepatic metabolism. Nutrients 2017; 9(4): 405.

14. Pósa A, Szabó R, Kupai K, Csonka A, Szalai Z, Veszelka M, et al. Exercise training and calorie restriction influence the metabolic parameters in ovariectomized female rats. Oxid Med Cell Longev 2015; 787063.

15. Weindruch R, Walford RL. The Retardation of Aging and Disease by Dietary Restriction. Springfield, Illinois: Charles C. Thomas, Publisher; 1988.

16. Beutler E. Glutathione. In: Red blood cell metabolism: A Manual of Biochemical Methods. 2nd ed. New York: Grune and Stratton; 1975, 112-4.

17. Ledwozyw A, Michalak J, Stepien A, Kadziolka A. The relationship between plasma triglycerides, cholesterol, total lipids and lipid peroxidation products during human atherosclerosis. Clin Chim Acta 1986; 155(3): 275-83.

18. Warren L. The thiobarbituric acid assay of sialic acids. J Biol Chem 1959; 234: 1971-5.

19. Winzler RJ. Determination of serum glycoproteins. Glick D, editors. Methods of Biochemical Analysis. New York: Interscience Publishers Inc. 1955; 2: 279-311.

20. Dische Z, Shettles LB. A specific color reaction of methylpentoses and a spectrophotometric micromethod for their determination. J Biol Chem 1948; 175; 595-603.

21. Shakeerabanu M, Sjahta K, Praveen R.C, Manimaran A. The defensive effect of quercetinon indomethacin induced gastric damage in rats. Adv Biol Res 2011; 5(1): 64-70.

22. Mylorie AA, Collins H, Umbles C, Kyle J. Erythrocyte superoxide dismutase activity and other parameters of copper status in rats ingesting lead acetate. Toxicol Appl Pharmacol 1986; 82(3): 512-20.

23. Aebi H. Catalase in vitro. Methods Enzymol 1984; 105:121-6.

24. Habig WH, Jacoby WB. Assays for differentiation of glutathione S-transferases. Methods in Enzymol 1981; 77: 398-405.

25. Walter K, Schült C. Acid and alkaline phosphatase in serum: two-point method. In: Methods of Enzymatic Analysis. 2nd ed. Bergmeyer HU, editors. Verlag Chemie: Academic Press, Inc. New York and London 1974; 2: 856-86.

26. Ingram GIC, Hills M. Reference method for the one-stage prothrombin time test on human blood. Thromb Haemost 1976; 36(1): 237-8.

27. Dalle-Donne I, Aldini G, Carini M, Colombo R, Rossi R, Milzani A. Protein carbonylation, cellular dysfunction and disease progression. J Cell Mol Med 2006; 10(2): 389-406.

28. Rutledge AC, Adele K. Fructose and the metabolic syndrome: Pathophysiology and molecular mechanisms. Nutr Rev 2007; 65: 13-23.

29. Abdullah MM, Riediger NN, Chen Q, Zhao Z, Azordegan N, Xu Z, et al. Effects of long-term consumption of a high fructose diet on conventional cardiovascular risk factors in Sprague-Dawley rats. Mol Cell Biochem 2009; 327(1-2): 247-56.

30. Paśko P, Bartoń H, Zagrodzki P, Gorinstein S. Effect of amaranth seeds (Amaranthus cruentus) in the diet on some biochemical parameters and essential trace elements in blood of high fructose-fed rats. Nat Prod Res 2011; 25: 844-9.

31. Babacanoğlu C, Yıldırım N, Sadi G, Pektas MB, Akar F. Resveratrol prevents high-fructose corn syrup-induced vascular insulin resistance and dysfunction in rats. Food Chem Toxicol 2013; 60: 160-7.

32. Masterjohn C, Park Y, Lee J, Noh SK, Koo SI, Bruno RS. Dietary Fructose Feeding Increases Adipose Methylglyoxal Accumulation in Rats in Association with Low Expression and Activity of Glyoxalase-2. Nutrients 2013; 5: 3311-28.

33. Zhao CX, Xu X, Cui Y, Wang P, Wei X, Yang S, et al. Increased endothelial nitric-oxide synthase expression reduces hypertension and hyperinsulinemia in fructose-treated rats. J Pharmacol Exp Ther 2009; 328(2): 610-20.

34. Giani JF, Mayer MA, Munoz MC, Silberman EA, Hocht C, Taira CA, et al. Chronic infusion of angiotensin-(1-7) improves insulin resistance and hypertension induced by a high-fructose diet in rats. Am J Physiol Endocrinol Metab 2009; 296(2): 262-71.

35. Wang DD, Sievenpiper JL, De Souza RJ, Cozma AI, Chiavaroli L, Ha V, et al. Effect of fructose on postprandial triglycerides: a systematic review and meta-analysis of controlled feeding trials. Atherosclerosis 2014; 232(1): 125-33.

36. Steinberg HO, Chaker H, Leaming R, Johnson A, Brechtel G, Baron AD. Obesity/insulin resistance is associated with endothelial dysfunction. Implications for the syndrome of insulin resistance. J Clin Invest 1996; 97(11): 2601-10.

37. Delbosc S, Paizanis E, Magous R, Araiz C, Dimo T, Cristol JP, et al. Involvement of oxidative stress and NADPH oxidase activation in the development of cardiovascular complications in a model of insulin resistance, the fructose-fed rat. Atherosclerosis 2005; 179(1): 43-9.

38. Singh I, Singh PK, Bhansali S, Shafiq N, Malhotra S, Pandhi P, et al. Effects of three different doses of a fruit extract of Terminalia chebula on metabolic components of metabolic syndrome, in a rat model. Phytother Res 2010; 24:107-12.

39. Castro-Barquero S, Ruiz-León AM, Sierra-Pérez M, Estruch R, Casas, R. Dietary strategies for metabolic syndrome: a comprehensive review. Nutrients 2020; 12(10): 2983.

40. Venditti P, Gomez-Cabrera MC, Zhang Y, Radak, Z. Oxidant antioxidants and adaptive responses to exercise. Oxid Med Cell Longev 2015; 290190.

41. Vincent HK, Powers SK, Demirel HA, Coombes JS, Naito H. Exercise training protects against contraction-induced lipid peroxidation in the diaphragm. Eur J Appl Physiol 1999; 79: 268-73.

42. Duarte J, Pérez-Palencia R, Vargas F, Ocete MA, Pérez-Vizcaino F, Zarzuelo A, Tamargo J. Antihypertensive effects of the flavonoid quercetin in spontaneously hypertensive rats. Br J Pharmacol 2001; 133:117-24.

43. Alipour M, Salehi I, Soufi FG. Effect of exercise on diabetes-induced oxidative stress in the rat hippocampus. Iran Red Crescent Med J 2012; 14(4): 222-8.

44. Lima TI, Monteiro IC, Valença S, Leal-Cardoso JH, Fortunato RS, Carvalho DP, Teodoro BG, Ceccatto VM. Effect of exercise training on liver antioxidant enzymes in STZ-diabetic rats. Life Sci 2015; 128: 64-71.

45. Hagopian K. Krebs cycle enzymes from livers of old mice are differantially regulated by caloric restriction. Physiol and Behavior 2005; 85: 581-92.

46. Speakman JR, Mitchell SE. Caloric restriction. Mol Aspects Med 2011; 32(3): 159-221.

47. He XY, Zhao XL, Gu Q, Shen JP, Hu Y, Hu RM. Calorie restriction from a young age preserves the functions of pancreatic β cells in aging rats. Tohoku J Exp Med 2012; 227(4): 245-52.

48. Horrillo D, Gallardo N, Lauzurica N, Barrus MT, San Frutos MG, Andres A, et al. Development of liver fibrosis during aging: effects of caloric restriction. J Biol Regul Homeost Agents 2013; 27(2): 377-88.

49. Mohammadi M, Ghaznavi R, Keyhanmanesh R, Sadeghipour HR, Naderi R, Mohammadi H. Caloric restriction prevents lead-induced oxidative stress and inflammation in rat liver. Scientific World J 2014; 20: 821524.

50. Mackman N. Tissue-specific hemostasis in mice. Arterioscler Thromb Vasc Biol 2005; 25: 2273-81.

51. Nemerson Y. Tissue factor: then and now. Thromb Haemost 1995; 74(1): 180-4.

52. Emekli-Alturfan E, Basar I, Malali E, Elemek E, Oktay S, Ayan F, et al. Plasma tissue factor and tissue factor activities of periodontitis patients with cardiovascular diseases. Pathophysiol Haemost Thromb 2010; 37: 77-81.

53. Yarat A, Tunali T, Pisiriciler R, Akyuz S, Ipbuker A, Emekli N. Salivary thromboplastic activity in diabetics and healthy controls. Clin Oral Investig 2004; 8: 36-9.

54. Aktop S, Emekli-Alturfan E, Ozer C, Gonul O, Garip H, Yarat A, et al. Effects of ankaferd blood stopper and celox on the tissue factor activities of warfarin-treated rats. Clin Appl Thromb Hemost 2014; 20: 16-21.

55. Emekli-Alturfan E, Kasikci E and Yarat A. Tissue factor activities of streptozotocin induced diabetic rat tissues and the effect of peanut consumption. Diabetes Metab Res Rev 2007; 23: 653-8.

56. Mehmetoğlu İ. Klinik Biyokimya El Kitabı. Konya: Nobel Tıp Kitabevleri; 2013. s. 155-6.

57. Koçyiğit Y, Aksak MC, Atamer Y, Aktaş A. Futbolcu ve basketbolcularda akut egzersiz ve C vitamininin karaciğer enzimleri ve plazma lipid düzeylerine etkisi. J Clin Exp Invest 2011; 2 (1): 62-8.

58. Emekli N, Yarat A, Akbay TT, Koç LÖ, Alturfan EI. Tükürük Biyokimyası. İçinde: Tükürük Histolojisi, Fizyolojisi, Mikrobiyolojisi ve Biyokimyası. Emekli N, Yarat A, editors. İstanbul: Nobel Tip Kitapevleri Ltd. Şti; 2008. pp.328-31.

59. Ünübol Aypak S, Uysal H. Glikoproteinlerin Yapısı ve Fonksiyonları. FÜ Sağ Bil Vet Derg 2010; 24 (2):107-14.

60. Crook MA, Tutt P, Pickup JC. Elevated serum sialic acid concentration in NIDDM and its relationship to blood pressure and retinopathy. Diabetes Care 1993; 16 (1): 57-60.

61. Porter-Turner MM, Sidmore JC, Khokher MA, Singh BM, Rea CA. Relationship between erythrocyte GLUT1 function and membrane glycation in type 2 diabetes. Br J Biomed Sci 2011; 68(4): 203-7.

62. Sacan O, Ertik O, Ipci Y, Kabasaka L, Sener G, Yanardag R. Protective effect of chard extract on glycoprotein compounds and enzyme activities in streptozotocin-induced hyperglycemic rat lungs. Bulg Chem Commun 2018; 50(1):119-23.

63. Mittal N, Kaur J, Mahmood A. Changes in tubular membrane glycosylation in diabetic, insulin and thyroxin treated rat kidneys. Indian J Exp Biol 1996; 34(8):782-5.

64. Spiro RG, SpiroMJ, Effect of diabetes on the biosynthesis of the renal glomerular basement membrane. Studies on the glucosyltransferase. Diabetes 1971; 20(10):641-8.

Acyclovir-Induced Nephrotoxicity: The Protective Benefit of Curcumin

Elias Adikwu[1] , James Kemelayefa[1]

[1]Niger Delta University, Faculty of Pharmacy, Department of Pharmacology and Toxicology, Bayelsa State, Nigeria

ORCID IDs of the authors: E.A. 0000-0003-4349-8227; J.K. 0000-0003-2713-9945

ABSTRACT

Objective: Nephrotoxicity may decrease the clinical use of acyclovir (ACV). Curcumin (CUM) is used traditionally as treatments for some diseases. This study examined the protective effect of CUM against ACV-induced nephrotoxicity in rats.

Materials and Methods: Forty-five male Wistar rats (240–250g) randomized into nine groups (n=5) were used. Group 1(Placebo control) received water (0.2mL/day) intraperitoneally (i.p) whereas group 2 (Solvent control) received corn oil (0.2mL/day) per oral (p.o) for 7 days. Groups 3-5 received CUM (25, 50 and 100 mg/kg/day p.o) for 7 days. Group 6 received ACV (150 mg/kg/day i.p) for 7 days. Groups 7-9 were pre-treated with CUM (25, 50 and 100 mg/kg/day p.o) before the treatment with ACV (150 mg/kg/day i.p) for 7 days. On day 8, the rats were anesthetized; blood samples were collected and evaluated for serum biochemical indices. The kidneys were weighed and assessed for histology and oxidative stress indices.

Results: ACV produced no significant (p>0.05) effects on the body and kidney weights of rats when compared to control. ACV caused significant (p<0.001) elevations in serum creatinine, urea, uric acid and kidney malondialdehyde levels when compared to control. ACV significantly (p<0.001) decreased kidney glutathione, catalase, glutathione peroxidase, superoxide dismutase, serum total protein, albumin, potassium, chloride, sodium and bicarbonate levels when compared to control. Tubular necrosis and hypercellular glomerulus with mesangial proliferation occurred in the ACV-treated rats. ACV-induced nephrotoxicity was abrogated in a dose-related fashion by CUM 25mg/kg (p<0.05), 50mg/kg (p<0.01) and 100mg/kg (p<0.001) when compared to ACV.

Conclusion: CUM may clinically prevent ACV-induced nephrotoxicity.

Keywords: Acyclovir, Curcumin, Kidney, Toxicity, Protection, Rat

INTRODUCTION

The kidney regulates body homeostasis through its excretory functions and important metabolic activities in the tubular epithelial cells. It is involved in the syntheses of hormones, and the degradation of low-molecular-weight proteins and peptides (1). The kidney is a major route of drug excretion, which predisposes it to nephrotoxicity. Drug-induced nephrotoxicity is an important cause of acute and chronic renal failure (2). Drugs have been responsible for 19%–25% of acute renal failure in patients admitted in hospitals (3, 4).

Acyclovir (ACV), an antiviral drug, is used for the treatment of varicella-zoster and herpes simplex virus infections (5, 6). It is well tolerated, but can cause nephrotoxicity, which often leads to acute renal failure (7, 8). Epidemiology showed it may cause nephrotoxicity in 12% to 48% of patients (6, 9). The nephrotoxic effect of ACV is primarily characterized by elevated plasma urea and creatinine levels and abnormal urine sediments (10, 11). It can also be characterized by degenerative alterations in tubular epithelial cells such as tubular necrosis (10, 11). The mechanisms by which ACV causes nephrotoxicity have been speculated to involve direct assault on renal tubular cells and oxidative stress (11, 12).

Curcumin (CUM) (1,7-bis(4-hydroxy-3-methoxyphenyl)-1,6-heptadiene-3,5-dione) also known as diferuloylmethane is a natural yellow orange dye derived from the rhizome of *Curcuma longa Linn.,* belonging to Zingiberaceae family (13, 14). CUM is a polyphenol, which has been shown to target multiple signaling molecules. It has activity at the cellular level with multiple health benefits (15). It is locally used as treatments for inflammation, metabolic syndrome, microbial infections, pain, and degenerative eye conditions (16-18). Potential effect of CUM as an antidote against toxicities, such as hepatotoxicity (19) nephrotoxicity (19) and cardiotoxicity (20) in animal models has been documented. Scientific information showed no study on the protective effect of CUM against animal models of ACV-induced nephrotoxicity, thus this study examined its protective effect against a rat model of ACV-induced nephrotoxicity.

MATERIALS AND METHODS

The guideline for the use of animals in experiments promulgated by the European Parliament and the Council was used for this study. Forty-five adult male Wistar rats were purchased from the animal breeding facility of the Department of Pharmacology/Toxicology, Faculty of Pharmacy, Niger Delta University, Bayelsa State, Nigeria. The rats were randomized into 9 groups of n=5 and allowed to acclimatize for 2 weeks prior to the experiment under 12/12-hour light and dark cycles with *ad libitum* access to diet and water. The study was approved by the Research Ethics Committee (NDU/PHARM/AEC/046) of the Department of Pharmacology/Toxicology, Faculty of Pharmacy, Niger Delta University, Bayelsa State Nigeria.

Animal Treatment
Group I (Placebo control) was treated with water (0.2mL) intraperitoneally (i.p) daily for 7 days. Group 2 (Solvent control) was treated with corn oil (0.2mL) per oral (p.o) daily for 7 days. Groups 3-5 were treated with CUM (25, 50 and 100 mg/kg/p.o) in corn oil (21) daily for 7 days. Group 6 was treated with ACV (150 mg/kg/i.p) (22) daily for 7 days. Groups 7-9 were supplemented with CUM (25, 50 and 100 mg/kg/p.o) prior to the treatment with ACV (150 mg/kg/i.p) for 7 days. Peperine (20mg/kg) was added to CUM to improve bioavailability (21).

Animal Sacrifice and Collection of Samples
On day 8, the rats were anesthetized in a diethyl ether chamber and blood samples were collected through cardiac puncture and allowed to clot. The clots were centrifuged (1500 rmp for 20 min) and serum samples were extracted. The serum samples were used for biochemical investigations. The kidneys were collected through dissection, rinsed in physiological saline and homogenized in buffered (pH 7.4) 0.1 M Tris-HCl solution. The homogenates were centrifuged (2000 rmp for 20 min), and the supernatants were decanted and used for oxidative stress markers investigations.

Assessment of Serum Biochemical Markers
Serum total protein, albumin, creatinine, uric acid, urea, sodium, potassium, chloride and bicarbonate concentrations were measured using laboratory test kits according manufacturer's specification.

Assessment of Kidney Oxidative Stress Markers
Malondialdehyde (MDA) was measured according to the method reported by Buege and Aust, 1978 (23). Catalase (CAT) was measured as described by Aebi, 1984 (24). Superoxide dismutase (SOD) was analyzed as described by Sun and Zigman, 1978 (25). Glutathione (GSH) was determined using the method described by Sedlak and Lindsay, 1968 (26). Glutathione peroxidase (GPx) was determined as reported by Rotruck*et al.* 1973 (27).

Statistical Analysis
Values are expressed as mean ± SEM, n=5. Values were analyzed using one-way analysis of variance (ANOVA) followed by Dunnett's multiple comparison tests. Graph Pad prism 5 (San Diego, CA) soft ware was used for computation. A probability value less than 0.05. 0.01, 0.001 was considered significant.

RESULTS

Effect of Curcumin on Body and Kidney Weights of Acyclovir-Treated Rats
The rats treated with CUM showed (p>0.05) no difference in body and kidney weights when compared to control. Also, body and kidney weights were not different in the ACV-treated rats (p>0.05) when compared to control (Table 1).

Table 1. Effects of curcumin on body and kidney weights of acyclovir-treated rats.

Group	Final body weight (g)*	Absolute kidney weight (g)*	Relative kidney weight (%)*
Control (Placebo)	240.8±13.5	0.65±0.07	0.27±0.06
Control(Solvent)	245.0±15.9	0.67±0.01	0.28±0.01
CUM 25 mg/kg	250.1±16.0	0.60±0.03	0.24±0.01
CUM 50 mg/kg	245.7±14.1	0.66±0.01	0.27±0.07
CUM 100 mg/kg	257.3±16.4	0.61±0.04	0.24±0.05
ACV 150 mg/kg	240.8±17.2	0.67±0.06	0.29±0.01
CUM 25 mg/kg+ACV	245.4±14.0	0.63±0.07	0.26±0.03
CUM 50 mg/kg+ACV	244.7±18.2	0.60±0.08	0.25±0.06
CUM 100mg/kg+ACV	245.0±16.6	0.59±0.05	0.24±0.02

*Values are shown as mean±SEM; n=5; CUM: Curcumin; ACV: Acyclovir; SEM: Standard error of mean.

Effect of Curcumin on Serum Biochemical Markers of Acyclovir-Treated Rats

Treatment with CUM did not produce significant (p>0.05) effects on serum total protein, albumin, uric acid, creatinine and urea levels in comparison to control. In contrast, serum uric acid, creatinine and urea levels were significantly (p<0.001) increased whereas total protein and albumin levels were significantly (p<0.001) decreased in the ACV-treated rats when compared to control (Table 2). However, CUM (25, 50 and 100 mg/kg) supplementation significantly decreased serum uric acid, creatinine and urea levels, but significantly increased serum albumin and total protein levels in a dose-related fashion at p<0.05, p<0.01 and p<0.001, respectively when compared to ACV (Table 2).

Effect of Curcumin on Serum Electrolytes of Acyclovir-Treated Rats

Treatment with CUM had no significant (p>0.05) effects on serum electrolytes in comparison to control. However, significant decreases in serum electrolytes were observed in the ACV-treated rats when compared to control (Table 3). Interestingly, CUM (25, 50 and 100 mg/kg) supplementation significantly increased serum electrolytes at p<0.05, p<0.01 and p<0.01, respectively when compared to ACV (Table 3).

Effect of Curcumin on Kidney Oxidative Stress Markers of Acyclovir-Treated Rats

Treatment with CUM did not produce significant (p>0.05) effects on kidney MDA and antioxidant (GPx, SOD, GSH, and CAT)

Table 2. Effect of curcumin on serum biochemical markers of acyclovir-treated rats.

Group	Urea (mg/dL)*	Creatinine (mg/dL)*	Uric Acid (mg/dL)*	Total Protein (g/dL)*	Albumin (g/dL)*
Control (Placebo)	14.84±1.32	0.67±0.45	1.41±0.06	4.00±0.52	3.09±0.22
Control (Solvent)	14.06±1.00	0.69±0.11	1.53±0.09	4.11±0.62	3.13±0.70
CUM 25 mg/kg	14.62±1.54	0.65±0.08	1.39±0.07	4.02±0.78	3.11±0.45
CUM 50 mg/kg	14.76±1.00	0.66±0.06	1.37±0.01	4.04±0.61	3.14±0.64
CUM 100 mg/kg	14.48±1.24	0.63±0.01	1.35±0.16	4.07±0.17	3.16±0.73
ACV 150 mg/kg	38.91±4.51 [a]	2.59±0.44 [a]	4.30±0.75 [a]	1.30±0.61 [a]	1.01±0.07 [a]
CUM 25 mg/kg+ACV	29.64±3.21 [b]	2.00±0.36 [b]	3.10±0.67 [b]	2.10±0.56 [b]	1.40±0.09 [b]
CUM 50 mg/kg+ACV	21.34±2.78 [c]	1.32±0.10 [c]	2.37±0.91 [c]	2.87±0.69 [c]	2.01±0.27 [c]
CUM 100mg/kg+ACV	16.16±1.48 [d]	0.80±0.06 [d]	1.63±0.55 [d]	3.88±0.75 [d]	2.87±0.86 [d]

*Values are shown as mean±SEM. n=5; CUM: Curcumin; ACV: Acyclovir; SEM: Standard error of mean. [a]p<0.001 when compared to control. [b]p<0.05 when compared to ACV, [c]p<0.01 when compared to ACV, [d] p<0.001 when compared to ACV.

Table 3. Effect of curcumin on serum electrolytes of acyclovir-treated rats.

Group	Potassium (mmo/L)*	Chloride (mmo/L)*	Sodium (mmo/L)*	Bicarbonate (mmo/L)*
Control (Placebo)	3.63±0.19	112.93±13.8	147.83±14.3	10.65±1.66
Control (Solvent)	3.71±0.23	117.02±10.1	149.27±16.7	10.91±1.91
CUM 25 mg/kg	3.62±0.04	111.60±13.0	146.24±16.0	10.26±1.46
CUM 50 mg/kg	3.60±0.30	110.05±10.4	149.05±13.8	11.03±2.49
CUM 100 mg/kg	3.58±0.06	109.84±15.2	145.91±17.1	10.31±1.01
ACV 150 mg/kg	2.40±0.17 [a]	58.73±5.33 [a]	78.50±5.64 [a]	4.10±0.27 [a]
CUM 25 mg/kg+ACV	3.10±0.06 [b]	79.92 ±4.17 [b]	99.14±7.16 [b]	6.00±0.07 [b]
CUM 50 mg/kg+ACV	3.51±0.43 [c]	99.26 ±8.33 [c]	139.87 ±9.66 [c]	8.70±1.01 [c]
CUM 100mg/kg+ACV	3.60±0.36 [c]	100.03±11.5 [c]	140.03±12.1 [c]	10.24±1.12 [c]

*Values are shown as mean±SEM. n=5; CUM: Curcumin; ACV: Acyclovir; SEM: Standard error of mean. [a]p<0.01 when compared to control. [b]p<0.05 when compared to ACV, [c]p<0.01.

Table 4. Effect of curcumin on kidney oxidative stress and antioxidant markers of acyclovir-treated rats.

Group	MDA (mmol/mg protein)*	GSH (μmole/mg protein)*	CAT (U/mg protein)*	SOD (U/mg protein)*	GPx (U/mg protein)*
Control (Placebo)	0.17±0.08	20.01±2.47	29.76±4.67	25.46±3.54	25.07±4.71
Control (Solvent)	0.18±0.01	20.53±1.67	29.93±3.88	26.03±2.37	25.35±3.35
CUM 25 mg/kg	0.16±0.05	20.47±2.55	30.07±4.21	25.61±3.75	25.16±3.03
CUM 50 mg/kg	0.16±0.01	20.70±3.86	30.25±3.72	25.72±3.32	25.36±4.22
CUM 100 mg/kg	0.15±0.08	21.04±2.73	30.44±4.21	25.91±3.68	25.52±3.51
ACV 150 mg/kg	3.12±0.16[a]	5.51±0.45[a]	8.11±1.27[a]	7.32±0.11[a]	8.065±0.93[a]
CUM 25 mg/kg+ACV	2.59±0.23[b]	8.84±0.86[b]	12.76±0.43[b]	11.74±3.17[b]	12.14±1.43[b]
CUM 50 mg/kg+ACV	2.00±0.44[c]	12.93±2.55[c]	18.35±1.07[c]	17.40±3.00[c]	17.56±2.25[c]
CUM 100mg/kg+ACV	0.23±0.09[d]	18.45±2.42[d]	26.27±3.24[d]	23.75±3.63[d]	22.15±2.11[d]

*Values are shown as mean±SEM. n=5; SEM: Standard error of mean; CUM: Curcumin; ACV: Acyclovir; MDA: Malondialdehyde; GSH: Glutathione; CAT: Catalase; SOD: Superoxide dismutase; GPx: Glutathione peroxidase; [a]p<0.001 when compared to control. [b]p<0.05 when compared to ACV, [c]p<0.01 when compared to ACV, [d]p<0.001 when compared to ACV.

levels when compared to control. On the other hand, treatment with ACV significantly (p<0.001) increased kidney MDA level, but significantly (p<0.001) decreased kidney antioxidant levels when compared to control (Table 4). However, significant increases in kidney antioxidants with significant decreases in kidney MDA levels were observed in CUM (25, 50 and 100 mg/kg) supplemented rats in a dose-related fashion at p<0.05, p<0.01 and p<0.001, respectively when compared to ACV (Table 4).

Effect of Curcumin on Kidney Histology of Acyclovir-Treated Rats

The kidney of the control rat showed normal glomerulus and renal tubule (Figure 1A), but the kidney of ACV-treated rat showed hypercellular glomerulus with mesangial proliferation and tubular necrosis (Figure 1B). The kidney of CUM (25 mg/kg and 50 mg/kg) supplemented rats showed hypercellular glomeruli with mesangial proliferation and normal renal tubules (Figures 1C and D) respectively. However, the kidney of CUM (100 mg/kg) supplemented rat showed normal glomerulus and renal tubule (Figure 1E).

DISCUSSION

ACV-induced nephrotoxicity is a serious adverse effect, which can affect treatment outcomes (28). Studies have reported various forms of nephrotoxicity caused by ACV including crystal nephropathy, acute interstitial nephritis, acute tubular necrosis and obstructive nephropathy (12, 29). Therapeutic outcomes and patients well-being can be significantly improved by curtailing the nephrotoxic menace of ACV. CUM has shown therapeutic activities against some animal models of diseases (30). This study assessed the protective effect of CUM on ACV-induced nephrotoxicity in rats. The current study supplemented the rats with CUM prior to the induction of nephrotoxicity with ACV. All

evaluated renal markers were normal in the CUM-treated rats. On the other hand, ACV had a negative impact on the kidneys of the treated rats by elevating serum creatinine, urea, and uric acid levels. Similarly, Lu et al. (31) reported elevated levels of the aforementioned renal biochemical markers in ACV-treated mice. The kidney accounts for about 60%–90% of ACV elimination. ACV is relatively insoluble in urine; it is filtered by glomeruli and secreted by renal tubules (32). Therefore, ACV crystals can be deposited in renal tubules leading to the obstruction of nephron causing increased resistance to renal blood flow and the elevation of serum creatinine, urea, and uric acid levels (31, 32). ACV might have also reduced glomerular filtration rate (GFR) through the induction of renal oxidative stress leading to increased serum creatinine, urea, and uric acid levels. Oxidative stress can induce vasoactive mediators, which can cause renal vasoconstriction or decreased glomerular filtration capacity (33). However, CUM supplementation restored serum creatinine, urea, and uric acid levels in a dose-related fashion. Similarly, Haung et al. (34) reported restored serum renal markers in cyclosporine-induced renal dysfunction in rats supplemented with CUM. In the current study, CUM might have restored the aforementioned renal markers by inhibiting ACV-induced renal obstruction, and oxidative stress, thereby increasing GFR.

The ACV-treated rats showed decreases in serum electrolytes (sodium, potassium, chloride and bicarbonate), total protein and albumin levels. Some studies have also documented electrolytes and protein abnormalities associated with ACV-administration (35). The observation in the current study can be ascribed to ACV-induced increased urinary excretion of the aforementioned parameters. However, serum electrolytes, total protein and albumin levels were stabilized by CUM supplementation in a dose-related fashion. In accordance with this finding,
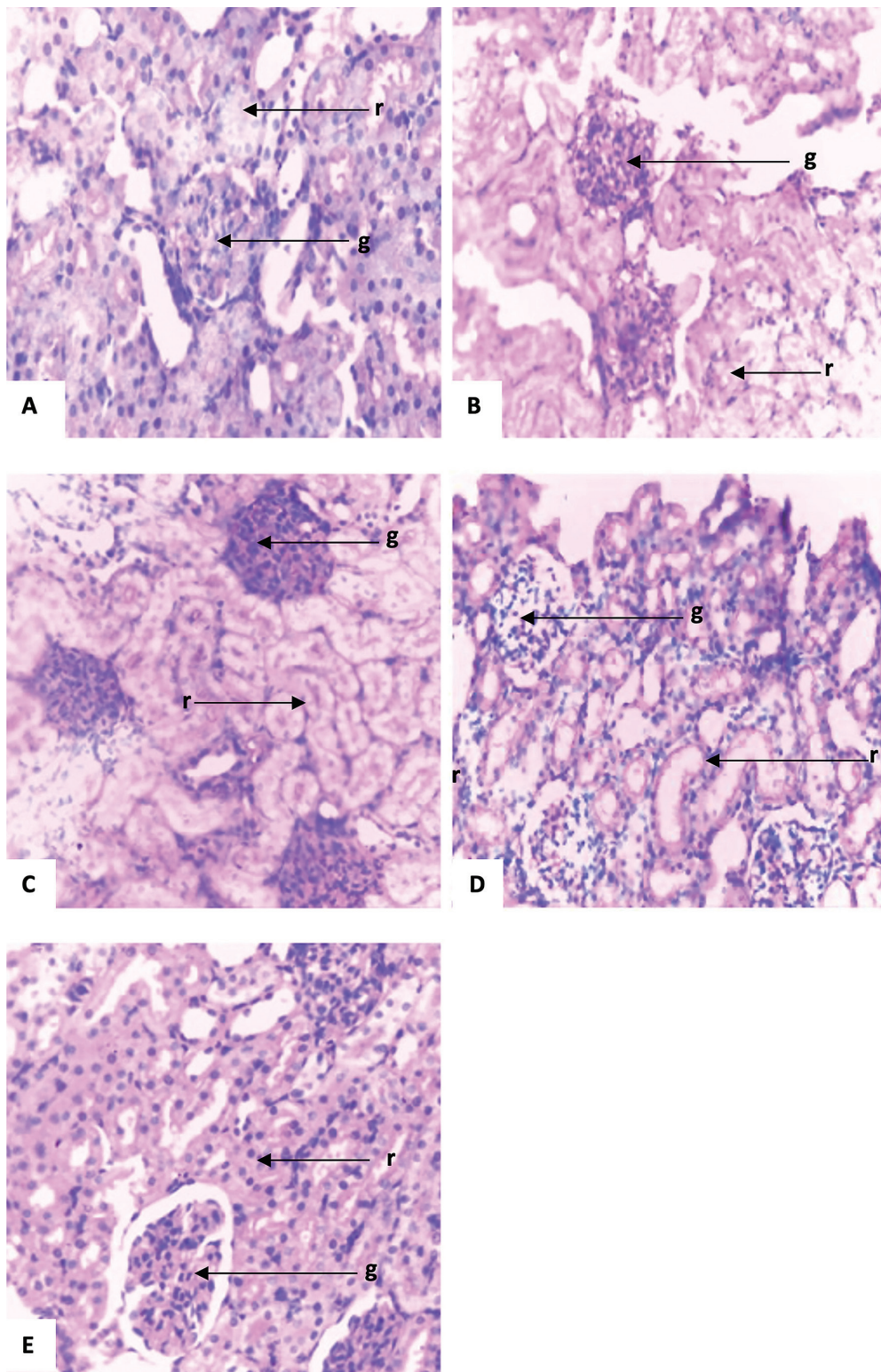
Figure 1. Kidney histology of control (A), ACV-treated (B), ACV+CUM (25 mg/kg)-treated (C), ACV+CUM (50 mg/kg)-treated (D) and ACV+CUM (100 mg/kg)-treated (E) rats. Control rats showed normal glomerulus and renal tubule (A), while ACV-treated rats were characterized by hypercellular glomerulus with mesangial proliferation and tubular necrosis (B). CUM (25 and 50 mg/kg) administrations to ACV-treated rats resulted in hypercellular glomerulus with mesangial proliferation and normal renal tubule (C and D). CUM (100mg/kg) supplementations led to normal glomerulus and renal tubule structure in ACV-treated rats. g: glomerulus; r: renal tubule. Hematoxylin-Eosin, x 400.

some scholars reported that CUM supplementation improved serum electrolytes and protein levels in a rat model of adriamycin-induced renal dysfunction (36). In the current study, CUM might have stabilized serum electrolytes, total protein and albumin levels by decreasing renal wastage.

ACV also had a negative impact on kidney redox status by decreasing kidney antioxidants (SOD, CAT, GSH and GPx) and increasing MDA concentrations. ACV might have decreased kidney antioxidant concentrations via the induction of oxidative stress as a consequence of ROS generation. The generated ROS might have depleted kidney antioxidants and caused the oxidation of renal lipids (polyunsaturated fatty acid), thereby increasing MDA level (34). Lu et al. (31) also suggested that oxidative damage may be an essential index for ACV-induced renal dysfunction. In the current study, antioxidants were increased whereas MDA levels were decreased in a dose-related fashion in CUM supplemented rats. This finding may be due to the inhibitory impact of CUM on ACV-induced renal oxidative stress by scavenging ROS. This might have increased kidney antioxidant activity, thus facilitating ROS incapacitation by antioxidants and decreased kidney MDA levels.

More so, the alteration in kidney morphology of ACV-treated rats was characterized by hypercellular glomerulus with mesangial proliferation and tubular necrosis. The observations in ACV-treated rats have been previously documented (37, 22). The observed changes in the kidney morphology of ACV-treated rats may be a consequence of oxidative stress-induced kidney biomolecular damage (38). Oxidative stress causes lipid peroxidation (LPO). LPO is a process by which free radicals attack lipids especially polyunsaturated fatty acids causing alterations in the physical properties of cellular membranes leading to covalent modifications of proteins and nucleic acids stimulating cytotoxicity, cell necrosis and apoptosis (39). In this study, kidney morphology was restored by CUM supplementation. This observation correlates with Tirkey et al. (40) who reported the ability of CUM to restore kidney morphology in cyclosporine-induced renal dysfunction in rats. Palipoch, et al. (41) also reported improved kidney histology caused by CUM supplementation against cisplatin-induced nephrotoxicity in rats. In the present study, the restored kidney morphology caused by CUM supplementation might be due to the inhibition of ACV-induced kidney oxidative stress, thus arresting kidney LPO and preventing structural and functional damage of kidney biomolecules. CUM might have offered renal protection as a chain-breaking antioxidant, which scavenges and eliminates free radicals such as singlet oxygen, hydroxyl radical, superoxide radicals and peroxyl radicals, which are inducers of oxidative stress (42-44). The inhibitory action of CUM on hydroxyl radical and peroxyl radicals might have prevented kidney proteins and nucleic acids modifications, which might have occurred due to LPO. CUM might have prevented ACV-induced kidney oxidative stress by inhibiting free radical-generating enzymes. Studies have associated CUM with inhibitory action on free radical-generating enzymes such as lipoxygenase/cyclooxygenase and xanthine hydrogenase/ox-

idase (45, 46). CUM might have also offered renal protection by inhibiting ACV-induced renal inflammation. Studies showed that CUM can reduce inflammation by inhibiting the activities of pro-inflammatory mediators including leukotrienes and cytokines (47).

CONCLUSION

Based on the findings in the current study, CUM supplementation abrogates ACV-induced nephrotoxicity in a dose-related fashion. It may have clinical application for ACV-associated nephrotoxicity.

REFERENCES

1. Klahr S. Nonexcretory Functions of the Kidney. In: Klahr S. (eds) The Kidney and Body Fluids in Health and Disease. Springer, Boston, MA,1983.

2. Arunvikram K, Mohanty I, Sardar KK, Palai S, Sahoo G, Patra RC. Adverse drug reaction and toxicity caused by commonly used antimicrobials in canine practice. Vet World 2014; 7(5): 299-5.

3. Mehta RL, Pascual MT, Soroko S, Savage BR, Himmelfarb J, Ikizler TA, et al. Spectrum of acute renal failure in the intensive care unit: The PICARD experience. Kidney Int 2004; 66: 1613-21.

4. Uchino S, Kellum JA, Bellomo R, Doig GS, Morimatsu H, Morgera S, et al. Acute renal failure in critically ill patients: A multinational, multicenter study. JAMA 2005; 294: 813-8.

5. Bryson YJ, Dillon M, Lovett M, Acuna G, Taylor S, Cherry JD, et al. Treatment of first episodes of genital herpes simplex virus infection with oral acyclovir. A randomized double-blind controlled trial in normal subjects. N Engl J Med 1983; 308(16): 916-21.

6. Keeney RE, Kirk LE, Bridgen D. Acyclovir tolerance in humans. Am J Med 1982; 73: 176-81.

7. Chou JW, Yong C, Wootton SH. Case 2: Rash, fever and headache first, do no harm. Paediatr Child Heal 2008; 13: 49-2.

8. Genc G, Ozkaya O, Acikgoz Y, Yapici O, Bek K, GulnarSensoy S, et al. Acute renal failure with acyclovir treatment in a child with leukemia. Drug ChemToxicol 2010; 33: 217-19.

9. Bean B, Aeppli D. Adverse effects of high-dose intravenous acyclovir in ambulatory patients with acute herpes zoster. J Infect Dis 1985; 151: 362-5.

10. Ahmad T, Simmonds M, McIver AG, McGraw ME. Reversible renal failure in renal transplant patients receiving oral acyclovir prophylaxis. PediatrNephrol 1994; 8: 489-91.

Eur J Biol 2021; 80(1): 22-28

Adikwu and Kemelayefa. Curcumin Prevents Acyclovir-Induced Nephrotoxicity in Rats

11. Vomiero G, Carpenter B, Robb I, Filler G. Combination of ceftriaxone and acyclovir an underestimated nephrotoxic potential? Pediatr Nephrol 2002; 17: 633-7.

12. Lu H, Han Y-J, Xu J-D, Xing W-M, Chen J. Proteomic Characterization of Acyclovir-Induced Nephrotoxicity in a Mouse Model. PLoS One 2014; 9(7): 1-6.

13. Aggarwal BB, Kumar A, Bharti AC. Anticancer potential of curcumin: Preclinical and clinical studies. Anticancer Res 2003; 23: 363-98.

14. Gounder DK, Lingmallu J. Comparison of chemical composition and antioxidant potential of volatile oil from fresh dried and cured turmeric (Curcuma longa) rhizomes. Ind Crops and Prod 2012; 38: 124-31.

15. Gupta SC, Patchva S, Aggarwal BB. Therapeutic roles of curcumin: Lessons learned from clinical trials. AAPS J 2013; 15: 195-218.

16. Hewlings SJ, Kalman DS. Curcumin: A review of its' effects on human health. Foods 2017; 6(92): 1-11.

17. Aggarwal BB, Harikumar KB. Potential therapeutic effects of curcumin, the anti-inflammatory agent, against neurodegenerative, cardiovascular, pulmonary, metabolic, autoimmune and neoplastic diseases. Int J Biochem Cell Biol 2009; 41: 40-59.

18. El Shemy MA. Protective effects of curcumin against Augmentin-induced hepatotoxicity in rats. Benha Vet MedJ 2018; 35: 375-86.

19. He L, Peng X, Zhu J, Liu G, Chen X, Tang C, et al. Protective effects of curcumin on acute gentamicininduced nephrotoxicity in rats. Can J PhysiolPharmacol 2015; 93(4): 275-82.

20. Miriyala S, Panchatcharam M, Rengarajulu P. Cardioprotective effects of curcumin. AdvExpMed Biol 2007; 595: 359-77.

21. Chakraborty M, Bhattacharjee A, Kamath JV. Cardioprotective effect of curcumin and piperine combination against cyclophosphamide-induced cardiotoxicity. Indian J Pharmacol 2017; 49(1): 65-70.

22. Campos SB, Seguro AC, Cesar KR, Rocha AS. Effects of acyclovir on renal function. Nephron 1992; 62: 74-9.

23. Buege JA, Aust SD. Microsomal lipid peroxidation. Meth Enzymol 1978; 52: 302-10.

24. Aebi H Catalase *in vitro*. In Method in Enzymology, Colowick SP and Kaplane NO, Eds., New York, NY, USA: Academic Press, 1984.

25. Sun M, Zigman S. An improved spectrophotometer assay of superoxide dismutase based on epinephrine, antioxidation. Anal Biochem 1978; 90: 81-9.

26. Sedlak J, Lindsay RH. Estimation of total, protein-bound and non-protein sulfhydryl groups in tissue with Ellman's reagent. Anal Biochem 1968; 25: 192-205.

27. Rotruck JT, Rope AL, Ganther HF, Swason AB. Selenium: biochemical role as a component of glutathione peroxidase. Sci 1973; 179: 588-90.

28. Izzedine H, Launay-Vacher V, Deray G. Antiviral drug-induced nephrotoxicity. Am J Kidney Dis 2005; 45: 804-17.

29. Tucker WE Jr, Macklin AW, Szot RJ, Johnston RE, Elion GB, de Miranda P, et al. Preclinical toxicology studies with acyclovir: Acute and subchronic tests. Fund ApplToxicol 1983; 3: 573-8.

30. Agrawal S, Goel RK. Curcumin and its protective and therapeutic uses. Natl J Physiol PharmPharmacol 2016; 6: 1-8.

31. Lu H, Han YJ, Xu JD, Xing WM, Chen J. Proteomic characterization of acyclovir-induced nephrotoxicity in a mouse model. PLoS One 2014; 9 (7): 1-9.

32. Perazella MA, Crystal-induced acute renal failure. Am J Med 1999; 106(4): 459-65.

33. Damiano S, Andretta E, Longobardi C, Prisco F, Paciello O, Squillacioti C, et al. Effects of curcumin on the renal toxicity induced by ochratoxin a in rats. Antioxid 2020; 9(332): 1-13.

34. Huang J, Yao X, Weng G, Qi H and Ye X. Protective effect of curcumin against cyclosporine A-induced rat nephrotoxicity. Mol Med Rep 2018; 17: 6038-44.

35. Chávez-Iñiguez JS, Medina-Gonzalez R, Aguilar-Parra, L. Torres-Vázquez EJ, Maggiani-Aguilera P, Cervantes-Pérez E *et al.* Oral acyclovir induced hypokalemia and acute tubular necrosis a case report. BMC Nephrol 2018; 19(324): 1-5.

36. Venkatesan N, Punithavathi D, Arumugam V. Curcumin prevents Adriamycin nephrotoxicity in rats. Br J Pharmacol 2000;129: 231-4.

37. Whitley RJ, Middlebrooks M, Gnann JW, Jr. Acyclovir: The past ten years. Adv Exp Med Biol 1990; 278: 243-53.

38. Dennis JM, Witting PK. Protective role for antioxidants in acute kidney disease. Nutr 2017; 9(7): 718.

39. Gaschler MM, Stockwell BR. Lipid peroxidation in cell death. BiochemBiophys Res Commun 2017; 15(482): 419-25.

40. Tirkey N, Kaur G, Vij G, Chopra K. Curcumin, a diferuloylmethane, attenuates cyclosporine-induced renal dysfunction and oxidative stress in rat kidneys. BMC Pharmacol 2005; 5(15): 1-10.

41. Palipoch S, Punsawad C, Chinnapun D, Suwannalert P. Amelioration of cisplatin-induced nephrotoxicity in rats by curcumin and α-tocopherol. Trop J Pharm Res 2013; 12: 973-9.

42. Yadav VR, Suresh S, Devi K, Yadav S. Effect of cyclodextrin complexation of curcumin on its solubility and antiangiogenic and anti-inflammatory activity in rat colitis model APPS Pharm Sci Tech 2009; 10: 752-62.

43. Maheshwari RK, Singh AK. Multiple biological activities of curcumin: a short review LifeSci 2006; 78: 2081-7.

44. Priyadarsini KI, Maity DK, Naik, GH, Kumar MS, Unnikrishnan MK, Satav JG, et al. Role of phenolic O-H and methylene hydrogen on the free radical reactions and antioxidant activity of curcumin. Free RadicBiol Med 2003; 35: 475-84.

45. Lin YG, Kunnumakkara AB, Nair A, Merritt WM, Han LY, Armaiz-Pena GN, et al. Curcumin inhibits tumor growth and angiogenesis in ovarian carcinoma by targeting the nuclear factor-κB pathway. Clin Cancer Res 2007; 13: 3423-30.

46. Marchiani A, Rozzo C, Fadda A, Delogu G, Ruzza P. Curcumin and curcumin-like molecules: From spice to drugs. Curr Med Chem 2014; 21: 204-22.

47. Kohli K, Ali J, Ansari MJ, Raheman Z. Curcumin: A natural anti-inflammatory agent. Indian J Pharmacol 2005; 37: 141-7.

ISTANBUL UNIVERSITY PRESS
ISTANBUL UNIVERSITY 1453

The Effect of Cell-Free Supernatants of Free-Living Amoeba against Some *Staphylococcus* Bacteria: First Findings from Turkey

Sevval Maral Ozcan[1,2] iD **, Zuhal Zeybek**[3] iD

[1]Istanbul University, Institute of Science, Istanbul, Turkey
[2]Biruni University, Faculty of Pharmacy, Department of Pharmacy, Pharmaceutical Microbiology Division, Istanbul, Turkey
[3]Istanbul University, Faculty of Science, Department of Biology, Fundamental and Industrial Microbiology Division, Istanbul, Turkey

ORCID IDs of the authors: S.M.O. 0000-0002-3336-5618; Z.Z. 0000-0002-9407-9519

ABSTRACT

Objective: Free-living amoeba (FLA) are protozoa living in soil and in natural and man-made water systems. They attract much attention owing to the illnesses associated with them and to their relationships with bacteria. In this study, the effect of cell-free supernatant (CFS) obtained from FLA against *Staphylococcus* was investigated.

Materials and Methods: Environmental FLA strains (A1, A2, A3) were obtained from lake water and swimming pools in Istanbul. *Acanthamoeba castellanii* ATCC 50373 was used as the standard strain. Clinical *Staphylococcus* strains (S1, S2, S3) were obtained from a culture collection at Istanbul University, Faculty of Pharmacy, Department of Pharmaceutical Microbiology. As standard strains, MRSA ATCC 43300, *S. epidermidis* ATCC 12228, *S. aureus* ATCC 29213 were used. FLA-CFS were obtained by centrifuging and filtering of axenic cultures. Colony counting technique was used to investigate the inhibition activities of FLA-CFS against *Staphylococcus* bacteria.

Results: Against MRSA ATCC 43300 strain, CFSs of *A. castellanii* ATCCC 50373 and A1 showed an inhibition efficiency of 78.36% and 73.47%, respectively. Against S1 strain, CFSs of *A. castellanii* ATCCC 50373 and A2 showed an inhibition of 65.64% and 15.14%, respectively. Against *S. aureus* ATCC 29213, only A1-CFS showed inhibitory effect (44%). It was found that *A. castellanii* ATCC 50373 and A2-CFSs inhibited the S2 strain 26.20% and 9.24% respectively. Against S3 strain, A2-CFS was inhibitory at 33.33%. No FLA-CFS could be inhibitory against *S. epidermidis* ATCC 12228.

Conclusion: It is necessary to devise new studies in which sample numbers are increased when using FLA strains in the inhibition of antibiotic-resistant bacteria.

Keywords: Free-living amoeba, *Staphylococcus* infections, *Acanthamoeba*, antibacterial effect, cell-free supernatant, antibiotic resistance

INTRODUCTION

Free-living amoeba (FLA) are eukaryotic microorganisms living in soil, air, sea water, fresh water and man-made water systems (pools, cooling towers, water pipes, etc.) (1-8). They have two stages in their lifecycle, namely trophozoite and cyst (9). Trophozoites are metabolically active, feeding, mobile forms which transform into cysts. The latter are inactive metabolically and

exist in adverse environmental conditions (starvation, temperature changes, pH changes, etc.) (10). Pathogenic FLA for humans are *Naegleria fowleri, Acanthamoeba spp., Balumuthia mandrillaris,* and *Sappinia spp* (5, 11). Along with their pathogenicities, FLA also attracted scientists' attention due to their interactions with other microorganisms in the environments in which they live. In this collective living, they play important roles in the

regulation of microorganism population and microbial ecology (12, 13): *i*) They use some bacteria, fungi, and algae as food (10, 14, 15). *ii*) Some bacteria which can enter inside FLA find themselves isolated from adverse environmental conditions (antibiotics, disinfectants, etc.) and they find the opportunity to multiply (16-19). After this, they can cause lysis of FLA cells (20). *iii*) They can inhibit some bacteria which does not enter inside FLA cells (non-fagocyting). Very scarce studies in recent years show these abilities (21-24).

Recently, increasing antibiotic resistance has become an important problem in the treatment of bacterial infections. Every year, about 2.9 million infections owing to the presence of antibiotic-resistant bacteria occur and about 36 thousand of them end in death (25). From past to present, antibacterial substances have been isolated from organisms like bacteria, fungi, algae, insects, and plants (26-29).

As is the case all around the world, new antibacterial compounds are also sought after in our country because antibiotic-resistant bacteria cause important problems in the treatment of these infections. However, the number of studies showing the antibacterial effect of FLA is quite limited in the literature (22, 23). So, in this context, this research aims to look for the antibacterial effect of cell-free supernatant (CFS) of FLA strains isolated in Turkish waters against infection-agent *Staphylococcus* bacteria.

MATERIALS AND METHODS

Test Microorganisms
In this study, the antibacterial activity of CFS obtained from four FLA (*Acanthamoeba castellanii* ATCC 50373, A1, A2, A3) was investigated against six *Staphylococcus* strains [Methicillin-resistant *Staphylococcus aureus* ATCC 43300 (MRSA ATCC 43300), *Staphylococcus aureus* ATCC 29213 (*S. aureus* ATCC 29213), *Staphylococcus epidermidis* ATCC 12228 (S. *epidermidis* ATCC 12228), Methicillin-resistant *Staphylococcus aureus* S1 (S1), Methicillin-sensitive *Staphylococcus aureus* S2 (S2), Methicillin-resistant *Staphylococcus epidermidis* S3 (S3)] (Table 1). Among the FLA strains used in this study, two of them (A1 and A2) were isolated from swimming pools in a previous study of ours (8), one of them (A3) was isolated from lake water, and *A. castellanii* ATCC 50373 was used as standard strain. Clinical *Staphylococcus* strains (S1, S2, S3) used in our study were obtained from the culture collection at Istanbul University (I.U.) Faculty of Pharmacy, Department of Pharmaceutical Microbiology. MRSA ATCC 43300, *S. aureus* ATCC 29213 and *S. epidermidis* ATCC 12228 were used as the standard strains.

Bacterial Cultures
MRSA ATCC 43300, *S. aureus* ATCC 29213, *S. epidermidis* ATCC 12228, S1, S2 and S3 strains were cultured in Trypticase soy agar (TSA) at 37°C for 24 hours and used in the experiment.

FLA Cultures
FLA strains (A1, A2) previously isolated and kept in the freezing medium (FM) at -86°C were first brought to room temperature. Petri dishes containing non-nutrient agar (NNA) spread on *Escherichia coli (E. coli)* pre-inactivated (121°C, 15 minutes) were used for the resuscitation of the strains. All Petri dishes were incubated for 3 to 4 weeks at 30°C and they were examined under inverted microscope every day (30, 31). Dense FLA trophozoite-bearing areas in NNA were marked and cut with a sterile lancet, and patched on fresh NNA medium surface (with inactivated *E. coli*) upside-down (2, 32, 33). All Petri dishes were incubated at 30°C.

Table 1. Microorganisms used in antibacterial activity experiments.

Microorganisms (Code)		Source
FLA Strains	*Acanthamoeba castellanii* ATCC 50373	Standard Strain
	A1	Swimming pool isolate
	A2	Swimming pool isolate
	A3	Lake water isolate
***Staphylococcus* Strains**	[a]MRSA ATCC 43300	Standard Strain
	[b]*S. aureus* ATCC 29213	Standard Strain
	[c]*S. epidermidis* ATCC 12228	Standard Strain
	[d]S1	Clinical isolate
	[e]S2	Clinical isolate
	[f]S3	Clinical isolate

a: Methicillin-resistant *Staphylococcus aureus* ATCC 43300, b: Methicillin-sensitive *Staphylococcus aureus* ATCC 29213,
c: Methicillin-sensitive *Staphylococcus epidermidis* ATCC 12228, d: Methicillin-resistant *Staphylococcus aureus,*
e: Methicillin-sensitive *Staphylococcus aureus,* f: Methicillin-resistant *Staphylococcus epidermidis*

First, A3-coded amoeba strain was isolated from Uluabat Lake (Bursa, Turkey) under aseptic conditions, and the water sample in a glass bottle was concentrated by passing through a Sartorius filtering device having a membrane filter (0.22 μm). Then, the filter paper was turned upside down and left on fresh NNA medium having inactivated *E. coli* and incubated at 30°C (4, 34). Petri dishes were examined on an inverted microscope on a daily basis.

FLA-Axenic Culture and FLA-CFS

To obtain FLA-axenic cultures, Pepton Yeast Extract Glucose medium (PYG) containing Page's amoeba saline (PAS) solution (PYG-PAS) was used (11, 35). Antibiotics (0.5 mg/mL penicillin and streptomycin) were added to PYG-PAS to avoid microbial contamination. Amoeba cells in the Petri dishes were collected with 2-3 mL of PAS solution and inoculated into T-25 tissue culture flask containing antibiotic-added PYG-PAS and incubated at 30°C (22, 36). When the mono-layered axenic culture was observed, the PYG-PAS containing antibiotics in the tissue culture flask was discharged and washed with fresh PAS three times, in order to clean the culture from antibiotics (17). After the last washing, fresh PYG-PAS was placed into the flask and incubated for 48-72 hours at 30°C. The FLA-axenic culture thus obtained was subjected to Thoma slide and trypan blue for counting (cell/mL) and vitality determination (37, 38). Cell-free supernatant of FLA (FLA-CFS) was obtained after centrifuging the FLA-axenic cultures (1000 g x 5 min) followed by passing the supernatant through 0.22 μm pore-diameter filters and were used in antibacterial experiments (22, 23).

Antibacterial Activity Experiments

Colony counting method was used to assess the antibacterial effect of FLA-CFSs against *Staphylococcus* bacterial strains (22, 23). Bacterial suspension (10^6 cfu/mL) in phosphate buffered saline (PBS) and FLA-CFS were mixed in a tube (1:10) and incubated for 18-24 hours at 37°C. After incubation, each mixture was diluted further with PBS 10 times to achieve a series of dilutions (10^{-1}–10^{-6}) and spread into Petri dishes containing TSA. All petri dishes were incubated for 24 hours at 37°C and after the period, colonies were counted. In the experiments, PYG-PAS and PBS were used as control groups. All experiments were performed in triplicate.

RESULTS

FLA-Axenic Culture and FLA- CFS

Figure 1 shows the images obtained under inverted microscopic examination (x100) of FLA-axenic cultures.

Each FLA-axenic culture had the following living FLA trophozoite numbers: For *A. castellanii* ATCC 50373, A1, A2, A3, the values are $3x10^5$, $8x10^5$, $5x10^5$, $1x10^5$ cell/mL, respectively. Trypan blue-dyed FLA-axenic cultures had the microscopic view (x100) of undyed/living FLA trophozoites in Figure 2.

Antibacterial Activity

The tested FLA-CFSs showed the highest inhibition effect on the MRSA ATCC 43300 strain among the *Staphylococcus* spe-
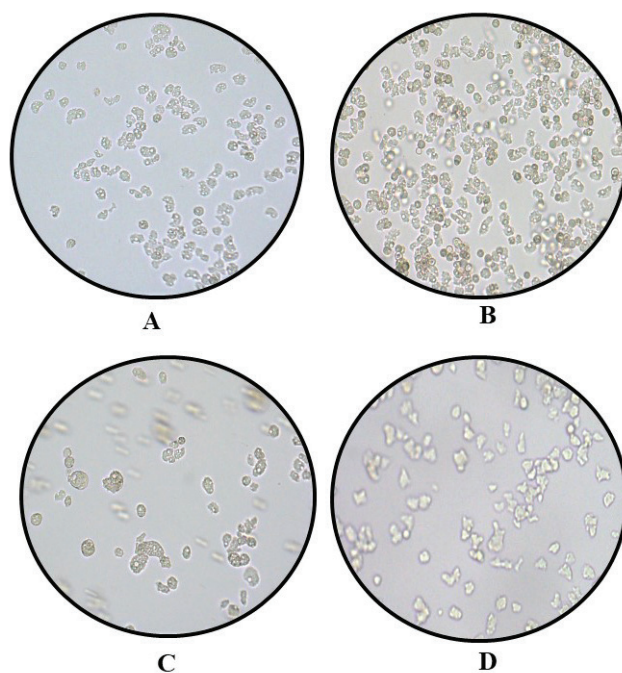
Figure 1. Microscopic images of axenic cultures obtained from each FLA (x100): A) *Acanthamoeba castellanii* ATCC 50373, B) A1, C) A2, D) A3.
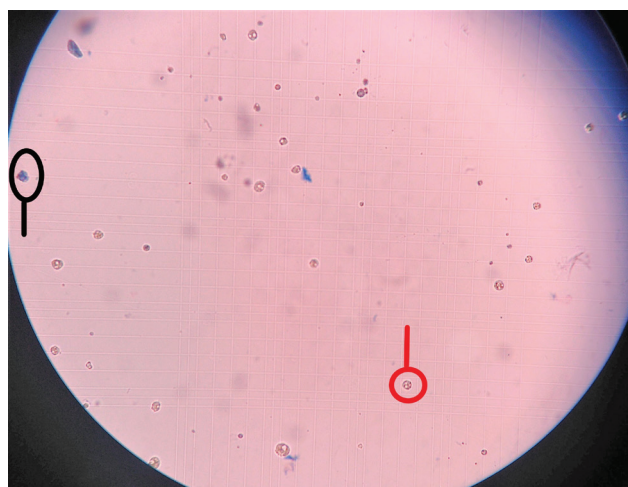
Figure 2. Light microscopic view (x100) of axenic culture of *Acanthamoeba castellanii* ATCC 50373 strain on the trypan blue-dyed Thoma slide; live trophozoite (red labelled) and dead trophozoite (black labelled).

cies tested (Figure 3). *A. castellanii* ATCCC 50373 coded FLA (*A. castellanii* ATCCC 50373-CFS) and A1 encoded FLA-CFS (A1-CFS) inhibited MRSA ATCC 43300 bacteria by 78.36% and 73.47%, respectively. *A. castellanii* ATCCC 50373 and A2-encoded FLA-CFS (A2-CFS) inhibited the S1 strain 65.64% and 15.14%, respectively. Against *S. aureus* ATCC 29213, only A1-CFS showed inhibitory effect (44%). It was found that *A. castellanii* ATCC 50373-CFS and

A2-CFS inhibited the S2 strain 26.20% and 9.24% respectively. Although A2-CFS inhibited S3 strain (33.33%), other FLA-CFSs did not show antibacterial effect against this strain. None of the tested FLA-CFSs were found to have an inhibitory effect on *S. epidermidis* ATCC 12228 strain. A3-CFS was found to have no inhibitory effect on any *Staphylococcus* strain tested. However, it was determined that *Staphylococcus* strains tested were inhibited by at least one native FLA-CFS (A1-CFS or A2-CFS), except for *S. epidermidis* ATCC 12228 strain (Figure 3).

Figure 3. Inhibitory effects of cell-free supernatants (CFSs) against *Staphylococcus* strains.

According to these data, it was understood that FLA-CFS had more inhibitory effect against *S. aureus* than *S. epidermidis* generally. *S. epidermidis* ATCC 12228 strain was not found to be inhibited by any FLA-CFS.

DISCUSSION

FLA have been attracting the attention of scientists for many years due to their role of regulating microorganism populations while living together with bacteria in the same environment. In the literature, FLA-bacteria relationship has frequently centered on the abilities of amoeba phagocyting bacteria, proliferation of bacteria in amoeba and therefore, causing lysis of them (16-19, 39, 40). However, there are few studies with narrow scope about amoeba inhibiting the proliferation of bacteria by secreting antibacterial substances (apart from phagocytosis) (21-24, 41, 42). Increasing the number of studies on this topic would help researchers to understand the FLA-bacteria relationship and would enhance microbial ecologic studies, leading to the discovery of new antibacterial substances for bacteria (especially antibiotic-resistant bacteria), which has been a great burden in these times. It was determined that the FLA tested in our study had an inhibitory effect on *S. aureus* and *S. epidermidis* (except phagocytosis). The highest inhibition against *Staphylococcus* bacteria (65.64%, 78.36%) was detected with *A. castellanii* ATCC 50373-CFS. A native aquatic FLA strain obtained

from our waters (A1-CFS) also yielded a similar (73.47%, 44%) inhibition effect. On the contrary, with the other native samples (for A2-CFS) these inhibitions were either low (15.14%, 9.24%, 33.33%) or (for A3-CFS) non-existent not at all (Figure 3). Nevertheless, these data show us that native FLA have the antibacterial potential against *Staphylococcus* bacteria. This study is the first one about the interaction/inhibition of FLA-*Staphylococcus* in which native strains were used. Our studies are ongoing, aiming to investigate more samples to reveal more bacteriostatic or bactericidal effects of FLA isolates against pathogen/potantial pathogen and antibiotic-resistant *Staphylococcus*. If this kind of effect were found, a new, native, and effective antibacterial substance, which would be applied to inhibition of *Staphylococcus* that are causing infections in humans, would be discovered.

Similar to our study, Nakışah and Chandrika reported that clinical and environmental (two sample) *Acanthamoeba* (FLA) lysates showed antibacterial activity against pathogen two *S. aureus* strains (21). Iqbal and co-workers reported that *A. castellanii*-CFS (one sample) was effective against clinical MRSA at 100% whereas it had a bactericidal activity against vancomycin-resistant *E. faecalis* at 8%. However, it did not show a bactericidal effect against *Acinetobacter sp., Pseudomonas aeruginosa (*22). Souza et al. reported that the relationship between a single clinical MRSA isolate and a single *Acanthamoeba polyphaga* ATCC 30461 (FLA) strain yielded that FLA culture lysate supported the growth of MRSA, but the same FLA culture supernatant inhibited the growth of the same bacteria (24). Martin et al. investigated the effects of different genus, kind, and or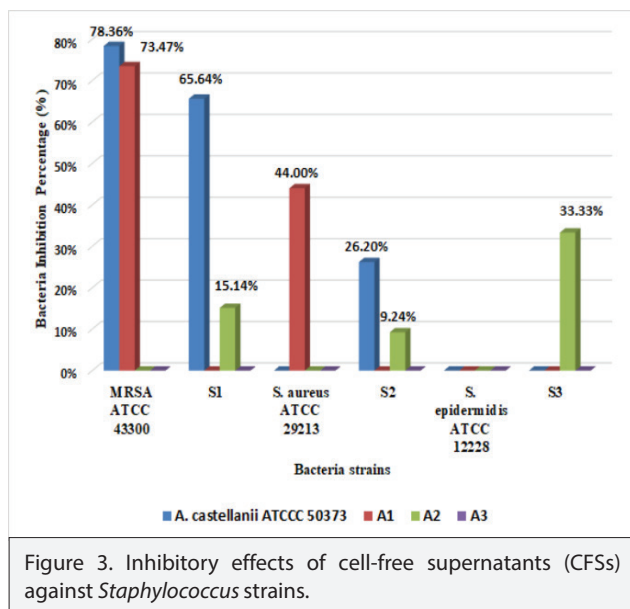igin of FLA-CFS against *Staphylococcus aureus* (MRSA typed as USA300) and found that *Mycobacterium bovis* biofilms and *A. polyphaga* CCAP 1501/18–CFS sample inhibited *Staphylococcus aureus* to a significant degree (42). As can be seen, there is a very low number of current studies testing a scarce number of strains. However, many more strains (four FLA strains and six *Staphylococcus* strains) were used in our study, thus making it more comprehensive. Moreover, our study used strains different from the standard strains used in other studies, including native strains. For these reasons, we are of the opinion that the inhibitory effect of FLA CFSs on *Staphylococcus* bacteria may vary depending on both FLA strains and *Staphylococcus* strains. The following data obtained from our study (Figure 3) also support this view: i) The tested FLA-CFSs had a greater inhibitory effect against *S. aureus* than *S. epidermidis*. ii) No FLA-CFS had antibacterial activity against *S. epidermidis* ATCC 12228 strain. iii) A3-CFS had no inhibitory effect on any of the Staphylococcus strains tested. iv) *Staphylococcus* strains tested were found to be inhibited by at least one native FLA-CFS (A1-CFS or A2-CFS), except for the *S. epidermidis* ATCC 12228 strain). Nevertheless, new studies are needed in which many more *Staphylococcus* and FLA strains would be used. This would be the only way to shed further light on the subject.

As stated above, since it is thought that the characteristics/abilities (pathogenicity factors) possessed by these microorganisms may play an important role among the factors affecting the relationship between FLA and bacteria living in the same environ-

ment, the subject should be investigated in detail. For example, it is known that the *S. epidermidis* ATCC 12228 strain, which was tested in our study and is avirulent, has molecules called bacteriocin that it releases into the external environment (43). This bacterium thus inhibits some species (eg *S. aureus*) that live in the same environment and are close to it. In our study, the reason why *S. epidermidis* ATCC 12228 strain was not inhibited by any FLA-CFS is perhaps because of these and similar molecules owned by the bacterium. In addition, it was found that the clinical (virulent) *S. epidermidis* strain (S3) tested in our study was inhibited by A2-CFS to a low extent (33.33%). These data suggest that virulent and avirulent *S. epidermidis* strains may be affected in different ways by FLA-CFS. In order to better understand the inhibition effect of FLA-CFS against *S. epidermidis*, new studies are planned in which more strains would be used (both virulent and avirulent *S. epidermidis*).

Souza Gonçalves et al. found that *A. castellanii* secreted different extracellular vesicles under different stress conditions and the CFS of these vesicles contained 69 proteins (41). In the light of this information, it is thought that the amoeba strains used in our study secrete inhibitory molecules against *Staphylococcus* strains, and new studies are planned to find the morphological and biochemical characterization of these possible molecules. Subsequent studies should relate to the purification of FLA-CFS with such activity and the active compound (s) that helped in the discovery of new anti-*Staphylococcus* active compound (s).

CONCLUSION

This is the first study showing the anti-*Staphylococcus* potential of FLA-CFS isolated from Turkey. In order to discover bactericidal FLAs against pathogen/potential pathogen and antibiotic resistant *Staphylococcus* bacteria, new studies using more strains should be planned.

REFERENCES

1. Thomas V, Herrera-Rimann K, Blanc DS, Greub G, Biodiversity of amoebae and amoeba-resisting bacteria in a hospital water network. Appl Environ Microbiol 2006; 72: 2428-38.
2. Zeybek Z, Üstüntürk M, Binay AR. Morphological characteristics and growth abilities of free living amoeba ısolated from domestic tap water samples in Istanbul. Eur J Biol 2010; 69: 17-23.
3. Penz T, Horn M, Schmitz-Esser S. The genome of the amoeba symbiont 'Candidatus Amoebophilus asiaticus' reveals common mechanisms for host cell interaction among amoeba-associated bacteria. J Bacteriol 2010; 1: 541-45.
4. Burak DM. and Zeybek Z. Investigation of legionella pneumophila and free living amoebas in the domestic hot water systems in Istanbul. Turkish J Biol 2011; 35: 679-85.
5. Trabelsi H, Dendana F, Sellami A, Sellami H, Cheikhrouhou F, Neji S, Ayadi A. Pathogenic free-living amoebae: epidemiology and clinical review. Pathol Biol 2012; 60: 399-405.
6. Üstüntürk M. and Zeybek Z. Microbial contamination of contact lens storage cases and domestic tap water of contact lens wearers. Wien Klin Wochenschr 2012; 24: 17-22.
7. Zeybek Z, Dogruoz Gungor N, Turetgen I. Investigation of heterotrophic bacteria, legionella and free - living amoeba in cooling tower samples by fish and culture methods. Eur J Biol 2017; 76: 7-13.
8. Zeybek Z and Türkmen A. Investigation of the incidence of legionella and free-living amoebae in swimming pool waters and biofilm specimens in istanbul by different methods. Microbiol Bull 2020; 54: 50-65.
9. Saburi E, Rajaii T, Behdari A, Kohansal MH, Vazini H. Free-living amoebae in the water resources of Iran: a systematic review. J Parasit Dis 2017; 41: 919-28.
10. Balczun C. and Scheid PL. Free-living amoebae as hosts for and vectors of intracellular microorganisms with public health significance. Viruses 2017; 9: 65.
11. Schuster FL. Cultivation of pathogenic and opportunistic free-living amebas. Clin Microbiol Rev 2002; 15: 342-54.
12. Lambrecht E, Baré J, Van Damme I, Bert W, Sabbe K. Houf K. Behavior of *Yersinia enterocolitica* in the presence of the bacterivorous *Acanthamoeba castellanii*. Appl Environ Microbiol 2013; 79: 6407-13.
13. Villanueva MP, Medina G, Fernández H. *Arcobacter butzleri* survives within trophozoite of *Acanthamoeba castellanii*. Rev Argent Microbiol 2016; 48: 105-9.
14. Şenler NG, Yıldız İ. Tatlı Su Protozoonları ve Önemi. Turk J Sci Rev 2010; 3: 7-16.
15. Cateau E, Delafont V, Hechard Y, Rodier MH. Free-living amoebae: What part do they play in healthcare-associated infections?. J Hosp Infect 2014; 87: 131-40.
16. Winiecka-Krusnell J. and Linder E. Bacterial infections of free-living amoebae. Res Microbiol 2001; 152: 613-9.
17. Akya A, Pointon A, Thomas C. Mechanism involved in phagocytosis and killing of Listeria monocytogenes by *Acanthamoeba polyphaga*. Parasitol Res 2009; 105: 1375-83.
18. Chekabab SM, Daigle F, Charette SJ, Dozois CM, Harel J. Survival of enterohemorrhagic Escherichia coli in the presence of *Acanthamoeba castellanii* and its dependence on Pho regulon. Microbiologyopen 2012; 1: 427-37.
19. Marciano-Cabral F and Cabral G. *Acanthamoeba spp.* as agents of disease in humans. Clin Microbiol Rev 2003; 16: 273-307.
20. Greub G, La Scola B, Raoult D. *Parachlamydia acanthamoeba* is endosymbiotic or lytic for *Acanthamoeba polyphaga* depending on the incubation temperature. Ann NY Acad Sci 2003; 990: 628-34.
21. Nakisah MA and Chandrika K. Antimicrobial activities of aqueous lysate of Acanthamoeba SPP against selected pathogenic bacteria. Malaysian Appl Bio 2012; 41: 45-9.
22. Iqbal J, Siddiqui R, Khan NA. Acanthamoeba and bacteria produce antimicrobials to target their counterpart. Parasites Vectors 2014; 7: 1-6.
23. Tashmukhambetov B. An investigation of the effects of an antimicrobial peptide on the survival of Acanthamoeba and intracellular bacteria associated with Cystic Fibrosis. University of Essex, Phd Thesis. 2016.

24. De Souza TK, Soares SS, Benitez LB, Rott MB. Interaction between Methicillin-Resistant *Staphylococcus aureus* (MRSA) and *Acanthamoeba polyphaga*. Curr Microbiol 2017; 74: 541-9.

25. CDC. Antibiotic resistance threats in the United States. *Cent. Dis. Control Prev.* 2019, https://www.cdc.gov/drugresistance/pdf/threats-report/2019-ar-threats-report-508.pdf

26. Ali SM, Siddiqui R., Ong SK, Shah MR, Anwar A, Heard PJ, Khan NA. Identification and characterization of antibacterial compound(s) of cockroaches (*Periplaneta americana*). Appl Microbiol Biotechnol 2017; 101: 253-86.

27. Ali S, Siddiqui R, Khan NA. Antimicrobial discovery from natural and unusual sources. J Pharm Pharmacol 2018; 70: 1287-300.

28. Akbar N, Siddiqui R, Iqbal M, Khan NA. Antibacterial activities of selected pure compounds isolated from gut bacteria of animals living in polluted environments. Antibiotics 2020; 9: 190.

29. Ali SM, Siddiqui R, Sagathevan KA, Khan, NA. Antibacterial activity of selected invertebrate species. Folia Microbiol 2021; 66: 285–91.

30. Borin S, Feldman I, Ken-Dror S, Briscoe D. Rapid diagnosis of *Acanthamoeba keratitis* using non-nutrient agar with a lawn of *E. coli*. J Ophth Inflame Inf 2013; 3: 1-2.

31. Özpınar N, Özçelik S, Yünlü Ö. Isolation and morphotyping of *Acanthamoeba spp.* and *Vermamoeba spp.* from hospital air-conditioning systems. Cumhur Medical J 2017; 39: 369-73.

32. Jacquier N, Aeby S, Lienard J, Greub. Discovery of new intracellular pathogens by amoebal coculture and amoebal enrichment approaches. JoVE 2013; 80.

33. Schuppler M. How the interaction of Listeria monocytogenes and Acanthamoeba spp. affects growth and distribution of the food borne pathogen. Appl Microbiol Biotechnol 2014; 98: 2907-16.

34. H. P. Agency. Isolation and Identification of *Acanthamoeba Species*. Nat Stand Method 2014; 17: 1-12.

35. Eroğlu F, Evyapan G, Koltaş İS. The cultivation of *Acanthamoeba* using with different axenic and monoxenic media. Mid Black Sea J Heal Sci 2015; 1: 13-7.

36. Üstüntürk M and Zeybek Z. Amoebicidal efficacy of a novel multi-purpose disinfecting solution: First findings. Exp Parasitol 2014; 145: 93-7.

37. Zeibig E. Clinical Parasitology-E-Book: A Prac App 2012.

38. Huang FC, Shih MH, Chang KF, Huang JM, Shin JW, Lin WC. Characterizing clinical isolates of *Acanthamoeba castellanii* with high resistance to polyhexamethylene biguanide in Taiwan. J Mıcrobiol Immunol 2017; 50: 570-77.

39. Barker J, Humphrey TJ, Brown MWR. Survival of *Escherichia coli* 0157 in a soil protozoan: Implications for disease. FEMS Microbiol Lett 1999; 173: 291-5.

40. Garcia, A, Goñi P, Cieloszyk J, Fernandez MT, Calvo-Beguería L, Rubio E, Clavel A. Identification of free-living amoebae and amoeba-associated bacteria from reservoirs and water treatment plants by molecular techniques. Environ Sci Technol 2013; 47: 3132-40.

41. Gonçalves DDS, Ferreira MDS, Liedke SC, Gomes KX, de Oliveira GA, Leão PEL, Guimaraes AJ. Extracellular vesicles and vesicle-free secretome of the protozoa acanthamoeba castellanii under homeostasis and nutritional stress and their damaging potential to host cells. Virulence 2018; 9: 818-36.

42. Martin KH, Borlee GI, Wheat, Jackson WHM, Borlee BR. Busting biofilms: Free-living amoebae disrupt preformed methicillin-resistant *Staphylococcus aureus* (MRSA) and *Mycobacterium bovis* biofilms. Microbiology 2020; 166: 695.

43. Jang, IT, Yang M, Kim HJ, Park JK. Novel Cytoplasmic Bacteriocin Compounds Derived from *Staphylococcus epidermidis* Selectively Kill *Staphylococcus aureus*, Including Methicillin-Resistant *Staphylococcus aureus* (MRSA). Pathogen 2020; 9: 87.

Variation of Response Patterns Associated with an Avirulent Plant Symbiont Directed Defense Gene Expressions in Maize Exposed to Toxic Elements

Necla Pehlivan[1]

[1]Recep Tayyip Erdogan University, Department of Biology, Rize, Turkey

ORCID IDs of the authors: N.P. 0000-0002-2045-8380

ABSTRACT

Objective: Microbe-assisted plant heavy metal (HM) tolerance is gaining momentum over a conventional breeding or transgenic approach being used to generate tolerant varieties capable of completing their life cycle in the metalliferous environments. To withstand toxicity, along with the current anthropogenic pressure, applications of fungi representing the largest group of eukaryotic organisms is considerably rising.

Materials and Methods: The hypothesis that a novel strain, which belongs to the *Trichoderma* genus (TS143), was previously identified as being multi HM-resistant, improves plant HM-tolerance by regulating hydraulic conductance and defense system was tested at a molecular level.

Results: While only a marginal increase in the expression level of 70 kDa chaperon protein (*HSP1*) gene was obtained, peroxidase (*POD1*) and plasma membrane intrinsic aquaporin (*PIP1-5*) genes were found to be upregulated (<2 fold) in the presence of chronic exposure to the HM-mix, (500 mg L^{-1} As, Cd, Cu, Pb, Zn) explaining the vivid metabolic modification underlying the metal stress response by target fungus. Up-regulation of the ROS-scavenging peroxidase and aquaporin genes affirming that the responses of *POD1* (9.44 fold) and *PIP1-5* (3.55 fold) expression may serve as potential sensitive biomarkers for HM-induced cellular toxicity monitoring with TS143 biostimulation.

Conclusion: Determining transcriptional level changes might pave the way for further applied research which would analyze gene level interactions of *Trichoderma*-HMs-plants.

Keywords: Heavy metal tolerance, maize, *Trichoderma*, stress markers, gene expressions

INTRODUCTION

Metal(oid)s, unlike other pollutants, are not biodegradable thus accumulating in soil over time (1). Hence these could readily be transmitted to the environment by two basic routes: the anthropogenic activities such as pesticide and fertilizer use (2) and the natural processes (rock sedimentation and soil erosion, volcanic eruptions, geothermal processes, forest fires, wind, etc.). However, several studies in the past decade have shown that metal(oid) pollution in the environment is mostly of anthropogenic origin (3). Thus, soils contaminated with high concentrations of metal(oid)s driven by anthropogenic input can cause significant yield losses in agricultural areas (4). In these areas, heavy metal(oid)s (HMs) are easily absorbed by plant roots (5) and migrated to the above-ground parts (6) causing dramatic physiological damage in plants (7). Impairments in the cell wall structure, cytoplasmic instability along with enzyme malfunction, decreased reactive oxygen species (ROS) scavenging capacity, nuclear DNA and organelle damage which would ultimately be blocking the photosynthesis are among the most serious

impacts which are the result of the accumulated HM amount/accumulation rate in a specific organ over a certain period of time (8). Particularly, multi-HM exposure such as simultaneous As, Cd, Cu, Pb, and Zn (HM mix) that could create synergistic damaging effects even at much lower concentrations more than a single HM does (9).

Fungi-plant associations can result in some degree of cleansing of the soil from toxic metals (10). It has also been widely reported that one of the most promising species in this regard belongs to the *Trichoderma* genus (11). Species in this genus, which are also commercially available today (12), show a beneficial bio-molecular significance in the plant rhizosphere via nutrient uptake efficiency increase, mycoparasitic activity, antibiosis, and competitiveness against plant pathogens commonly found in the soil (13, 14) thereby providing tolerance to both abiotic and biotic stressors (11, 15). These species have been widely reported to alleviate abiotic stresses through cellular processes such as osmolyte and seconder metabolite synthesis, Na cation elimination, or root improvement (16) by chemical signals after root penetration with the help of cysteine-rich hydrophobin proteins isolated from the fungus itself (17). In fact, it`s even been reported that the volatile metabolites of this micro fungus family do not cause any damage to plants, on the contrary, they develop various protection responses such as preventing excessive formation of ROS by anthocyanin accumulation and increase in the expression of defense genes (18).

Although studies are showing that HMs in soil are more bio-available thanks to the members of this genus (19, 20), the information on the contribution of these genus members to the HM response at the molecular level in plants is still scarce (18), particularly for new *Trichoderma* variants. Thereby, determination of the efficacy of the target fungal strain promoting defense response at the plant gene level give a more informative approach and can pave the way to further mechanistic research paths. In this study, the effect of *Trichoderma* TS143, a new, genetically characterized local isolate with high HM tolerance, which has a high potential for use in the rehabilitation of mine sites and biodiesel production (20) but whose effects on plant transcript dynamics are unknown was investigated at the gene level. The response triggered by TS143 directed regulation/target transcript on maize was targeted for analysis under multi-HM stress.

MATERIALS AND METHODS

Simultaneous TS143 and Multi-HM Exposure

A *Trichoderma* isolate, which is able to grow in HM concentrations between the range of 500-2500 ppm, was used in the experiments. This strain is one of the strains in which we analyzed the efficacy of its metal uptake in plants and proved that it increased the phytoremediation ability of maize plants (20). Based on the dry matter of the soil according to the US EPA method (21), 500g of soil was placed in glass jars then, solutions containing 500 mg L^{-1} As, Cd, Cu, Pb and Zn were added from the top. The solution mix was prepared by readily available

$Na_2HAsO_4 \cdot 7H_2O$, $Cd(NO_3)_2 \cdot 4H_2O$, $Cu(NO_3)_2 \cdot 3H_2O$, $Pb(NO_3)_2$, and $Zn(NO_3)_2 \cdot 6H_2O$ chemicals. After that, the jars were placed in a horizontal shaker at 24±1°C and 75 rpm for 2 days. The soil used in the pot experiments was ready after the solutions were evaporated at 40°C in an oven. TS143 was one of several members of the genus isolated by Dr. Rengin Eltem/Ege University from the soils sampled at a specific site of an active mining area in the Northeastern Black Sea region of Turkey. The strain was applied as a 10^8 colony forming unit (CFU) mL^{-1}/500g soil under in-vitro conditions.

Pot Experiments

Commercially supplied soil was autoclaved under 1.1 atm at 121°C and cooled down under sterile conditions. The pots used were pre-disinfected with bleach, then were rinsed through distilled water. The soil not contaminated with HMs was used as the control group (Control), while uncontaminated soil treated with the isolate only (TS143) was used as the positive control. To determine fungal efficacy, two more groups consisting of the HM cocktail only (HM mix) and As, Cd, Cu, Pb, Zn mix + TS143 (HM mix+TS143) were used to sow maize seeds (*Zea mays* L. *RX9292*) after a regular sterilization process. Six seeds were sown at a 2cm depth in the soil for all pots. After seven days, the seedlings were reduced to two plants in each pot to allow better future growth. The pots were watered every four days for 21 days (without using supportive fertilizers) to provide enough saturation of the soil. After the chronic HM exposure period with and without TS143, shoot samples taken for further use in RNA isolation were washed several times in distilled water then treated with liquid nitrogen and stored at -80°C.

Organ Specific Expression Analysis for Potential Target Genes

To measure changes at the transcriptional level in the marker genes belonging to enzymatic antioxidant and homeostasis mechanisms playing vital roles in free radical detoxification and/or possible water scarcity protection (due to the ionic toxicity under HM exposure), sequence-specific primers were synthesized. Heat shock 70 kDa protein1 (*HSP1*) which is one of the regulatory proteins that protect peroxidase1 (*POD1*) and plasma membrane intrinsic aquaporins 1-5 (*PIP1-5*) as an indicator of possible disruption related to water intake were selected. The maize glyceraldehyde 3-phosphate dehydrogenase (*GAPDH*) gene was used as an internal reference for the normalization of the gene expression (22, 23).

RNA Isolation, cDNA Synthesis and Quantitative RT-PCR Analysis

The shoot samples of plants grown in the climate cabinet (Daihan, South Korea) for 21 days under the conditions of 16h light (120 μmol m²sec⁻¹ light intensity), eight hours dark mode at 25°C day/22°C night, and 70% humidity, were powdered in liquid N_2. The RNAs that belonged to the samples were isolated according to Chomczynski (24) using TRIzol®Reagent (AMBION). All solutions during isolation were used after being treated with diethyl pyrocarbonate (DEPC) and autoclaved.

Table 1. Primers of the target and reference genes used in the real time q-PCR experiments

Database entry#	gene_name	amplicon size (bp)	primers (F-R)
GRMZM2G137839	Peroxidase1 ZmPOD1	136	5'-CTGCTGAGTGACCCTGTCTTC-3' 5'-GGATAGGGTCTATTTAAGCATCAG-3'
GRMZM2G310431	Heat Shock 70 kDa Protein1 ZmHSP1	128	5'-CCACCAACACCGTCTTCGAT-3' 5'-TACAATCATGGGTTTGTCACCAG-3'
GRMZM2G081843	Plasma membrane intrinsic aquaporins 1-5 ZmPIP1-5	90	5'-CACGTGGTCATCATCAGGG-3' 5'-CGTATGCTGCATGGTTGCT-3'
GRMZM2G176307	glyceraldehyde 3-phosphate dehydrogenase ZmGAPDH	105	5'-AGCAGGTCGAGCATCTTCG-3' 5'-CTGTAGCCCCACTCGTTGTC-3'

cDNA synthesis (55°C 15s and 95°C 3 min) and qPCR were not performed sequentially, thus an EvaGreen 20X (Biotium, CA, US) and a commercial 2X One-Step RT-PCR mix was used to amplify fragments ranging between 90-136 bp for target genes by using 0.5 µg RNA for each. The expression level of the specific transcripts for each different RNA sample consisting of 3 replicates (biological) for each group was determined. Negative control (No Template Controls-NTC) and non-amplification control groups (No Amplification Controls-NAC, a minus-reverse transcriptase control) was added in the reactions (45X of 15s at 95°C-denaturation, the 30s at 60°C-annealing and 40s at 72°C-extension for the amplification and 5s at 95°C, 1 min at 65°C, continued up to 97°C and 30s at 40°C cooling for melting peak quantification). Respective fluorescence was measured by LightCycler 480 Software (Roche). The Standard Curve Set Efficiency was 2.00. The comparative CT method ($2^{-\Delta\Delta Ct}$) for relative quantitation of gene expression was used (25) in data analysis.

Statistical Analysis

SigmaPlot 13 Software (Systat, CA) was used for T-test analysis to see if there were any biologically significant differences between treatments and the control groups. The significance was determined at 5% confidence level.

RESULTS

The Combined Effects of HM Mix and the Fungus on the Seedling Phenotype

Various HMs can impair almost all stages of the plant life cycle including germination, growth development, and reproduction (22). In this work, the response of soil-grown maize seedlings was studied to tackle the following question: whether *Trichoderma* could be beneficial in terms of diminishing the injurious potential of the metal(oid) cocktail when maize seedlings grown under combined HM mixture conditions by interfering and affecting antagonistically. Compared with the control seedlings, the group of plants belonging to TS143 only/HM mix-free (-HM) exhibited no significant growth difference however, phenotypic compositions were remarkably distinguishable in the HM mix-exposed (+HM) groups with and without fungal species application compared to either control or TS143

only groups (Figure 1, lower panel). While a slight difference in green leaf number (data not shown) was observed on the TS143+HM mix plants, growth was significantly retarded in the +HM only groups indicating plant phenotype and survival was influenced by 15 days of exposure when fungus was absent. Before the experiments (Figure 1, upper panel) no plants, in different application groups, performed significantly better than the other.

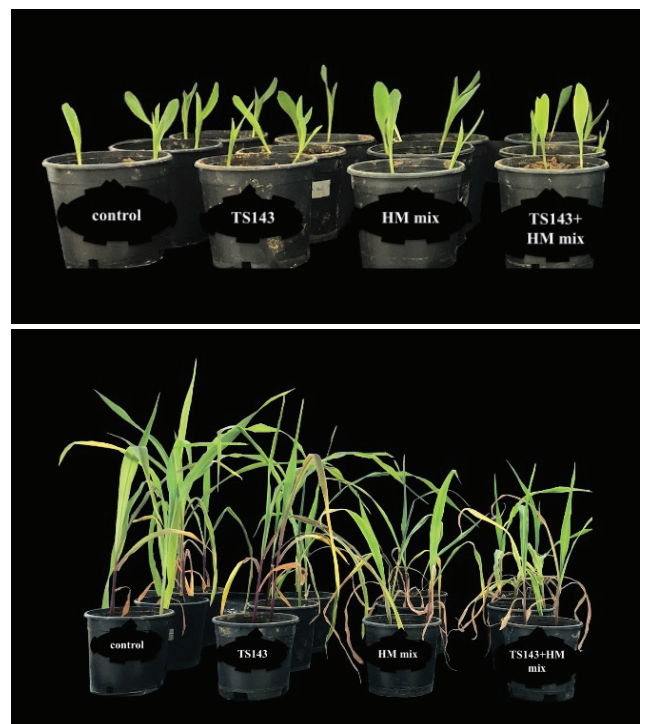Figure 1. Maize phenotypes after simultaneous *Trichoderma* and chronic multi-HM exposure. Upper panel: Images of seven day old seedlings with no application. Lower panel: *Trichoderma* and multi-HM exposed maize seedlings for 15 days (21 days after sowing). Control: untreated; TS143: *Trichoderma* applied; HM mix: As, Cd, Cu, Pb, Zn-exposed, TS143+HM mix: *Trichoderma*+As, Cd, Cu, Pb, Zn exposed maize seedlings.

HM Cocktail Alters Response Patterns of Plasma Intrinsic Protein, Peroxidase and Heat Shock Defense Genes in Maize

To find evidence for a possible connection and/or interlinking between combined HM stress, TS143 bio- stimulation, and plant response against an oxidative burst caused by ROS, four experimental groups with maize seedlings were prepared to test the protection potential of the target strain under As, Cd, Cu, Pb, Zn-applied conditions. In this context, the mRNA expression profiles of previously identified defense gene expressions reported to be induced by different HMs (34) were analyzed (yet, despite these proteins conferring putative trace element caused stress tolerance, *HSP*, *PIP*, and *POD*-encoding genes cannot be listed as sole protection components for HMs). Activation under HM mix conditions in the gene encoding *ZmPIP1-5* (1.40-fold), *ZmHSP1* (1.8-fold) and *ZmPOD1* (5.55-fold) respectively showed molecular evidence of cellular damage that overlapped with phenotypic changes (Figure 2). On the other hand, TS143 only gene expressions for all three genes tested were found dramatically lower than the control seedlings. However, HM mix+TS143 induced elevated gene expressions higher than that of the HM mix only conditions not for *ZmHSP1* (0.04-fold difference), but *ZmPIP1-5* and *ZmPOD1* (approximately 4-and 9.5-fold respectively).

TS143 Regulates Maize Plasma Intrinsic Aquaporin 1-5 and Peroxidase1 under Chronic HM Stress

This study found a strong direct (positive) correlation between the *ZmPIP1-5* and *Zmperoxidase1* quantified *mRNA* expression and the phenotypic performance of the TS143 supported maize plants continuously grown in soil with +As, Cd, Cu, Pb, Zn concentrations (Figure 2) as compared to the HM mix only

group, indicating positive effects yielding water uptake aid and triggered cellular defense signaling. Relative expression for *ZmHSP1*, *ZmPIP1-5*, and *ZmPOD1* was calculated (mean±standart error) as 0.08±0.01, 0.35±0.06 and 0.09±0.01 in TS143 only groups respectively, while expression was 1.89±0.2, 1.40±0.2, 5.55±0.3 for HM mix only group and 0.04±0.01, 3.58±0.3 and 9.44±0.6 for TS143+HM mix groups. Almost no change or a complete decline compared to the other two genes, in *ZmHSP1* transcript expression detected below intermediate levels (0.04-fold) which could indicate destructive effects of the heavy metal(oid)s used on the crosstalk between molecular chaperons, protein labeling, and degradation pathways of maize cells. Particularly, *Zmperoxidase1* which was calculated to be expressed at a relatively higher level than that of *ZmPIP1-5* and *ZmPIP1-5* in maize subjected to the same exact regime (TS143+HM mix) shows that an enzymatic antioxidant gene differed markedly, while it remained unchanged under control conditions with almost no difference.

DISCUSSION

Plants yield significant changes in gene expression to counteract HM stress if they are not hyperaccumulators able to complete life cycles without major symptoms due to toxicity (26). However, according to the recent plant HM stress reports, there is still scarce data on gene transcript changes driven by the fungal genus *Trichoderma* that recently emerged as a group of symbionts with immense impact on human welfare (27). The concepts designated to analyze the physiological outcomes of HM cocktails on plants under a fungus effect were even rarer (28) compared to other reports showing the efficacy of different *Trichoderma* genotypes under a single HM element (e.g., Pb (29) or Cu (30). Also, reports mostly focused on biotic stress-triggered gene expression dynamics in plants induced by the genus (31) rather than abiotic factors. In addition, research on the efficacy of newly identified genetic variants isolated from a mining niche might be more valuable in terms of showing the molecular plant protection potential of a novel strain in plant molecular HM tolerance which has not previously been investigated. This background along with evidence showing that the Trichoderma genus has been shown to dissolve oxidative zinc (Zn^{2+}) via ligand complex release (32) and Cd extraction (33), allowed this study to prepare four experimental groups with maize seedlings exposed to HM mix-free (-HM) and HM mix-exposed (+HM) with/without fungal species (Figure 1) to test the protection potential of the target strain.

Given the metal(oid) uptake and/or transport was reported to be more a quantitative trait subject to crosstalk of multiple genes and the regulation of HM transport/tolerance in plants requires more than one physiological pathway (8), of particular interest, the transcriptional expression pattern of an aquaporin gene and analogue mechanisms of one of the enzymatic antioxidants (peroxidase1) and stress proteins, protecting enzyme malfunction (HSP1) were chosen to be analyzed and confirmed by quantitative PCR.
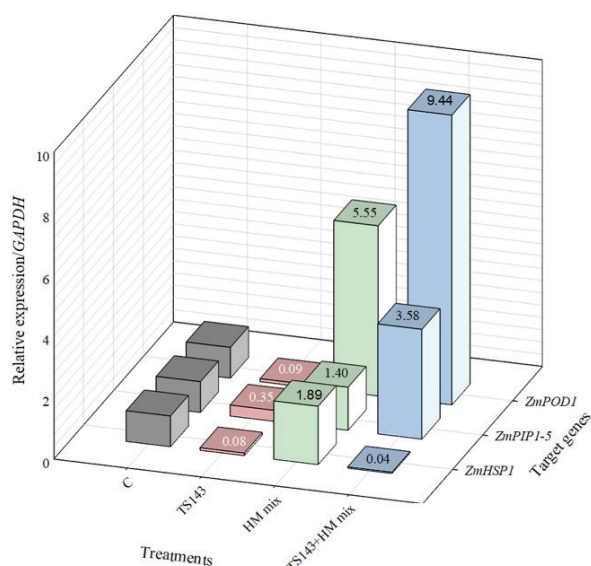

Figure 2. Profiling of representative genes expressing *peroxidase1_ZmPOD1, plasma membrane intrinsic aquaporins 1-5_ ZmPIP1-5* and *heat shock protein1_ZmHSP1* in maize. Data is given as mean (n=3). Control: untreated; TS143: *Trichoderma* applied; HM mix: As, Cd, Cu, Pb, Zn-exposed, TS143+HM mix: *Trichoderma*+As, Cd, Cu, Pb, Zn exposed maize seedlings (for 15 days).

While PODs are one of the major enzymatic antioxidants catalyzing the breakdown of H_2O_2 to scavenge radicals, or sometimes generating H_2O_2 themselves as signal molecules (34), the HSPs are the quality controllers of PODs , assisting conformational changes (35). They belong to multi-gene superfamilies whose proteins are present in the mitochondria or chloroplasts showing induced expression not only by thermo-stress but also by HMs (35). Hence, validation of these related gene expressions in maize seedlings interacting simultaneously with HMs and TS143 was performed. As shown in the Figure 2, the TS143 was found actively mediating HMs up-take and translocation by possibly playing with reduction kinetics of the metal(oid)s or facilitating vacuolar storage in maize seedlings under chronic multi-HM exposure, given the analysis was performed in shoot tissues (translocation). Simultaneous exposure of the HM-mix along with TS143 did not exhibit increased expression in *HSP1,* possibly indicating that the *HSP1* might not be a very sensitive biomarker, would serve for HM-induced toxicity monitoring for the current experimental set up in maize. Only slight distinctive expression levels indicating *HSP1* involvement were obtained for the HM-mix-only group. In this group, given the used dose in the experiments (500 mg L^{-1}) was relatively high, excretion was expected to be decreased and xylem loading would increase gradually which in turn would trigger a rapid involvement of molecular detoxification elements, potentially including the over-expression of HSPs (as confirmed almost 2-fold increase in *ZmHSP1*). The confounding levels of expression (0.04-fold) in the HM mix+TS143 groups could be attributed to an avoidable action in the *HSP1* up-regulation with the help of TS143 protection, given the primary function of this gene is to prevent the damage-induced aggregation of proteins under stress (35). However, this could be valid only if there was not a complete breakdown in the metal regulatory network of the seedlings consisting of HSPs, because the proteins of the HSP gene family were reported to be found at significant levels even in non-stressed plant cells when none of the stress factors were present (36). However, the HM mix-only exposure caused an almost 2-fold increase in *ZmHSP1* (Figure 2) gene of the seedlings, in direct opposition to the control and TS143-applied only groups. *POD1* expression, on the other hand, was significantly induced (p<0.05; t-test) by chronic exposure of HMs+TS143. The 9.44-fold increase might be showing the cytotoxic range for an applied HM dose that is exceedingly difficult to avoid for seedlings. The *POD1* increase rate in the HM-mix exposed-only group was calculated 5.5-fold more (p<0.05; t-test) compared to the control. This data may be grounded on the TS143 colonization induced signaling cascades improving POD-arbitrated redox state by regulating the downstream genes while adjusting the molecular defense machinery. Similar results were exemplified by several other studies (37, 38, 29) proving enhanced antioxidative defense were characterized by higher expressions of *POD* genes.

Beyond generating free radicals that attack cells, HMs also generate ionic stress due to water scarcity (39). The data interpreting that the aquaporin genes of a hyperaccumulator, *Pteris vittata TIP4;1* might be responsible for metal uptake as a metal transporter (40) confirms the functionality and involvement of PIPs in this notion and a lead to analyze maize aquaporin expression change. Relative expression was calculated 2-fold more than HM mix-exposed only seedlings and *PIP1-5* expression reached almost 3.6-fold (p<0.05; t-test) which was more than both the control and TS143- applied only group, following two weeks of application. Up-regulation of maize aquaporin expression (>2 fold) might be pinpointing the contribution of TS143 in the reduction of water scarcity by trapping metals and not permitting translocation from roots to the shoots. Certain studies confirm the current data and reporting that the genus is effective on plant-water relations via co-metabolic exchange by breaking down the robust chemistry of toxicants (14).

CONCLUSION

Besides the fact that the fungi belong to *Trichoderma* genus produce the strongest mycotoxins in the world along with its Aspergillus counterparts (41), this research further affirmed the increased potential in alleviating trace toxic elements which caused cellular injuries in plants (29, 30). A transcriptional perspective of molecular protection was interpreted in this work by showing selected gene expression dynamics lead by TS143. The particular species used is an isolate whose molecular phylogeny and major physiological effects have recently been characterized under HM-stress and its effective use was recommended to provide agro-ecological benefits in environmental biotechnology (20). This research data provides further supports that the target isolate triggers plant molecular antioxidant defense and water dynamics via coordinating aquaporin, peroxidase, and molecular chaperon genes to a certain extent.

Researching the impacts on plant molecular physiology lead by more novel genotypes occupying a wide variety of natural/artificial niches as in the case of TS143, would be useful in either further plant-fungus methods or exploitation and effective use of fungi in the areas of agricultural and environmental biotechnology.

REFERENCES

1. Nriagu JO, Bhattacharya P, Mukherjee AB, Bundschuh J, Zevenhoven R, Loeppert RH. Arsenic in soil and groundwater: an overview. Bhattacharya P, Mukherjee AB, Bundschuh J, Zevenhoven R, Loeppert RH, editors. Trace Metals and other Contaminants in the Environment. Elsevier; 2007.p.3-60.

2. Goutam J, Sharma J, Singh R, Sharma D. Fungal-mediated bioremediation of heavy metal-polluted environment. In microbial rejuvenation of polluted environment 2021; 51-76. Springer, Singapore.

Eur J Biol 2021; 80(1): 35-41

Pehlivan. Gen Expression Patterns Linked to TS143 in HM Stressed Maize

3. Xu Y, Shi H, Fei Y, Wang C, Mo L, Shu M. Identification of soil heavy metal sources in a large-scale area affected by industry. Sustainability 2021; 13(2): 1-15.

4. Ma Y, Rajkumar M, Zhang C, Freitas H. Beneficial role of bacterial endophytes in heavy metal phytoremediation. J Environ Manage 2016; 174: 14-25.

5. Pečiulytė D, Repečkienė J, Levinskaitė L, Lugauskas A, Motuzas A, Prosyčevas I. Growth and metal accumulation ability of plants in soil polluted with Cu, Zn and Pb. Ekologija 2006; 1: 48-52.

6. Song Y, Cui J, Zhang H, Wang G, Zhao FJ, Shen Z. Proteomic analysis of copper stress responses in the roots of two rice (*Oryza sativa L.*) varieties differing in Cu tolerance. Plant and soil 2013; 366(1): 647-58.

7. Yan A, Wang Y, Tan SN, Yusof ML, Ghosh S, Chen Z. Phytoremediation: a promising approach for revegetation of heavy metal-polluted land. Front Plant Sci 2020; 30(11): 1-15.

8. Zhang H, Xin L, Zisong X, Yue W, Zhiyuan T, Meijun A, et al. Toxic effects of heavy metals Pb and Cd on mulberry (*Morus alba L.*) seedling leaves: Photosynthetic function and reactive oxygen species (ROS) metabolism responses. Ecotoxicology and Environmental Safety 2020; 195: 1-11.

9. Redha A, Al-Hasan R, Afzal M. Synergistic and concentration-dependent toxicity of multiple heavy metals compared with single heavy metals in *Conocarpus lancifolius*. Environ Sci Pollut Res 2021; 14: 1-5.

10. Skowrońska M, Bielińska EJ, Szymański K, Futa B, Antonkiewicz J, Kołodziej B. An integrated assessment of the long-term impact of municipal sewage sludge on the chemical and biological properties of soil. Catena 2020; 189: 1-6.

11. Druzhinina IS, Kopchinskiy AG, Kubicek CP. The first 100 *Trichoderma* species characterized by molecular data. Mycoscience 2006; 47: 55-64.

12. Sood M, Kapoor D, Kumar V, Sheteiwy MS, Ramakrishnan M, Landi M, et al. *Trichoderma*: the "secrets" of a multitalented biocontrol agent. Plants 2020; 9(6): 1-25.

13. Harman GE, Kubicek PK. *Trichoderma* and *Gliocladium*. Enzymes, biological control and commercial applications (Vol 2) London: Taylor and Francis 1998.

14. Harman GE, Howell CR, Viterbo A, Chet I, Lorito M. *Trichoderma* species-opportunistic, avirulent plant symbionts. Nat Rev Microbiol 2004; 2(1): 43-56.

15. Garbeva PV, Van Veen JA, Van Elsas JD. Microbial diversity in soil: selection of microbial populations by plant and soil type and implications for disease suppressiveness. Annu Rev Phytopathol 2004; 8(42): 243-70.

16. Contreras-Cornejo HA, Macías-Rodríguez L, Alfaro-Cuevas R, López-Bucio J. *Trichoderma spp.* improve growth of *Arabidopsis* seedlings under salt stress through enhanced root development, osmolite production, and Na+ elimination through root exudates. Mol Plant-Microbe Int 2014; 27: 503-14.

17. Samolski I, Rincon AM, Pinzón LM, Viterbo A, Monte E. The qid74 gene from *Trichoderma harzianum* has a role in root architecture and plant biofertilization. Microbiology 2012; 158(1): 129-38.

18. Kottb M, Gigolashvili T, Großkinsky DK, Piechulla B. *Trichoderma* volatiles effecting Arabidopsis: from inhibition to protection against phytopathogenic fungi. Front Microbiol 2015; 29(6): 1-14.

19. Babu AG, Shim J, Bang KS, Shea PJ, Oh BT. *Trichoderma* virens PDR-28: a heavy metal-tolerant and plant growth-promoting fungus for remediation and bioenergy crop production on mine tailing soil. J Environ Manage 2014; 132: 129-34.

20. Pehlivan N, Gedik K, Eltem R, Terzi E. Dynamic interactions of *Trichoderma harzianum* TS 143 from an old mining site in Turkey for potent metal (oid)s phytoextraction and bioenergy crop farming. J Hazard Mater 2021; 403: 1-10.

21. US EPA. Risk Assessment Guidance for Superfund Volume I: Human Health Evaluation Manual (Part E, Supplemental Guidance for Dermal Risk Assessment)-Interim Guidance. 2001.

22. Zhao L, Hu Q, Huang Y, Keller AA. Response at genetic, metabolic, and physiological levels of maize (*Zea mays*) exposed to a Cu (OH)$_2$ nanopesticide. ACS Sustain Chem Eng 2017; 5(9): 8294-301.

23. Qiao Y, Ren J, Yin L, Liu Y, Deng X, Liu P, et al. Exogenous melatonin alleviates PEG-induced short-term water deficiency in maize by increasing hydraulic conductance. BMC Plant Biol 2020; 20: 1-4.

24. Chomczynski P. A reagent for the single-step simultaneous isolation of RNA, DNA and proteins from cell and tissue samples. Biotechniques 1993; 15(3): 532-4.

25. Schmittgen TD, Livak KJ. Analyzing real-time PCR data by the comparative CT method. Nat Protoc 2008; 3(6): 1101-8.

26. Li JT, Gurajala HK, Wu LH, van der Ent A, Qiu RL, Baker AJ, et al. Hyperaccumulator plants from China: a synthesis of the current state of knowledge. Environ Sci Technol 2018; 52(21): 11980-94.

27. Gorai PS, Barman S, Gond SK, Mandal NC. Chapter 28 – *Trichoderma*. Editor(s): Amaresan N, Senthil M, Kumar KA, Krishna K, Sankaranarayanan A. Beneficial microbes in agro-ecology, Academic Press 2020; 571-591, ISBN 9780128234143.

28. Adams P, De-Leij FAAM, Lynch JM. *Trichoderma harzianum Rifai* mediates growth promotion of crack willow (*Salix fragilis*) saplings in both clean and metal-contaminated soil. Microb Ecol 2007; 54(2): 306-13.

29. Sun X, Sun M, Chao Y, Wang H, Pan H, Yang Q, et al. Alleviation of lead toxicity and phytostimulation in perennial ryegrass by the Pb-resistant fungus *Trichoderma asperellum* SD-5. Funct Plant Biol 2020; 48(3): 333-341.

30. Vargas JT, Rodríguez-Monroy M, Meyer ML, Montes-Belmont R, Sepúlveda-Jiménez G. *Trichoderma asperellum* ameliorates phytotoxic effects of copper in onion (*Allium cepa L.*). Environ Exp Bot 2017; 136: 85-93.

31. Schmidt J, Dotson BR, Schmiderer L, van Tour A, Kumar B, Marttila S, et al. Substrate and plant genotype strongly influence the growth and gene expression response to *Trichoderma afroharzianum* T22 in Sugar Beet. Plants 2020; 9(8): 1-14.

32. Altomare C, Norvell WA, Björkman T, Harman GE. Solubilization of phosphates and micronutrients by the plant-growth-promoting and biocontrol fungus *Trichoderma harzianum Rifai* 1295-22. App Env Microb 1999; 65(7): 2926-33.

33. Cao L, Jiang M, Zeng Z, Du A, Tan H, Liu Y. *Trichoderma atroviride* F6 improves phytoextraction efficiency of mustard (Brassica juncea (L.) Coss. var. foliosa Bailey) in Cd, Ni contaminated soils. Chemosphere 2008; 71(9): 1769-73.

34. Chen S, Yu M, Li H, Wang Y, Lu Z, Zhang Y, et al. SaHsfA4c from *Sedum alfredii* hance enhances cadmium tolerance by regulating ROS-scavenger activities and heat shock proteins expression. Front Plant Sci 2020; 11: 1-14.

35. Zhang K, Ezemaduka AN, Wang Z, Hu H, Shi X, Liu C, et al. A novel mechanism for small heat shock proteins to function as molecular chaperones. Sci Rep 2015; 5(1): 1-8.

36. Vierling E. The roles of heat shock proteins in plants. Annu Rev Plant Physiol 1991; 42(1): 579-620.

37. Mastouri F, Björkman T, Harman GE. *Trichoderma harzianum* enhances antioxidant defense of tomato seedlings and resistance to water deficit. Mol Plant Microbe Interact 2012; 25(9): 1264-71.

Eur J Biol 2021; 80(1): 35-41

Pehlivan. Gen Expression Patterns Linked to TS143 in HM Stressed Maize

38. Zhang S, Gan Y, Xu B. Application of plant-growth-promoting fungi *Trichoderma longibrachiatum* T6 enhances tolerance of wheat to salt stress through improvement of antioxidative defense system and gene expression. Front Plant Sci 2016; 7: 1-11.

39. Rucińska-Sobkowiak R. Water relations in plants subjected to heavy metal stresses. Acta Physiol Plant 2016; 38(11): 1-13.

40. He Z, Yan H, Chen Y, Shen H, Xu W, Zhang H, Shi L, Zhu YG, Ma M. An aquaporin Pv TIP 4; 1 from *Pteris vittata* may mediate arsenite uptake. New Phytol 2016; 209(2): 746-61.

41. Abbott SP. Mycotoxins and indoor molds. Indoor Env Con 2002; 3: 14-24.

ISTANBUL
UNIVERSITY
PRESS

Differential Effects of Bisphenol A and Di (2-Ethylhexyl) Phthalate Exposure on Crestin and the Expression of Some Genes Related to Apoptosis and Inflammation in Zebrafish Embryos

Perihan Seda Ates-Kalkan[1] ![ORCID], **Tugce Ayik[2]** ![ORCID], **Unsal Veli Ustundag[3]** ![ORCID], **Ebru Emekli-Alturfan[2]** ![ORCID]

[1]University of Oxford, Radcliffe Department of Medicine, Oxford, England
[2]Marmara University, Faculty of Dentistry, Deparament of Basic Medical Sciences, Istanbul, Turkey
[3]Istanbul Medipol University, Faculty of Medicine, Department of Medical Biochemistry, Istanbul, Turkey

ORCID IDs of the authors: P.S.A.K. 0000-0002-4905-1912; T.A. 0000-0001-9655-2122; U.V.U. 0000-0003-0804-1475; E.E.A. 0000-0003-2419-8587

ABSTRACT

Objective: Endocrine disrupting chemicals (EDC) in plastics may disrupt proper endocrine system functioning. Zebrafish embryos are formed through external fertilization, and their rapid development, short life cycle, and transparency provide imaging advantages. In zebrafish embryos, neural crest development occurs similarly to other vertebrate embryos and crestin is found in the neural crest during embryogenesis. The aim of our study is to evaluate the effects of bisphenol A (BPA) and Di (2-ethylhexyl) phthalate (DEHP), which are the most widely used EDCs, on the expression of crestin, apoptosis, and inflammation-related parameters in zebrafish embryos.

Materials and Methods: The embryos were exposed to either DEHP or BPA in well plates for 72 h post fertilization (hpf). Expressions of crestin were evaluated by *in situ* hybridization, while the expressions of *bax, casp8, casp3a, ifng1, fas,* and *tp53* were evaluated by RT-PCR.

Results: Expressions of *bax* and *casp8* increased and *casp3a, ifng1,* and *fas* decreased in BPA and DEHP groups. *tp53* expression increased in the BPA group but decreased in the DEHP group compared with the control group. In the DEHP group, *casp3a, ifng1, fas, bax, casp8,* and *tp53* expressions decreased compared with the BPA group. No significant change was observed in the crestin expressions in the groups. When compared with the control group, an inverse relation between *ifng1* expression and apoptosis, as evidenced by increased *bax* and *casp8* expressions, was observed in the BPA and DEHP groups.

Conclusion: Our study provided important data on the effects of EDCs on the relationship between inflammation and apoptosis.

Keywords: Bisphenol A, Di (2-ethylhexyl) phthalate, Apoptosis, Inflammation, Crestin

INTRODUCTION

Containers and packages made of plastic are widely used in the food industry because they are lighter, unbreakable and more affordable. However, the possibility of transferring toxic additives to foods and beverages through the monomers contained in plastics has become a serious cause of concern and risk in terms of public health. Factories producing plastic and plastic derivatives release various chemicals into nature in an uncontrolled manner, and discussions about the possible effects of these chemicals on living things are in-

creasing day by day (1). Chemicals commonly found in plastics and derivatives that disrupt endocrine functions are called endocrine disrupting chemicals (EDC) (2). In this study we aimed to examine apoptosis and inflammation-related parameters in zebrafish embryos exposed to bisphenol A (BPA) and Di (2-ethylhexyl) phthalate (DEHP), which are the most widely used EDCs.

Polyethylene terephthalate (PET) is widely used in the production of plastic materials and bottles. DEHP is used as a plasticizing agent in PET bottles. Polycarbonate plastic (PC) is widely used, especially in food and medical equipment, and BPA is needed for its production (1, 2). EDC exposure, which has become one of the important public health problems of our time, is related to various diseases, such as cancer. On the other hand, metabolic disease such as obesity and diabetes have also been connected to EDC exposure. It has been shown that BPA can pass into foods when it comes into contact, and this transition increases with heat. It has been shown that BPA consumed through plastic bottles can cause serious damage to the prostate, liver, and reproductive system and brain development and may lead to cancer and heart diseases (2-5).

Zebrafish, the popular model organism of recent years, is a vertebrate organism. Females lay 50 to 300 eggs per day, embryos are formed with external fertilization and have rapid development, they have short life cycles, and their transparency provides imaging advantages (6, 7).

It has been shown in animal models that the expression of the *tp53* tumor suppressor gene can be altered by the effects of various EDCs (8). It is known that steroids and sex hormones have major roles in modulating inflammatory and immune responses, so endocrine disruptors may also affect the formation of immune responses (9). In a study conducted in rats, it was shown that IFN-expression was affected by endocrine disruptors (10, 11). Caspase-3 is a caspase protein encoded by the *casp3* gene that interacts with caspase-8. The interaction of the fas receptor with its ligand causes the formation of the death-inducing signaling complex. Sequential caspase activation regulates the execution phase of apoptosis and Bcl-2 inhibits Bax-triggered apoptosis (9-11). In this study we aimed to determine the possible effects of DEHP and BPA on *tp53*, *ifn-γ*, *casp3*, *casp8*, *bcl2*, *bax*, and *fas* associated with apoptosis and inflammation in zebrafish embryos.

Crestin is expressed in zebrafish during embryogenesis and it is first observed at the beginning of somitogenesis in neural crest cells of the ectoderm (12). Although BPA and DEHP have been previously demonstrated to cause several malformations in zebrafish embryos (13), the effects of BPA and DEHP on crestin, which is an important developmental marker, have not been previously reported. Accordingly, we also aimed to evaluate the effects of BPA and DEHP on crestin expression in developing zebrafish embryos.

MATERIALS AND METHODS

Embryo Exposures
Embryos were obtained from zebrafish (wild type AB/AB strain) that were housed in apparently disease-free conditions. Animal husbandry and spawning were performed according to the protocols approved by the University of Marmara Institutional Animal Care and Use Committee. As the zebrafish embryos used were no more than 5 days old, no ethical approval was required for the protocols applied as stated by the Council of Europe (1986), Directive 86/609/EEC. Reverse osmosis water that contains 0.018 mg L−1 Instant Ocean™ salt was used for all of the experiments. After natural spawning, fertilized embryos were gathered and staged according to their development and morphology as described previously. Zebrafish embryos were exposed to BPA and DEHP at doses below the LC50 values as determined and reported previously by Üstündağ et al. (13). Accordingly, embryos were exposed to BPA 1 μg /L and DEHP 2,5 μg/L. The embryos were exposed to either DEHP or BPA in well plates for 72 h post fertilization (hpf). DMSO and methanol were used as the solvent control, and the embryo medium was used as the blank control. Three replicates, each containing 30 embryos, were prepared. BPA (CAS no: 80-05-7), DEHP (CAS no: 117-81-7), dimethyl sulfoxide (DMSO) (CAS no: 67-68-5), and methanol (CAS no: 67-56-1) were purchased from Sigma-Aldrich Co. (St. Louis, Missouri, USA).

Gene Expression Analyses
Embryos in each pool were placed in a 1.5 ml microfuge tube, water was removed, and TRIzol reagent was added. Then the embryos were homogenized with a pellet pestle. RNA isolations from the embryo homogenates were made by using the RNeasy Mini kit using the Qiacube (Qiagen) instrument. cDNA synthesis from the obtained RNA samples was carried out using One Script (ABM). The expression of *bax* (forward primer, 5′-GGC-TATTTCAACCAGGGTTCC-3′; reverse primer, 5′-TGCGAATCAC-CAATGCTGT-3′) *casp3* (forward primer, 5′-ATGAACGGAGACTGT-GTG-3′; reverse primer, 5′-TTAAGGAGTGAAGTACATCTCTTTG-3′) *casp8* (forward primer, 5′-GCTTCAATGGGTGCTTTTGT-3′; reverse primer, 5′-TCCGGCAAAAGGCAGTGTAA-3′), *ifng1* (forward primer, 5′-GCTGGATCTTCAAAGTCGGGTGTA-3′; reverse primer, 5′-TGTGAGTCTCAGCACACTTCCATC-3′), *fas* (forward primer, 5′-GTGACGCTAATGCAAAAATGAAG-3′; reverse primer, 5′-CGATGTCCTGCAGAGTGGTG-3′), and *tp53* (forward primer, 5′-GGGCAATCAGCGAGCAAA-3′; reverse primer 5′-GGGCAAT-CAGCGAGCAAA-3′) was determined using the Rotor-Gene Q instrument by adding the obtained cDNA samples to the RT2 SYBR Green Master Mix mixture. *actb1* (forward primer, 5′-AAG-CAGGAGTACGATGAGTCTG-3′; reverse primer, 5′- GGTAAAC-GCTTCTGGAATGAC-3′) was used as the housekeeping gene. The samples were studied in triplicate. Analysis of the data was performed using the delta delta Ct method based on normalization with the housekeeping gene *actb1* (14).

Crestin Expression Analysis by *In Situ* Hybridization Method
In order to determine the expression of the crestin by the *in situ* hybridization method, a previously prepared RNA probe targeting the crestin was used. 10 embryos reaching 72 hours were homogenized and RNA was isolated with the RNeasy mini kit. After the RNA was converted to cDNA, the desired region was amplified by PCR with previously designed crystalline primers. In order to check the accuracy of the proliferating area, it was

validated by the gel electrophoresis method. Then, after the desired region was reproduced by PCR, unwanted molecules (dntps etc.) were removed, except for the area replicated with the clean-up kit. Then, the PCR product obtained by the *in vitro* transcription method was transformed into a DIG-labeled RNA. The obtained RNA was made usable by cleaning with the RNA clean-up kit. The probe obtained in this way was compared with the embryos to which BPA and DEHP had been administered by using the *in situ* hybridization method and the control group embryos (15).

Statistical Analysis

Statistical analysis of the data was done with the Graph Pad 7 Statistical program using Tukey Multiple Comparison Analysis after One Way Anova. The Shapiro–Wilk test was performed to test the normality. Results are given as Mean±Standard Deviation; $p < 0.05$ was considered significant.

RESULTS

As the data analysis did not show any difference between the solvent control and blank control for the parameters investigated in this study, accordingly, the blank control test data are given in the following sections. It was determined that there was a significant increase in *bax* and *casp8* mRNA expression levels in BPA and DEHP groups compared to the control group ($p < 0.05$). When the DEHP group was compared with the BPA group, it was observed that there was a significant decrease in *bax* and *casp8* mRNA expression levels ($p < 0.05$) (Figure 1).
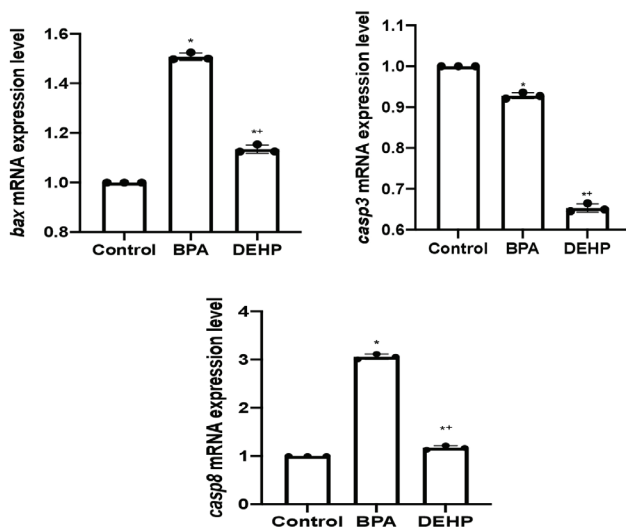
Figure 1. *bax, casp3* and *casp8* transcripts quantified by RT-PCR. All RT-PCR results are normalized to β-actin, the housekeeping gene and expressed as fold change from their respective controls. Data presented are mean±SD. *significantly different from the control group, $p < 0.05$; +significantly different from the BPA group; SD: standard deviation; BPA: Bisphenol A; DEHP: Di (2-ethylhexyl) phthalate.

A significant decrease was found in *casp3a*, *ifng1*, and *fas* mRNA expression levels in both the BPA and DEHP groups ($p < 0.05$). In the DEHP group, a significant decrease was observed in *casp3a*, *ifng1*, and *fas* mRNA expression levels compared to the BPA group and compared to the control group (Figures 1 and 2) ($p < 0.05$).
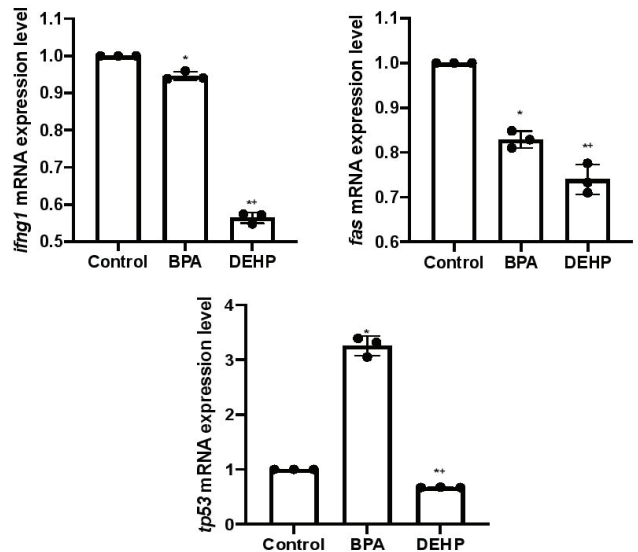
Figure 2. *ifng1, fas* and *tp53* transcripts quantified by RT-PCR. All RT-PCR results are normalized to β-actin, the housekeeping gene and expressed as fold change from their respective controls. Data presented are mean±SD. *significantly different from the control group, $p < 0.05$; +significantly different from the BPA group; SD: standard deviation; BPA: Bisphenol A; DEHP: Di (2-ethylhexyl) phthalate.

tp53 mRNA expression levels were found to be increased in the BPA group compared to the control group ($p < 0.05$). On the other hand, in the DEHP group, a significant decrease was observed in the *tp53* mRNA expression level compared to both the control and BPA groups ($p < 0.05$) (Figure 2). Crestin-expressing cells were found to be distributed along the anterior-posterior axis, in the neural crest migratory pathways. No significant change was observed in the crestin expressions in the groups (Figure 3).

DISCUSSION

In our study, we examined the effects of exposure to BPA and DEHP on the expression of apoptosis-associated *p53*, *casp3*, *casp8*, and *bax* genes and the inflammation-related *ifn-γ* gene, as well as the expression of crestin, which is an important marker in the embryonic period.

BPA is used to produce polycarbonate plastic and it acts as synthetic estrogen. BPA is found in different products such as food containers, toys, baby bottles, and dental and medical devices. Plastics are widely used in modern life and therefore

Control   **BPA**   **DEHP**
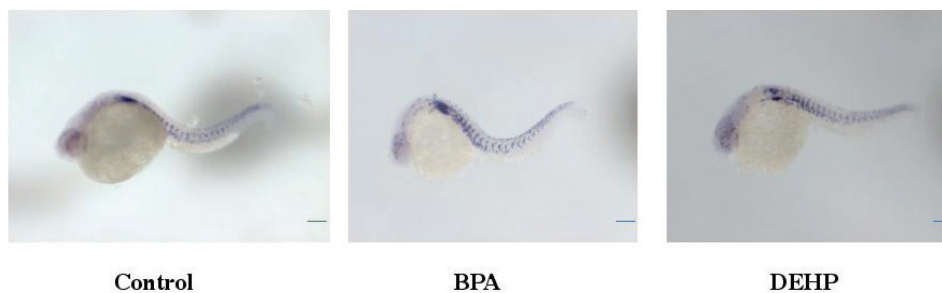
Figure 3. Crestin expressions of the control, Bisphenol A (BPA) and Di (2-ethylhexyl) phthalate (DEHP) groups determined by in situ hybridization. Crestin expressing cells are distributed along the anterior-posterior axis, in the neural crest migratory pathways. Scale bar: 60 µM.

BPA is released into the environment directly or under normal conditions due to incomplete polymerization. Hydrolysis of the ester bonds binding BPA monomers due to acid, base, or heat exposures lead to the release of BPA and increase the migration rate. BPA can be found in water sources such as streams and rivers, and even in drinking water. The main source of exposure is suggested to be by food and drink (16). We have shown previously that BPA and DEHP induced axial malformations, pericardial edema, and yolk sac edema in the zebrafish embryos (13). BPA affects different physiological processes related to development, reproduction, and metabolism. These effects can be attributed to its estrogen-like effect, whereby it binds to the estrogen receptors, altering the hormone system. BPA exposure has been related to many diseases affected by changes in estrogen levels, such as ovarian disease and breast cancer. Moreover, body fat distribution has been shown to correlate with blood BPA levels in women (17).

Increased *bax* and *casp8* expressions in the BPA- and DEHP-exposed groups is consistent with some other studies showing the apoptotic effects of these EDCs. Apoptosis is a programmed event that plays an important role in the normal development of living things, in the elimination of defective germ cells, in maintaining the proportion of Sertoli cells with appropriate germ cells, and in controlling sperm production. It has been reported that BPA induces autophagy and apoptosis in Sertoli and Leyding cells in rats (18). In testicular Leydig cells, it has been shown that BPA can activate protein kinase A (PKA) and Akt. In different models, BPA has been shown to affect proliferation of cells, apoptosis, and steroidogenesis by binding specific receptors in signaling pathways. On the other hand, information on the mechanism of germ cell apoptosis activated by BPA and the role of apoptosis-signaling pathways is scarce (16-18). In our study, although *bax* and *casp8* expressions were found to be increased in the BPA and DEHP groups, *casp3* expressions were found to be decreased when compared with the control group. The inhibition of *casp3* may be related to developmental defects, as reported by Oka et al. (19), who aimed to evaluate how BPA affected the early development of *Xenopus laevis* embryos. For this purpose, they exposed the embryos to 10-100 µM BPA and reported that the developmental abnormalities were found in embryos exposed to 20 µM BPA. As apoptosis is induced through various stimuli, inside the cell the apoptotic signal within the cell is transmitted through two main molecular pathways. These pathways are the death receptor pathway, known as the extrinsic-external pathway, and the mitochondrial pathway, known as the intrinsic or internal pathway. The intrinsic pathway can be induced by various extracellular or intracellular signals. These signals may include radiation, oxidative stress, and reactive oxygen species, as well as the intermediates of xenobiotic metabolism. BPA and some chemotherapeutic drugs may also lead to the dysfunction of mitochondria. Mitochondria is the control point of the intrinsic apoptotic pathway that is modulated by Bcl-2 family proteins and results in cell death by cytochrome c and other proapoptotic effectors (18).

In our study, *p53* expression levels increased significantly in embryos exposed to BPA compared to the control group. Lloyd et al. (20) showed that BPA led to increased P53 protein levels through the western blot analysis method in the breast cancer cell line. Although cytolocalization of P53 was not affected by BPA administration, an increase in cell proliferation was observed. Jiang et al. (21) reported that BPA exposure increased the levels of casp 3, 8, 9, and 10 in the kidney and showed an apoptotic effect in rats with BPA added to their feed for five weeks. Xu et al. (22) studied the effect of BPA on ovarian granulosa cells in rats. They exposed ovarian granulosa cells to BPA for 24 hours to 72 hours and reported that BPA reduced the viability of granulosa cells in a dose- and time-dependent manner. Researchers have reported that BPA increases Bax expression and decreases Bcl2 expression in granulosa cells. These results show that low doses of BPA reduce the granulosa cell viability through the induction of apoptosis. It has been suggested that increased Bax expression and decreased Bcl2 are effectively involved in this apoptotic effect.

The mechanism of BPA-induced apoptosis may proceed through three distinct pathways: the DNA damage response signaling pathway, the mitogen-activated protein kinase (MAPK) signaling cascade, and the insulin-like growth factor-1 signaling pathway. In our previous study, we showed that BPA increased nitric oxide levels and decreased glutathione S-transferase and superoxide dismutase activities (5). Accordingly, increased oxidative stress may be the reason for increased *bax* and *casp8* expressions in the BPA group.

In our study, *ifng1* expression levels decreased significantly in BPA group embryos compared to the control group. Although structurally different from estrogen, BPA binds to estrogen receptor (ER) subtypes, especially ER-beta, with 6 times greater affinity. Immune system cells respond to sex hormones, including estrogen. Upon ER binding of estrogen, the ligand-receptor complex mediates the transcription activity of genes containing estrogen response elements (EREs). Estrogen regulates IFN-γ as well as the interleukin-10 (IL-10). The *ifn*-promoter contains sequences similar to ERE and estrogen has been reported to activate the production of IFN-γ (23). BPA has been shown to decrease IFN-γ levels in both male and female mice (24).

Üstündağ et al. (13) observed increased vitellogenin levels and *wnt3a* and *gsk3* expressions in zebrafish embryos exposed to BPA. They reported that increased apoptosis in embryos exposed to BPA can be because of Wnt3a-induced pro-apoptotic changes. However, in DEHP exposure, it has been suggested that Wnt3a has a lesser effect. In the same study, vitellogenin levels and apoptosis did not significantly increase in embryos exposed to DEHP. In the study by Üstündağ et al. (13), apoptosis was evaluated using the acridine orange method.

DEHP is toxic to zebrafish embryos and larvae and has been shown to cause developmental anomalies. It has been shown that DEHP exposure may lead to increased activity of estrogen under 1.50 ppm and that DEHP leads to ER transactivation (25). It has been shown in previous studies that DEHP can induce apoptosis and mitochondrial damage, break the DNA strand, and lead to reactive oxygen species (ROS) production. The damage to the DNA causes the weakening of the mitochondrial function regulator known as SIRT1, and thus suppressed ATP levels. ATP is needed for spermatozoa motility, therefore decreased ATP levels caused by DEHP have been accepted as a very important problem for male fertility (26). It has been reported that the toxic effects of DEHP on ovaries and follicles may occur due to apoptosis. For proper steroidogenesis regulation and to survive atresia, follicles should function properly. Atresia is suggested to be a naturally occurring apoptotic event that occurs with the death of follicles, which detrimentally affects the reproductive system. Atresia of ovarian follicles is regulated through proapoptotic factors, including Bad and Bax, and antiapoptotic factors, including Bcl2, which are usually inhibited due to DEHP exposure. Increased oxidative stress with DEHP may lead to follicular atresia. DEHP may lead to the inhibition of follicle growth through oxidative stress (27). In accordance with these reports in our study, we found that as a result of DEHP exposure, *bax* and *casp8* expressions increased in zebrafish embryos compared to the control group, and *casp3a*, *ifng1*, *fas*, and *tp53* expressions decreased. In addition, the expressions of *bax*, *casp3a*, *casp8*, *fas*, *ifng1*, and *tp53* decreased when embryos exposed to DEHP were compared with those exposed to BPA.

Cell death plays an important role in the regulation of inflammation and may also be observed as a result of inflammation. For the maintenance of tissue homeostasis, both the recognition and removal of invading pathogens, as well as the clearance of dying cells, are necessary (28). Although induction of apoptosis was not initially considered an action of IFNs, *in vitro* studies have shown that IFN-α, IFN-β or IFN-γ have induced characteristic apoptotic cell changes in the morphology of cells, such as rounding up and detachment of cells (29-31). In our study, increased *bax* and *casp8* expressions in the BPA and DEHP groups might be induced by IFN-γ, which in turn decreased after the induction of apoptosis. Activation of the caspase 8 cascade may lead to the release of cytochrome c from mitochondria, disrupt the mitochondrial potential, cause changes in the plasma membrane symmetry, and finally lead to DNA fragmentation (29-31).

In our study BPA and DEHP exposures did not change the crestin expressions. Neural crest cells develop in the third week of embryo development in humans. These cells are pluripotent in character and migrate to different places in the embryo to differentiate into different cell types. The migration of these cells is required for morphogenesis for the roles where they will function (32, 33). The development of the head and face region occurs as a result of more than one biological process, including the growth, proliferation, migration, and differentiation of neural crest cells (32, 33). The development of the neural crest occurs similarly to other vertebrate embryos in zebrafish embryos. However, since zebrafish embryos are transparent initially and have bigger but fewer neural crest cells than other species, in living embryos viable premature neural crest cells can be observed and manipulated (33). During embryogenesis, it is known that crestin is expressed in zebrafish. Crestin expression was first determined at the beginning of somitogenesis in neural crest cells of the ectoderm (33).

CONCLUSION

We have shown that as a result of BPA and DEHP exposure, while *casp3a*, *ifng1*, and *fas* expressions decreased, *bax* and *casp8* expressions increased in zebrafish embryos compared to the control group. *tp53* expression increased in BPA compared to the control group, but it decreased in the DEHP group. The expressions of *bax*, *casp3a*, *casp8*, *fas*, *ifng1*, and *tp53* decreased when embryos exposed to DEHP were compared with those exposed to BPA. An inverse relation between *ifng1* expression and apoptosis was observed by increased *bax* and *casp8* expressions in the BPA and DEHP groups. Accordingly, our study provided important data on the effects of EDCs on the relationship between inflammation and apoptosis.

BPA and DEHP exposures did not lead to a significant change in the crestin expressions of the embryos. However, this subject is open to research, as it is possible that different doses and different exposure durations may cause different results.

REFERENCES

1. Alabi OA, Ologbonjaye KI, Awosolu O, Alalade OE. Public and Environmental Health Effects of Plastic Wastes Disposal: A Review. J Toxicol Risk Assess 2019; 5: 021.

2. Sax L. Polyethylene terephthalate may yield endocrine disruptors. Environ Health Persp 2010; 118(4): 445-8.

3. Durusoy R, Karababa AO. Plastik gıda ambalajları ve sağlık. TAF Prevent Med Bull 2011; 10(1): 87-96.

4. Strakovsky RS, Schantz SL. Impacts of bisphenol A (BPA) and phthalate exposures on epigenetic outcomes in the human placenta. Environ Epigenet 2018; 4(3): 022.

5. Ustundag U, Unal İ , Ates P , Alturfan A , Yigitbasi T , Emekli-Alturfan E. Oxidant-Antioxidant Status and c-myc Expression in BPA- and DEHP-Exposed Zebrafish Embryos. Eur J Biol 2017; 76 (1): 26-30.

6. Mudbhary R, Sadler KC. Epigenetics, development, and cancer: zebrafish make their mark. Birth Defects Res C Embryo Today 2011; 93(2): 194-03.

7. Westerfield M. The Zebrafish Book, A Guide for the Laboratory Use of Zebrafish. University of Oregon Press, Oregon, USA (1995).

8. Lee YM, Rhee JS, Hwang DS, Kim IC, Raisuddin S, Lee JS. p53 gene expression is modulated by endocrine disrupting chemicals in the hermaphroditic fish, Kryptolebias marmoratus. Comp Biochem Physiol C Toxicol Pharmacol 2008; 147(2): 150-7.

9. Diamanti-Kandarakis E, Bourguignon JP, Giudice LC, Hauser R, Prins GS, Soto AM, et al. Endocrine-disrupting chemicals: An Endocrine Society scientific statement. Endocr Rev 2009; 30(4): 293-42.

10. Jocsak G, Ioja E, Kiss DS, Toth I, Barany Z, Bartha T, et al. Endocrine Disruptors Induced Distinct Expression of Thyroid and Estrogen Receptors in Rat versus Mouse Primary Cerebellar Cell Cultures. Brain Sci 2019; 5;9(12): 359.

11. Anway MD, Skinner MK. Transgenerational effects of the endocrine disruptor vinclozolin on the prostate transcriptome and adult onset disease. Prostate 2008; 68(5): 517-29.

12. Mayor R, Theveneau E. The neural crest. Development 2013; 140: 2247-51.

13. Üstündağ ÜV, Ünal İ, Ateş PS, Alturfan AA, Yiğitbaşı T, Emekli-Alturfan E. Bisphenol A and di(2-ethylhexyl) phthalate exert divergent effects on apoptosis and the Wnt/β-catenin pathway in zebrafish embryos: A possible mechanism of endocrine disrupting chemical action.Toxicol Ind Health 2017; 33(12): 901-10.

14. Livak KJ, Schmittgen TD. Analysis of relative gene expression data using real-time quantitative PCR and the 2(-Delta Delta C(T)) Method. Methods 2001; 25(4): 402-8.

15. Thisse C, Thisse B. High resolution in situ hybridization on wholemount zebrafish embryo. Nat Protoc 2008; 3: 59-69.

16. Lakind JS, Naiman DQ. Daily intake of bisphenol A and potential sources of exposure: 2005–2006 National Health and Nutrition Examination Survey. J Expo Sci Environ Epidemiol 2011; 21: 272-9.

17. Valentino R, D'Esposito V, Passaretti F, Liotti A, Cabaro S, Longo M, et al. Bisphenol-A impairs insulin action and up-regulates inflammatory pathways in human subcutaneous adipocytes and 3T3-L1 cells. PLoS ONE 2013; 8: e82099.

18. Shamas-Din A, Kale J, Leber B, Andrews DW. Mechanisms of action of Bcl-2 family proteins. Cold Spring Harb Perspect Biol 2013; 5(4): a008714.

19. Oka T, Adati N, Shinkai T, Sakuma K, Nishimura T, Kurose K. Bisphenol A induces apoptosis in central neural cells during early development of Xenopus laevis. Biochem Biophys Res Commun 2003; 312(4): 877-82.

20. Lloyd V, Morse M, Purakal B, Parker J, Benard P, Crone M, et al. Hormone-like effects of bisphenol A on p53 and estrogen receptor alpha in breast cancer cells, BioResearch Open Access 2019; 8(1): 169-84.

21. Jiang W, Zhao H, Zhang L, Wu B, Zha Z. Maintenance of mitochondrial function by astaxanthin protects against bisphenol A-induced kidney toxicity in rats. Biomed Pharmacother 2020; 121: 109629.

22. Xu J, Osuga Y, Yano T, Morita Y, Tang X, Fujiwara T, et al. Bisphenol A induces apoptosis and G2-to-M arrest of ovarian granulosa cells. Biochem Biophys Res Commun 2002; 292(2): 456-62.

23. Karpuzoglu-Sahin E, Zhi-Jun Y, Lengi A, Sriranganathan N, Ansar Ahmed S. Effects of long-term estrogen treat- ment on IFN-gamma, IL-2 and IL-4 gene expression and protein synthesis in spleen and thymus of normal C57BL/6 mice. Cytokine 2001; 14: 208-17.

24. Sawai C, Anderson K, Walser-Kuntz D. Effect of Bisphenol A on murine immune function: Modulation of interferon-γ, IgG2a, and disease symptoms in NZB × NZW F1 mice. Environ Health Perspect 2003; 111(16).

25. Chen X, Xu S, Tan T, Lee ST, Cheng SH, Lee FW, et al. Toxicity and estrogenic endocrine disrupting activity of phthalates and their mixtures. Int JEnv Res Pub He 2014; 11(3): 3156-68.

26. Li X, Fang EF, Scheibye-Knudsen M, Cui H, Qiu L, Li J, et al. Di-(2-ethylhexyl) phthalate inhibits DNA replication leading to hyperPARylation, SIRT1 attenuation, and mitochondrial dysfunction in the testis. Sci Rep 2014; 4: 6434.

27. Wang W, Craig ZR, Basavarajappa MS, Gupta RK, Flaws JA. Di (2-ethylhexyl) phthalate inhibits growth of mouse ovarian antral follicles through an oxidative stress pathway. Toxicol Appl Pharmacol 2012; 258(2): 288-95.

28. Yang Y, Jiang G, Zhang P, Fan J. Programmed cell death and its role in inflammation. Mil Med Res 2015; 2: 12.

29. Chawla-Sarkar M, Leaman DW, Borden EC. Preferential induction of apoptosis by interferon (IFN)-β compared with IFN-α2: Correlation with TRAIL/Apo2L induction in melanoma cell lines. Clin Cancer Res 2001; 7: 1821-31.

30. Morrison BH, Bauer JA, Kalvakolanu DV, Lindner DJ. Inositol hexakisphosphate kinase 2 mediates growth suppressive and apoptotic effects of interferon-beta in ovarian carcinoma cells. J Biol Chem 2001; 276: 24965-70.

31. Chen Q, Gong B, Mahmoud-Ahmed AS, Zhou A, Hsi ED, Hussein M, et al. Apo2L/TRAIL and Bcl2 related proteins regulate type I interferon induced apoptosis in mutiple myeloma. Blood 2001; 98: 2183-92.

32. Berke N, Keklikoğlu N. Nöral krest kökenli hücrelerin ağız ve çeneyüz oluşumuna katkilari ve neden oldukları anomaliler. JIUFD 2010; 44: 39-43.

33. Luo R, An M, Arduini BL, Henion PD. Specific pan-neural crest expression of zebrafish Crestin throughout embryonic development. Dev Dyn 2001; 220(2): 169-74.

ISTANBUL
UNIVERSITY
P R E S S

The Effects of a Probiotic (*Bacillus clausii*) in Acute Kidney Injury in a Rat Model of LPS-Induced Endotoxemia

Asli Kandil[1]

[1]Istanbul University, Faculty of Science, Department of Biology, Istanbul, Turkey

ORCID IDs of the authors: A.K. 0000-0001-8408-2610

ABSTRACT

Objective: This study aims to examine the role of a probiotic bacterium, *Bacillus clausii*, on oxidative stress in a lipopolysaccharide (LPS)-induced acute kidney injury (AKI) rat model.

Materials and Methods: The rats were divided into four groups: Control group, LPS group (1.5 mg/kg, LPS), Probiotic+LPS group in which LPS was given after administration of *Bacillus clausii* as a probiotic for 21 days, and Probiotic group. The kidneys of the rats were removed 24 hours after LPS injection. Total antioxidant status, total oxidant status, oxidative stress index, malondialdehyde and myeloperoxidase (MPO) values were biochemically determined in the kidneys. Furthermore, the kidney tissue samples were immunohistochemically stained for interleukin-6 (IL-6) and tumor necrosis factor (TNF)-α expression, and leukocyte distribution.

Results: Endotoxemia caused an increase in oxidative stress (p<0.001), lipid peroxidation (p<0.01), MPO activity (p<0.001), and the expression of IL-6 (p<0.001) and TNF-α (p<0.001). The administration of probiotic ameliorated oxidative stress, lipid peroxidation, and myeloperoxidase activity, and resulted in decreased IL-6 and TNF-α reactions that were elevated with LPS treatment.

Conclusion: The results suggest that *Bacillus clausii* as a probiotic bacterium may have an antioxidative property in LPS-induced AKI.

Keywords: Probiotic, acute kidney injury, endotoxemia, oxidative stress, *Bacillus clausii*

INTRODUCTION

Microbiota consists of various microorganisms (bacteria, fungi, and protozoa) (1). There is a symbiotic and mutualistic relationship between microorganisms in the gut microbiota and host (2). In mammals, the microbiota is composed mainly of four main phyla of eubacteria: Bacteroidetes, Firmicutes, Actinobacteria, and Proteobacteria (3, 4). The microbiota plays significant roles in various physiological events, such as protection against infection, recovery from disease, drug metabolism, nutritional status, and vitamin synthesis (3, 5).

The change in gut microbiota is called dysbiosis, leading to a disrupted interaction between host and microbes. The resulting systemic complications and disease may follow deterioration in microbiota homeostasis caused by excessive increase or depletion of specific bacterial species (6). Dysbiosis relates to several diseases such as obesity, diabetes, and inflammatory bowel and critical disease (7, 8). It was shown that the loss of "health promoting" bacteria and dysbiosis could contribute to infections, organ failure, and sepsis in the intensive care unit (ICU) (7). Some members of the gut microbiota generate anti-inflammatory molecules and proteins, while the microbiota can cause inflammatory responses. It is thought that the loss of useful microorganisms can disrupt nutrition in humans and trigger inflammatory responses. Hence, modification of the

microbiota composition can restore nutritional deficiencies and anti-inflammatory effects (9).

Probiotics have attracted attention as an opportunity to treat and prevent different diseases such as diabetes, obesity, allergies, and infections (10-12). In recent years, the question has been raised as to whether restoration of ICU patients through probiotics or synbiotics to interfere with the preservation and degradation of the microbiota would be an optimal interference to prevent infection and improve recovery.

The supplementation of probiotics offers a significant approach to critical illness therapy because of the important roles of microbiota in the modulation of nutrient production and absorption, and inflammation (9). Probiotics are live microorganisms which, when they are administered in adequate amounts, confer a health benefit on the host (13).

Different dietary supplements, functional foods, or probiotic strains that can be beneficial for human health have been designed. Data obtained from studies have supported the use of bacterial spore formers as probiotics and food supplements (14).

Bacillus spp., one of the spore-forming probiotics, are Gram-positive, aerobic or facultative anaerobic bacteria, and can survive in heat, acidic stomach, and other extreme environmental conditions (15-17). Therefore, spores of *Bacillus* spp. are generally used as probiotic preparations for different purposes (18).

Acute kidney injury (AKI) is a serious and common complication of sepsis in ICU patients (19). The pathophysiology of AKI in endotoxemic shock or sepsis is complex, and contains hemodynamic changes, inflammation, and damage. Moreover, sepsis-induced immune responses include the activation of both pro-inflammatory and anti-inflammatory events (20, 21). In the literature, it has been shown that the gut microbiota plays a role in kidney disease (22-25). Although the function of gut microbiota has been determined in kidney disease, the relationship between AKI and microbiota is not yet fully understood.

This study aimed to investigate the effects of the probiotic bacterium *Bacillus clausii* on renal oxidative stress in a lipopolysaccharide (LPS)-induced AKI model.

MATERIALS AND METHODS

Animals and Experimental Protocol
The experiments were designed with 27 male *Wistar albino* rats (3 months old, 300-400 g) supplied from Bezmiâlem Vakıf University, Istanbul, Turkey. The animals were allowed free access to a pelleted diet and tap water. The study was approved and reviewed by Bezmiâlem Vakıf University Animal Experiments Local Ethics Committee (Decision no: 2021/54).

The rats were divided into four groups. The control group (n=6) was injected intraperitoneally (ip) with 0.9% NaCl solution (physiological saline) after physiological saline was given by gavage for 21 days. In the LPS group (n=7), LPS (1.5 mg/kg LPS,

ip, *E. coli*, Serotip 0111: B4, Sigma, Missouri, USA) was injected ip after physiological saline was given by gavage for 21 days. In the Probiotic+LPS group (n=6), LPS was injected ip into animals after the administration of *B. clausii* (1.25 ml, 1×10^9 CFU per animal via gavage) as a commercial probiotic (Enterogermina®, Sanofi, Turkey) for 21 days. Probiotic group (n=8) was ip treated with physiological saline after *B. clausii* was given by gavage for 21 days. All applications were done at the same time every day.

The rats were anesthetized 24 hours after LPS injection. The kidney samples were removed for biochemical and immunohistochemical analyses.

Biochemical Analyses
The tissue samples were homogenized and centrifuged at 3000 rpm for 20 minutes at +4 ºC (Sorvall Super T21, Benchtop Centrifuge). The supernatants were collected from homogenates.

Total oxidant status (TOS) (µmol H_2O_2 eq/L), total antioxidant status (TAS) (mmol Trolox eq/L), and oxidative stress index (OSI) (arbitrary unit) were measured in the kidney tissues using commercial kits (Rel Assay Diagnostics; Gaziantep, Turkey).

Malondialdehyde (MDA) in the kidney was measured using the spectrophotometric method (26). The results were expressed as nmol/mg protein.

Myeloperoxidase (MPO) activity was measured according to the method of Krawisz et al. (1984) (27). The results were expressed as µmol/mL.

Protein levels in homogenate/postmitochondrial fractions were measured using the bicinchoninic acid reaction (28).

Immunohistochemical Analyses
The kidney samples were fixed in a neutral buffer formaldehyde solution, and histologically processed as previously described (29). The kidney sections (5 µm thick) were stained with tumor necrosis factor (TNF)-α (diluted 1/200) (Abcam ab66579), interleukin-6 (IL-6) (diluted 1/200) (Abcam, 6672), and MPO (diluted 1/75) (Thermo Fisher Scientific, RB-373-A) antibodies. The antibody staining was scored as previously described by Legrand et al. (29).

Statistical Analysis
Significant differences between groups were estimated using one-way ANOVA with Tukey's post-test using GraphPad Prism version 5.0 for Windows (GraphPad Software, San Diego, CA, USA). A value $p<0.05$ was considered statistically significant. The results were expressed as the mean±SEM.

RESULTS

Biochemical Results
TOS levels increased in renal tissues of LPS-injected animals ($p<0.001$), and diminished in the Probiotic+LPS group, but was high with respect to the control ($p<0.001$). In the Probiotic group, TOS levels elevated according to the control ($p<0.05$)
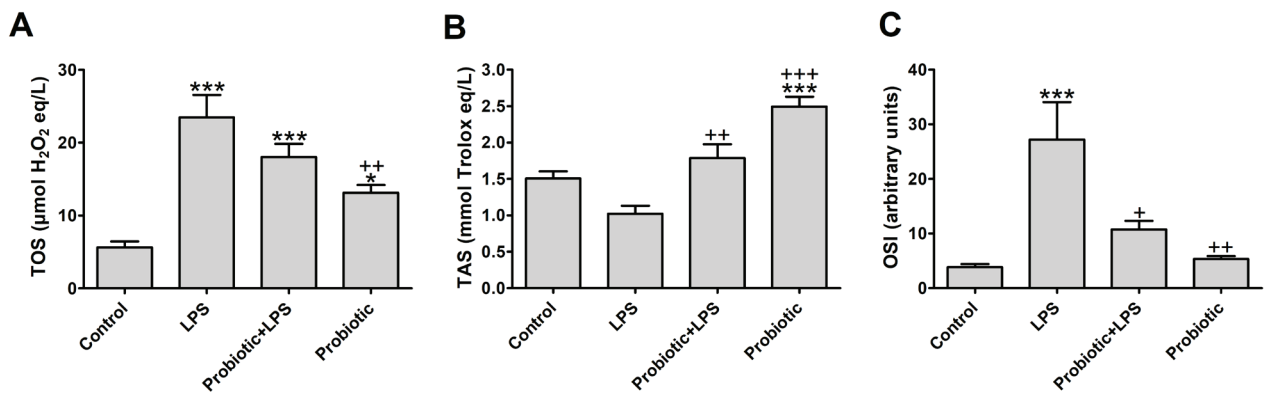
Figure 1. Effects of a probiotic bacterium *Bacillus clausii* on renal oxidative stress in lipopolysaccharide (LPS)-induced endotoxemia. (A) Kidney total oxidant status (TOS), (B) total antioxidant status (TAS) and (C) oxidative stress index (OSI) values in the experimental groups. ***$p<0.001$,*$p<0.05$ vs. Control group. +++$p<0.001$, ++$p<0.01$, +$p<0.05$ vs. LPS group.
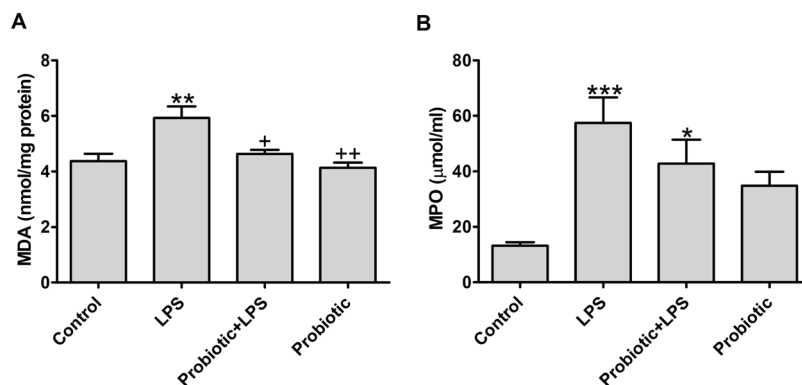
Figure 2. Effects of a probiotic bacterium *Bacillus clausii* on kidney malondialdehyde (MDA) levels (A) and myeloperoxidase (MPO) activity (B) in lipopolysaccharide (LPS)-induced endotoxemia. ***$p<0.001$, **$p<0.01$, *$p<0.05$ vs. Control group. ++$p<0.01$, +$p<0.05$ vs. LPS group.

(Figure 1A). TAS levels reduced in renal tissues of the LPS group. Administration of the probiotic caused an increase in TAS levels ($p<0.01$) in the Probiotic+LPS group. Moreover, TAS level was similar to the control group. TAS levels increased in the Probiotic group compared with the control group ($p<0.001$) (Figure 1B). OSI values increased ($p<0.001$) in the LPS group compared with the control group. In the Probiotic+LPS group, OSI values decreased compared with the LPS group ($p<0.05$). OSI values of probiotic treated groups were similar to the control (Figure 1C).

MDA levels increased in LPS-treated animals ($p<0.01$) and reduced in the Probiotic+LPS group ($p<0.05$) when compared to this group. MDA levels of the Probiotic+LPS and Probiotic groups resembled the control group (Figure 2A). MPO activity elevated in the LPS group ($p<0.001$) and diminished in the Probiotic+LPS group when compared to this group. In the Probiotic+LPS group, it was high with respect to the control group ($p<0.01$). MPO activity of the Probiotic group was higher than the control group, but it was not statistically significant (Figure 2B).

Immunohistochemical Results

IL-6 and TNF-α reaction and MPO-stained leukocytes are presented in Figure 3. LPS-induced endotoxemia caused an increase in TNF-α and IL-6 reactions in the kidney tissues ($p<0.001$). The probiotic administration decreased IL-6 ($p<0.001$) and TNF-α reaction ($p<0.01$) compared with the LPS group. The distribution of MPO-stained leukocytes was marked in both glomeruli and peritubular areas in the LPS groups ($p<0.001$) in comparison to the control group. The probiotic did not affect the distribution of MPO-stained leukocytes in the kidney tissue in LPS given animals (Figure 3).

DISCUSSION

AKI is an important health problem (19). Sepsis, endotoxemia, ischemia reperfusion, or nephrotoxins cause AKI (30). The fundamental interaction between kidney and gut microbiota is an important regulating factor in AKI (22, 23). Gut microbes are associated with physiological and pathophysiological processes
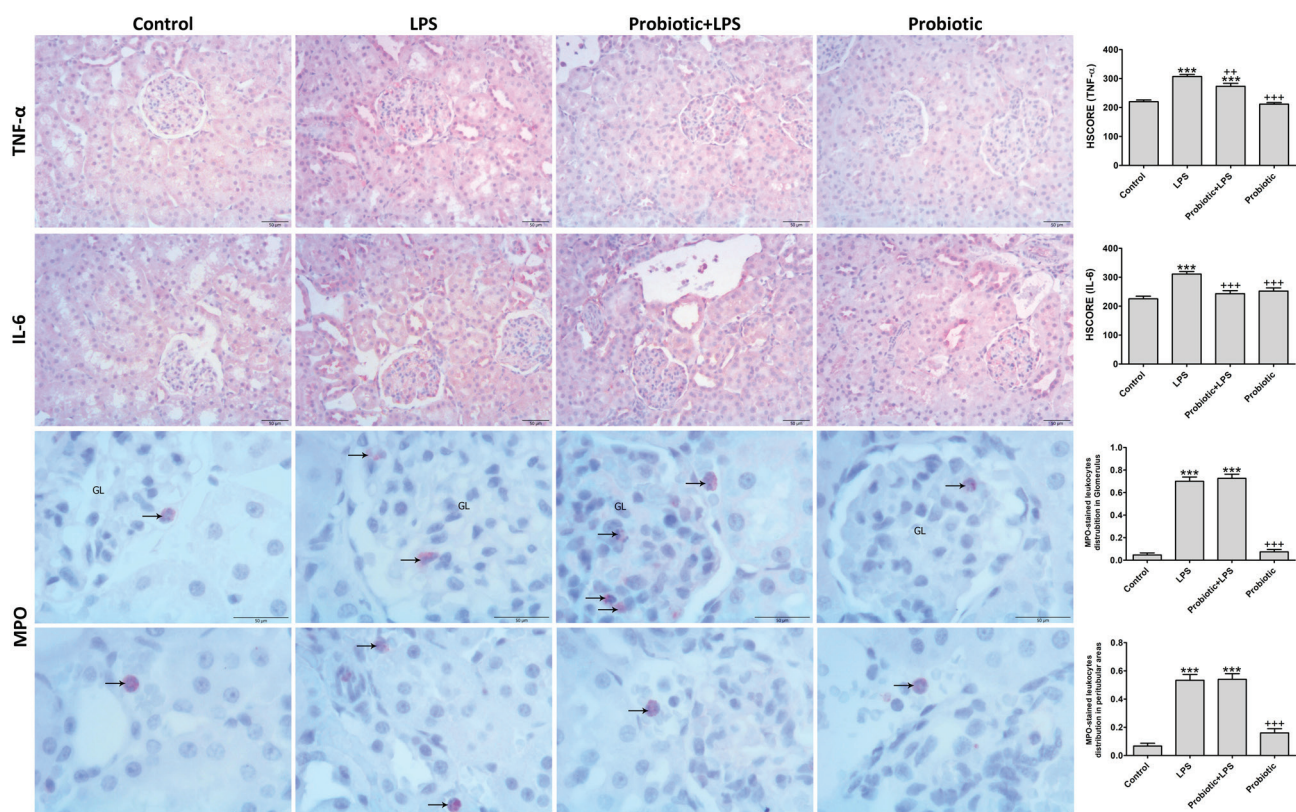
Figure 3. The immunoreactivity and distribution of tumor necrosis factor (TNF)-α, interleukin-6 (IL-6), and myeloperoxidase (MPO)-stained leukocytes (→) in kidney sections, and HSCORE values of immunoreactive reactions in the experimental groups. Bar: 50 μm. LPS: lipopolysaccharide. ***p<0.001 vs. Control group. +++p<0.001, ++p<0.01 vs. LPS group.

in the kidneys (23). Short chain fatty acids (SCFAs) that gut microbes produce improved sepsis-induced AKI (24) and reduced kidney damage and levels of reactive oxygen species and cytokines after kidney ischemia-reperfusion injury (25). Renal structural injury and functional decline following ischemia-reperfusion injury were more severe in germ-free mice compared with control mice (31). It was reported that severely abnormal gut microbiota in patients with renal failure led to aggravate kidney disease (32). Protecting the balance of the gut microbiota was stated to be important for ameliorating dysbiosis that results in immunological dysfunction, inflammation, and renal disease (23). Although the function of gut microbiota has been determined in kidney disease, the link between AKI and microbiota is not yet fully understood. Major advances in studies of the composition and functions of gut microbiota have opened up the opportunity for application of treatment strategies for AKI patients (22).

Changes in gut microbiota control metabolic endotoxemia characterized by translocation of lipopolysaccharides in systemic circulation, and induction of oxidative stress and inflammation in obesity and diabetes (12). Ávila et al. suggest that probiotics and fecal microbiota transplantation could present immunomodulatory advances and may be functional for treatment of pediatric septic patients (33). The different probiotics could reduce the oxidative damage and inflammation in intestines of animals with sepsis (33). Probiotics prevent intestinal and liver damage in sepsis induced with administration of LPS and D-galactosamine (11). The selected probiotic isolates reduced the LPS-caused inflammation in murine macrophage cell line (34). *Lactobacillus salivarius* reduced inflammation and oxidative stress in cisplatin-induced AKI. These effects were partially mediated by modulating the gut environment (35). In a rat study of sepsis that was induced by injection of LPS after the administration of *Lactobacillus rhamnosus gg* as probiotic (1×10^7 CFU/day) for 10 days, the probiotic was revealed to have exerted protective effects (36). Similarly, LPS induced oxidative stress and inflammation in the present study. Moreover, the pre-treatment with a probiotic prevented oxidative stress, and exerted protective effects in endotoxemia that was induced by LPS. The probiotic administration after LPS treatment induced a humoral immune response by increasing the levels of immunoglobulins E, A, G, and M (37).

A number of *Bacillus* strains as probiotic have been studied for their potential functions *in vivo* and *in vitro* models (38, 39). *B. clausii* is an endospore-forming, gram-positive, facultative alkaliphilic rod bacterium (15), and is able to grow under aerobic and anaerobic conditions and survive gastric acidity (16, 17). The role of the *Bacillus* species ranges from the probiotic nature

of *B. clausii, B. subtilis, B. pumilus, B. coagulans* and other strains, to biological control agents (*B. sphaericus* and *B. thuringiensis*) and pathogenicity (*B. cereus* and *B. anthracis*) (18). The effects of *B. clausii* have been associated with antimicrobial and immunomodulatory properties (40). *B. clausii* had a role in production of pro-inflammatory and anti-inflammatory cytokines (41). Furthermore, *B. clausii* strains release antimicrobial substances (40). The probiotic *B. clausii* strain inhibits the cytotoxic effects caused by *B. cereus* and *Clostridium difficile* toxins (38). *B. clausii* may reveal immunomodulating activity in nasal lavage of allergic children (10). *B. clausii* inhibited secretion of pro-inflammatory cytokines and reactive oxygen species production in rotavirus-infected cells (39). It was demonstrated that pretreatment with probiotic capsules of *Bacillus* species spores caused a significant decrement in pro-inflammatory cytokines (42). Treatment with *B. clausii* UBBC07 importantly attenuated oxidative stress by increasing catalase and SOD, and decreasing MDA in acetaminophen-induced uremia in rats (43). In our study, the treatment with *B. clausii* importantly ameliorated the oxidative stress and lipid peroxidation caused by LPS injection.

Current data showed that Enterogermina, a spore-based probiotic formulation of *Bacillus spp.*, is a trusted probiotic to manage acute diarrhea and intestinal infections (44) and to decrease anti-*Helicobacter pylori* treatment (45, 46), and exhibits immunomodulatory and antimicrobial activities (10, 40).

In the study, the effects of probiotic *B. clausii*, marketed as Enterogermina®, on rat kidneys were examined in LPS-induced AKI. Similar to current data, the present study indicated that probiotic *B. clausii* has antioxidant and anti-inflammatory properties. The results revealed that LPS gave rise to increase TOS and decrease TAS. It can be said that LPS-induced endotoxemia caused oxidative stress as indicated with an increase in the oxidative stress index. Furthermore, it was found that endotoxemia increased the levels of lipid peroxidation and inflammation in the kidney tissue. In addition, expression of pro-inflammatory cytokines such as TNF-α and IL-6 and leukocytes infiltration was determined in kidney tissues of endotoxemic rats. The pre-treatment with *B. clausii* ameliorated the oxidative stress, lipid peroxidation, and inflammation, and decreased expression of pro-inflammatory cytokines in LPS-induced endotoxemic rats. However, probiotic treatment did not affect the distribution of leukocytes in kidney tissues.

CONCLUSION

Our results suggested that probiotic *B. clausii* may have an antioxidative and anti-inflammatory property in LPS-induced AKI. Therefore, the present study supports the efficacy of *B. clausii* in the attenuation of LPS-induced AKI. Nevertheless, further studies should be performed to determine the exact role and effect mechanisms of this probiotic in kidney disease.

Peer-review: Externally peer-reviewed.

Conflict of Interest: The author declares that she has no conflicts of interest to disclose.

REFERENCES

1. Cani PD. Human gut microbiome: hopes, threats and promises. Gut 2018; 67(9): 1716-25.
2. Eloe-Fadrosh EA, Rasko DA. The human microbiome: from symbiosis to pathogenesis. Annu Rev Med 2013; 64: 145-63.
3. Turnbaugh PJ, Ley RE, Hamady M, Fraser-Liggett CM, Knight R, Gordon JI. The human microbiome project. Nature 2007; 449(7164): 804-10.
4. Rinninella E, Raoul P, Cintoni M, Franceschi F, Miggiano GAD, Gasbarrini A, et al. What is the healthy gut microbiota composition? A changing ecosystem across age, environment, diet, and diseases. Microorganisms 2019; 7(1): 14.
5. Levy M, Blacher E, Elinav E. Microbiome, metabolites and host immunity. Curr Opin Microbiol 2017; 35: 8-15.
6. Petersen C, Round JL. Defining dysbiosis and its influence on host immunity and disease. Cell Microbiol 2014; 16(7): 1024-33.
7. Wischmeyer PE, McDonald D, Knight R. Role of the microbiome, probiotics, and 'dysbiosis therapy' in critical illness. Curr Opin Crit Care 2016; 22(4): 347-53.
8. Kho ZY, Lal SK. The human gut microbiome - A potential controller of wellness and disease. Front Microbiol 2018; 9: 1835.
9. Davison JM, Wischmeyer PE. Probiotic and synbiotic therapy in the critically ill: State of the art. Nutrition 2019; 59: 29-36.
10. Ciprandi G, Tosca MA, Milanese M, Caligo G, Ricca V. Cytokines evaluation in nasal lavage of allergic children after *Bacillus clausii* administration: a pilot study. Pediatr Allergy Immunol 2004; 15(2): 148-51.
11. Ewaschuk J, Endersby R, Thiel D, Diaz H, Backer J, Ma M, et al. Probiotic bacteria prevent hepatic damage and maintain colonic barrier function in a mouse model of sepsis. Hepatology 2007; 46(3): 841-50.
12. Cani PD, Bibiloni R, Knauf C, Waget A, Neyrinck AM, Delzenne NM, et al. Changes in gut microbiota control metabolic endotoxemia-induced inflammation in high-fat diet-induced obesity and diabetes in mice. Diabetes 2008; 57(6): 1470-81.
13. FAO/WHO working group report on drafting guidelines for the evaluation of probiotics in food London, Ontario, Canada, April 30 and May 1, 2002.
14. Elshaghabee FMF, Rokana N, Gulhane RD, Sharma C, Panwar H. *Bacillus* as potential probiotics: status, concerns, and future perspectives. Front Microbiol 2017; 8: 1490.
15. Cenci G, Trotta F, Caldini G. Tolerance to challenges miming gastrointestinal transit by spores and vegetative cells of *Bacillus clausii*. J Appl Microbiol 2006; 101(6): 1208-15.
16. Jenson I., Encyclopedia of food microbiology (Second Edition), Editor(s): Carl A. Batt, Mary Lou Tortorello, Bacillus, Introduction, London, Academic Press, 2014, Pages 111-7.
17. Delbrassinne L., Mahillon J., Encyclopedia of food and health, Editor(s): Benjamin Caballero, Paul M. Finglas, Fidel Toldrá, Bacillus: Occurrence, Academic Press, 2016, Pages 307-11.
18. Khatri I, Sharma G, Subramanian S. Composite genome sequence of *Bacillus clausii*, a probiotic commercially available as Enterogermina®, and insights into its probiotic properties. BMC Microbiol 2019; 19(1): 307.
19. Hoste EA, Bagshaw SM, Bellomo R, Cely CM, Colman R, Cruz DN, et al. Epidemiology of acute kidney injury in critically ill patients: the multinational AKI-EPI study. Intensive Care Med 2015; 41(8): 1411-23.
20. Zarbock A, Gomez H, Kellum JA. Sepsis-induced acute kidney injury revisited: pathophysiology, prevention and future therapies. Curr Opin Crit Care 2014; 20(6): 588-95.

21. Gómez H, Kellum JA. Sepsis-induced acute kidney injury. Curr Opin Crit Care 2016; 22(6): 546-53.

22. Rabb H, Pluznick J, Noel S. The microbiome and acute kidney injury. Nephron 2018; 140(2): 120-3.

23. Stavropoulou E, Kantartzi K, Tsigalou C, Konstantinidis T, Romanidou G, Voidarou C, et al. Focus on the gut-kidney axis in health and disease. Front Med (Lausanne) 2021; 7: 620102.

24. Al-Harbi NO, Nadeem A, Ahmad SF, Alotaibi MR, Al Asmari AF, Alanazi WA, et al. Short chain fatty acid, acetate ameliorates sepsis-induced acute kidney injury by inhibition of NADPH oxidase signaling in T cells. Int Immunopharmacol 2018; 58: 24-31.

25. Andrade-Oliveira V, Amano MT, Correa-Costa M, Castoldi A, Felizardo RJ, de Almeida DC, et al. Gut bacteria products prevent AKI induced by ischemia-reperfusion. J Am Soc Nephrol 2015; 26(8): 1877-88.

26. Ohkawa H, Ohishi N, Yagi K. Assay for lipid peroxides in animal tissues by thiobarbituric acid reaction. Anal Biochem 1979; 95(2): 351-8.

27. Krawisz JE, Sharon P, Stenson WF. Quantitative assay for acute intestinal inflammation based on myeloperoxidase activity. Assessment of inflammation in rat and hamster models. Gastroenterology 1984; 87(6): 1344-50.

28. Smith PK, Krohn RI, Hermanson GT, Mallia AK, Gartner FH, Provenzano MD, et al. Measurement of protein using bicinchoninic acid. Anal Biochem 1985; 150(1): 76-85.

29. Legrand M, Bezemer R, Kandil A, Demirci C, Payen D, Ince C. The role of renal hypoperfusion in development of renal microcirculatory dysfunction in endotoxemic rats. Intensive Care Med 2011; 37(9): 1534-42.

30. Bonavia A, Singbartl K. A review of the role of immune cells in acute kidney injury. Pediatr Nephrol 2018; 33(10): 1629-39.

31. Jang HR, Gandolfo MT, Ko GJ, Satpute S, Racusen L, Rabb H. Early exposure to germs modifies kidney damage and inflammation after experimental ischemia-reperfusion injury. Am J Physiol Renal Physiol 2009; 297(5): F1457-65.

32. Wang X, Yang S, Li S, Zhao L, Hao Y, Qin J, et al. Aberrant gut microbiota alters host metabolome and impacts renal failure in humans and rodents. Gut 2020; 69(12): 2131-42.

33. Ávila PRM, Michels M, Vuolo F, Bilésimo R, Burger H, Milioli MVM, et al. Protective effects of fecal microbiota transplantation in sepsis are independent of the modulation of the intestinal flora. Nutrition 2020; 73:110727.

34. Khanna S, Bishnoi M, Kondepudi KK, Shukla G. Isolation, characterization and anti-inflammatory mechanism of probiotics in lipopolysaccharide-stimulated RAW 264.7 macrophages. World J Microbiol Biotechnol 2020; 36(5): 74.

35. Lee TH, Park D, Kim YJ, Lee I, Kim S, Oh CT, et al. *Lactobacillus salivarius* BP121 prevents cisplatininduced acute kidney injury by inhibition of uremic toxins such as indoxyl sulfate and pcresol sulfate via alleviating dysbiosis. Int J Mol Med 2020; 45(4): 1130-40.

36. Yılmaz M, Erdem AO. The protective role of probiotics in sepsis-induced rats. Ulus Travma Acil Cerrahi Derg 2020; 26(6): 843-6.

37. Kadafi KT, Wibowo S. Differences in systemic humoral immune response among Balb/c mice administered with probiotic, LPS *Escherichia coli*, and probiotic-LPS *E. coli*. Iran J Microbiol 2019; 11(4): 294-9.

38. Ripert G, Racedo SM, Elie AM, Jacquot C, Bressollier P, Urdaci MC. Secreted compounds of the probiotic *Bacillus clausii* strain O/C inhibit the cytotoxic effects induced by *Clostridium difficile* and *Bacillus cereus* toxins. Antimicrob Agents Chemother 2016; 60(6): 3445-54.

39. Paparo L, Tripodi L, Bruno C, Pisapia L, Damiano C, Pastore L, et al. Protective action of *Bacillus clausii* probiotic strains in an in vitro model of Rotavirus infection. Sci Rep 2020; 10(1): 12636.

40. Urdaci MC, Bressollier P, Pinchuk I. *Bacillus clausii* probiotic strains: antimicrobial and immunomodulatory activities. J Clin Gastroenterol 2004; 38(6 Suppl): S86-90.

41. Di Caro S, Tao H, Grillo A, Franceschi F, Elia C, Zocco MA, et al. *Bacillus clausii* effect on gene expression pattern in small bowel mucosa using DNA microarray analysis. Eur J Gastroenterol Hepatol 2005; 17(9): 951-60.

42. Neag MA, Catinean A, Muntean DM, Pop MR, Bocsan CI, Botan EC, et al. Probiotic Bacillus spores protect against acetaminophen induced acute liver injury in rats. Nutrients 2020; 12(3): 632.

43. Patel C, Patel P, Acharya S. Therapeutic prospective of a spore-forming probiotic-*Bacillus clausii* UBBC07 against acetaminophen-induced uremia in rats. Probiotics Antimicrob Proteins 2020; 12(1): 253-8.

44. Mazza, P. The use of *Bacillus subtilis* as an antidiarrhoeal microorganism. Bollettino chimico farmaceutico 1994; 133.1: 3-18.

45. Nista EC, Candelli M, Cremonini F, Cazzato IA, Zocco MA, Franceschi F, et al. *Bacillus clausii* therapy to reduce side-effects of anti-*Helicobacter pylori* treatment: randomized, double-blind, placebo controlled trial. Aliment Pharmacol Ther 2004; 20(10): 1181-8.

46. Plomer M, Iii Perez M, Greifenberg DM. Effect of *Bacillus clausii* capsules in reducing adverse effects associated with *Helicobacter pylori* eradication therapy: A randomized, double-blind, controlled trial. Infect Dis Ther 2020; 9(4): 867-78.

Evaluation of the Relationship between Epiphytic Diatoms and Water Quality Parameters in the Büyükçekmece Reservoir

Tumer Orhun Aykut[1] ⓘ**, Neslihan Balkis-Ozdelice[2]** ⓘ**, Turgay Durmus[2]** ⓘ**,
Cuneyt Nadir Solak[3]** ⓘ

[1]Istanbul University, Institute of Science, Istanbul, Turkey
[2]Istanbul University, Faculty of Science, Department of Biology, Istanbul, Turkey
[3]Kütahya Dumlupınar University, Faculty of Arts and Sciences, Kütahya, Turkey

ORCID IDs of the authors: T.O.A. 0000-0002-0791-8127; N.B.O. 0000-0001-8030-7480; T.D. 0000-0002-8242-1823;
C.N.S. 0000-0003-2334-4271

ABSTRACT

Objective: In this study carried out in Büyükçekmece Reservoir, the composition, distribution, seasonal changes of epiphytic diatoms that live on the surfaces of plants, and the effects of environmental parameters on these organisms were investigated, and it was aimed to reveal the water quality of the reservoir.

Materials and Methods: In order to determine the seasonal changes of epiphytic diatom species in Büyükçekmece Reservoir, water and material samples were collected from five stations in 2019. In the study, water temperature, salinity, conductivity, dissolved oxygen, and pH values, which are among the basic ecological variables, were measured. Epiphytic diatom samples were obtained from *Phragmites* sp. species. Also, Spearman's rank correlation, Shannon–Weaver diversity index, Cluster (Bray–Curtis and Euclidean Distance), and ordination analysis (DCA and CCA) were applied in the study.

Results: 66 epiphytic diatom species were identified in this study, and 36 of these species are new records for the reservoir. Most epiphytic diatom species were obtained in August, and the lowest number was obtained in November. According to the pH values, it was determined that the reservoir is alkaline. In addition, it was determined that the main factors affecting the distribution of epiphytic diatom species in the reservoir are temperature and conductivity, and it was revealed that ecological variables affect species distribution.

Conclusion: According to conductivity and DO values, it was determined that the reservoir was of very good and of good quality, and in terms of DO values, the reservoir was mainly oligotrophic. However, station 5 was mesotrophic during the August sampling period, station 4 was mesotrophic, and station 5 was eutrophic in November. Also, Büyükçekmece Reservoir was found in poor and moderate status according to *H'* classification.

Keywords: Epiphytic diatom, Bacillariophyceae, Correlation, Water quality, Istanbul, Turkey

INTRODUCTION

Diatoms (Bacillariophyceae) are among the unicellular, microscopic groups of algae with high distribution in freshwaters. Their existence on Earth, dating back 185 million years ago, has been proven by the fossil records

(1). Diatoms are responsible for almost 20-25% of the oxygen produced on Earth in aquatic ecosystems (2). Diatoms constitute the vast majority of benthic algae species in freshwater and seas (3,4), and they are distributed in almost all habitats. Due to their high tolerance range against environmental factors, they

spread in a wide variety of aquatic environments (5-7). In their environment, they play an important role in the food chain for other aquatic organisms (8). By taking part in the carbon cycle through the photosynthesis process they perform, these organisms present in the photic zone play a key role in the elimination of atmospheric greenhouse gases that significantly contribute to global warming (9). They are used in biological monitoring studies because they respond to environmental parameters and the changes of these parameters faster than other living things. The presence of diatoms in all kinds of aquatic ecosystems, their ability to reach a high number of species even in small areas, including polluted and clean waters, and easy sampling are why they are preferred for comparing aquatic ecosystems with each other.

In recent years, the growths in industrialization, the excessive proliferation of the human population, and human insensitivity to the ecosystem have brought many environmental problems. It is worrying for humanity that freshwater reserves necessary for life are rapidly depleted or have become unusable. Protection of surface water resources and monitoring water pollution are among the priority points of many countries. For this reason, the use of biological organisms has increased in recent years in monitoring water pollution situations. Many countries have defined the biological quality steps by continuously following their current water potentials and have developed a national water quality system to monitor these resources in certain periods. While European Union member countries carry out these studies within the scope of the EU Water Framework Directive (WFD) (10), in Turkey, according to the Water Pollution Control Regulation (11) and the Surface Water Quality Control Regulation (12), determinations can be made about the water quality status of the resources. Although the commonly used parameters are various basic ecological variables such as water temperature, pH, dissolved oxygen, and nutrients, the excessive increase or decrease of some biological groups depending on these variables are observed. In particular, species composition and the abundance status of diatoms change depending on these variables and are used as an important indicator in determining the trophic status of lakes (13-16).

When the studies carried out in Büyükçekmece Reservoir are evaluated, it has been seen that the studies include all algae groups which are generally living in benthic and pelagic plankton (17–24). Also, studies on benthic algae have also been carried out, and it has been revealed that the diatoms are dominant organisms compared to the other groups in terms of the number of species in all of the studies. Among these studies, Temel (17) conducted a study on epipelic algae in the reservoir and defined the benthic flora of the lake as very poor in terms of species and abundance. The same researcher studied epiphytic and epilithic algae in another study and reported that 43 diatom species were encountered in the epiphytic habitat in the Büyükçekmece Reservoir (18). In addition to these studies carried out in the reservoir, the importance of the water catchment areas is another reason for this study. Lakes, one of the most important freshwater reserves, are important natural areas with

many features such as their biological life and their roles in fishing, recreation, tourism, and the hydrological cycle. Since the water catchment basins of the reservoirs are wider than natural lakes, they are more affected by the pollution in the basin. Therefore, it is necessary to carry out monitoring studies, especially in areas where drinking water is supplied (25). In this context, in this study carried out in Büyükçekmece Reservoir, the composition, distribution, seasonal changes of epiphytic diatoms that survive on plants, and the effects of environmental parameters on these organisms were investigated, and it was aimed to reveal the water quality of the reservoir.

MATERIALS AND METHODS

Study Area
While Büyükçekmece Reservoir was one of the coastal lagoons of the Sea of Marmara until 1989, it was disconnected from the sea with an earth-filled embankment and took its current form (26). The reservoir, which is one of the drinking water resources of Istanbul today, is located between the Büyükçekmece, Çatalca, and Esenyurt districts on the European continent of Istanbul. The surface area of this reservoir, which is 2 km wide and 7 km long, is 43 km^2. 400,000 m^3 of drinking water is obtained per day from the reservoir, which has a maximum water accumulation volume of approximately 149×10^6 m^3 (27).

Sampling and Analysis of Biotic and Abiotic Variables
In order to determine the seasonal changes of epiphytic diatom species in the Büyükçekmece Reservoir, water and material samples were collected from five stations in 2019 (February, May, August and November) (Figure 1). The main ecological variables of the environment; water temperature, salinity, conductivity, dissolved oxygen, (DO) and pH values; were measured during the field studies with the YSI–556 model multiprobe.

Diatom samples were obtained by taking 10 cm long sections from the part of the *Phragmites* sp. species within the water and 30 cm below the water surface. In November, it was observed that the water level in the reservoir decreased by up to 40% (28). In this season, since *Phragmites* sp. was not found within the water in stations except for station 2, no epiphytic diatom sampling was performed at other stations. The sections taken from the *Phragmites* sp. species were repeated as three replications for each station. These sections, which were taken into plastic containers with 100 ml of distilled water, were shaken moderately to mix the diatom species with the water, and 4% formaldehyde (buffered with borax) was added to ensure fixation (29). The samples brought to the laboratory immediately after the field study were kept at room temperature.

Pre-Treatment of Diatom Samples, Preparations of Permanent Slides and Identification
Diatom frustules were burned and permanent slides prepared according to Hendey (30) and Battarbee et al. (31). Accordingly, in order to eliminate the organic material in the cells, the samples were first kept in a 10% hydrochloric acid (HCl) solution overnight and then washed with distilled water. Then, hydrogen peroxide (H$_2$O$_2$) was added to the samples on a hotplate,
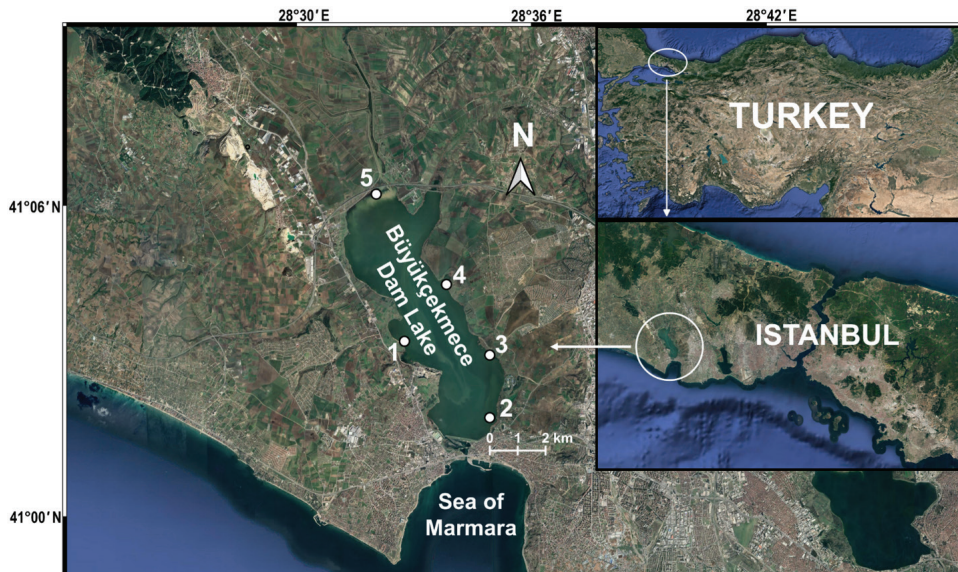
Figure 1. Sampling area and location of stations in the Büyükçekmece Reservoir.

the samples were boiled at 150°C for about 5 hours, and their SiO_2-containing skeletons were exposed. Naphrax was used in the preparation of permanent slides, and the prepared slides were examined under an Olympus BX51 light microscope at ×1000 magnification. In the identification of the species, Hustedt (32), Patrick and Reimer (33,34), Round et al. (2), and Krammer and Lange–Bertalot (35-38) were used. For each sample from the permanent slides prepared for counting, 300 diatom frustules were counted randomly under the microscope, and the relative abundance of the species was computed as a percentage.

Statistical Analysis of the Biotic and Abiotic Variables

Spearman's rank correlation was used in determining the relationship between biotic and abiotic variables (39), Shannon–Weaver diversity index (40) was used in determining the species diversity of stations, and Bray–Curtis similarity analysis was used in determining the similarity of stations according to epiphytic diatom species and individual numbers. Euclidean Distance was used in determining the similarity of stations in terms of ecological variables (41). Before clustering analysis, Bray–Curtis (log x + 1) and Euclidean Distance (Normalisation) data were transformed. From statistical analysis, Spearman's rank correlation was analyzed in the SPSS v.25 package program, while Shannon–Weaver diversity index, Bray–Curtis similarity analysis, and Euclidean Distance were analyzed in the Primer v.6 programs.

Ordination analysis was carried out to reveal the relationship between environmental variables and the relative abundance data of the species. While the method was preferred, firstly, the detrended corresponding analysis (DCA) stated by Lepš and Šmilauer (42) was employed by means of the PC–ORD 6.0 program (43). As the longest gradient was obtained as 4.002 (Axis 1, *Eigenvalue*: 0.81737) as a result of DCA analysis, the direct gra-

dient analysis canonical correspondence analysis (CCA) was preferred for ordination analysis. The first two CCA axes explained a total of 37.9% of the cumulative variance in species data, and the correlation between the response variable (epiphytic diatoms) and the predictive variables (ecological parameters) was determined as 93.5%. Environmental variables used in CCA were tested in the SPSS 25.0 program with the Monte Carlo test (with 499 permutations) (p<0.05). The abundance data of diatoms were analyzed by including all sampling periods and species with an observation frequency of "> 5%" at stations (42), and the CCA ordination diagram was drawn in the PAST 4.0 program (44). In addition, according to the Surface Water Quality Control Regulation (12), the water quality classes and trophic status of the reservoir were revealed. Also, the ecological status of the reservoir has been classified according to Molvær et al. (45), and this classification was based on H' values. In this classification, they have been classified into 5 ecological groups as follows: "High status" > 3.8; "Good status" 3.0–3.8; "Moderate status" 1.9–3.0; "Poor status" 0.9–1.9; "Bad status" < 0.9.

RESULTS

Ecological Variables

Results of ecological variables recorded at five stations in Büyükçekmece Reservoir are given in Figure 2. In the measurements performed in the reservoir, it was recorded that the water temperature was between 5.01-26.65°C. The lowest water temperature was measured at station 3 in the February sampling, and the highest water temperature was measured at station 4 in the August sampling. The values measured in the February sampling are much lower than in the other sampling periods. The highest water temperature in this period was determined as 5.64°C. During the sampling periods, the highest water temperature variation between stations was observed in the May sampling. Considering the salinity values of the lake during the
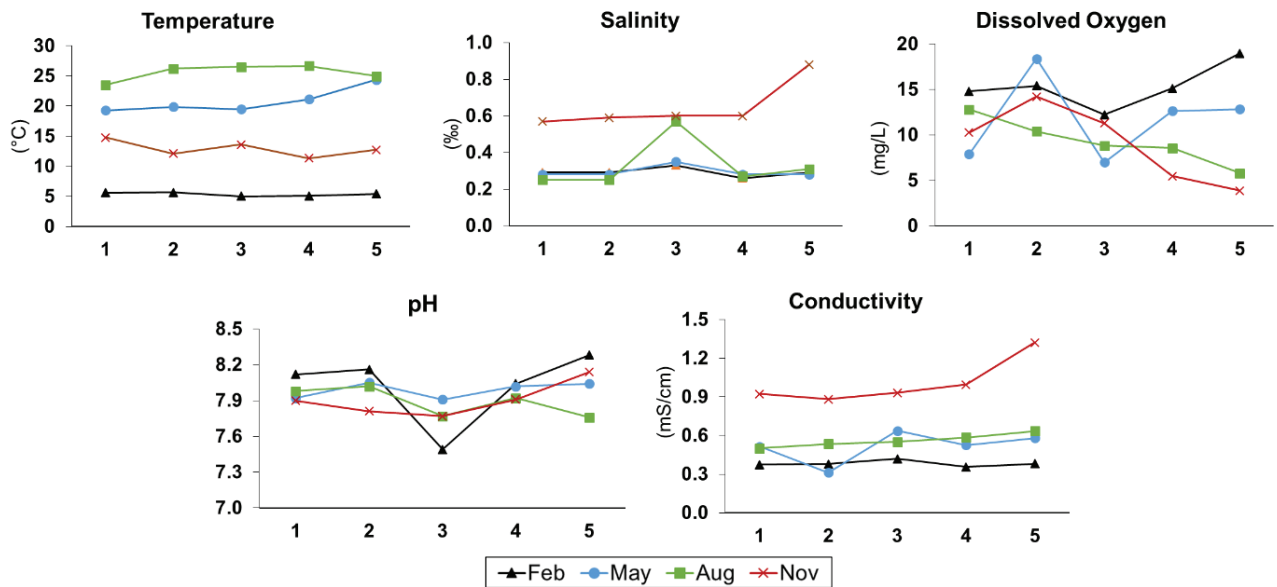
Figure 2. Changes of ecological variables in the Büyükçekmece Reservoir.

year, it was observed that it was below 1% in all sampling periods and varied between 0.25-0.88 ‰. The lowest value was measured from stations 1 and 2 in the August period, and the highest value was measured from station number 3 in November. During the study, it was observed that the salinity rate of the reservoir was higher in the November sampling, which is the period when the occupancy rate of the reservoir is the lowest, compared to other periods. Dissolved oxygen (DO) values were recorded between 3.87 and 18.96 mg/L. The lowest DO value was measured from station 5 in the November sampling, and the highest value was measured from station 5 in the February sampling.

Conductivity in water was measured as 0.312-1.322 mS/cm between sampling periods. The lowest conductivity was recorded at station 2 in the May sampling, and the highest was recorded at station 5 in the November sampling. The highest conductivity difference between the stations was obtained in the November sampling. As the pH values in the reservoir varied between 7.49 and 8.28, it was determined that the reservoir is of alkaline characteristics. The highest (St.5) and lowest (St.3) pH values were measured in the February sampling, and the highest pH difference between stations was observed in this period.

Epiphytic Diatoms Composition and Abundance
In this seasonal study conducted in Büyükçekmece Reservoir, 66 epiphytic diatom species were identified, 5 of which were genus level (Figure 3-5). In the study, one (1.5%) species from centric diatom and 65 (98.5%) species from pennate diatoms were obtained (Table 1). 36 of the identified species are new records for the reservoir, and the genera *Eunotia*, *Geissleria*, *Hippodonta*, and *Tabularia* were reported for the first time with this study (Table 1). Most species in the study belonged to *Navicula* (8 species), followed by *Gomphonema* (7 species) and

Cymbella (6 species). While the highest number of epiphytic diatom species was obtained in August (43 species) and May (38 species), fewer species numbers were obtained in February (28 species) and November (25 species).

When the number of species obtained at stations was evaluated, the highest number of species was obtained from station 5 (18 species), and the lowest number of species was obtained from station 3 (5 species) in the February sampling. During this sampling period, *Fragilaria vaucheriae*, *Fragilaria* sp.2, and *Gomphonella olivacea* were found in all stations (100%). When evaluated in terms of relative abundance (Figure 6a), it was determined that *G. olivacea* was dominant in all stations (>49%) and reached the highest abundance (74%) at station 1. In the study, *Fragilaria* sp.1, *Gomphonema* sp., *Navicula capitatoradiata*, *Nitzschia intermedia*, and *Tabularia fasciculata* were observed only in this period, and their relative abundance at the stations where they were observed remained below 2%. During this period, a total of 8 cells were found at station 3, and the targeted 300 cells in terms of relative abundance could not be reached. Among the obtained cells, *G. olivacea* (50%) was found to be dominant as in other stations.

In the May sampling, the highest number of species was obtained from station 4 (21 species) and the least number of species from station 2 (12 species). During this period, *Achnanthidium* sp., *Cymbella affinis*, *Encyonopsis minuta*, *Fragilaria perminuta*, and *Gomphonema pumilum* were recorded from all stations and in terms of relative abundance (Figure 6b). *Cymbella lange-bertalotii* (34%) at station 1, *C. affinis* (56%) at station 2, *Achnanthidium* sp. (40%) at station 3, *Encyonema auerswaldii* at station 4 (22%), and *G. pumilum* (29%) at station 5 were observed to be dominant. *Eunotia bilunaris*, *Geissleria decussis*, *Hippodonta hungarica*, *Navicula novaesiberica*, and *Tryblionella*
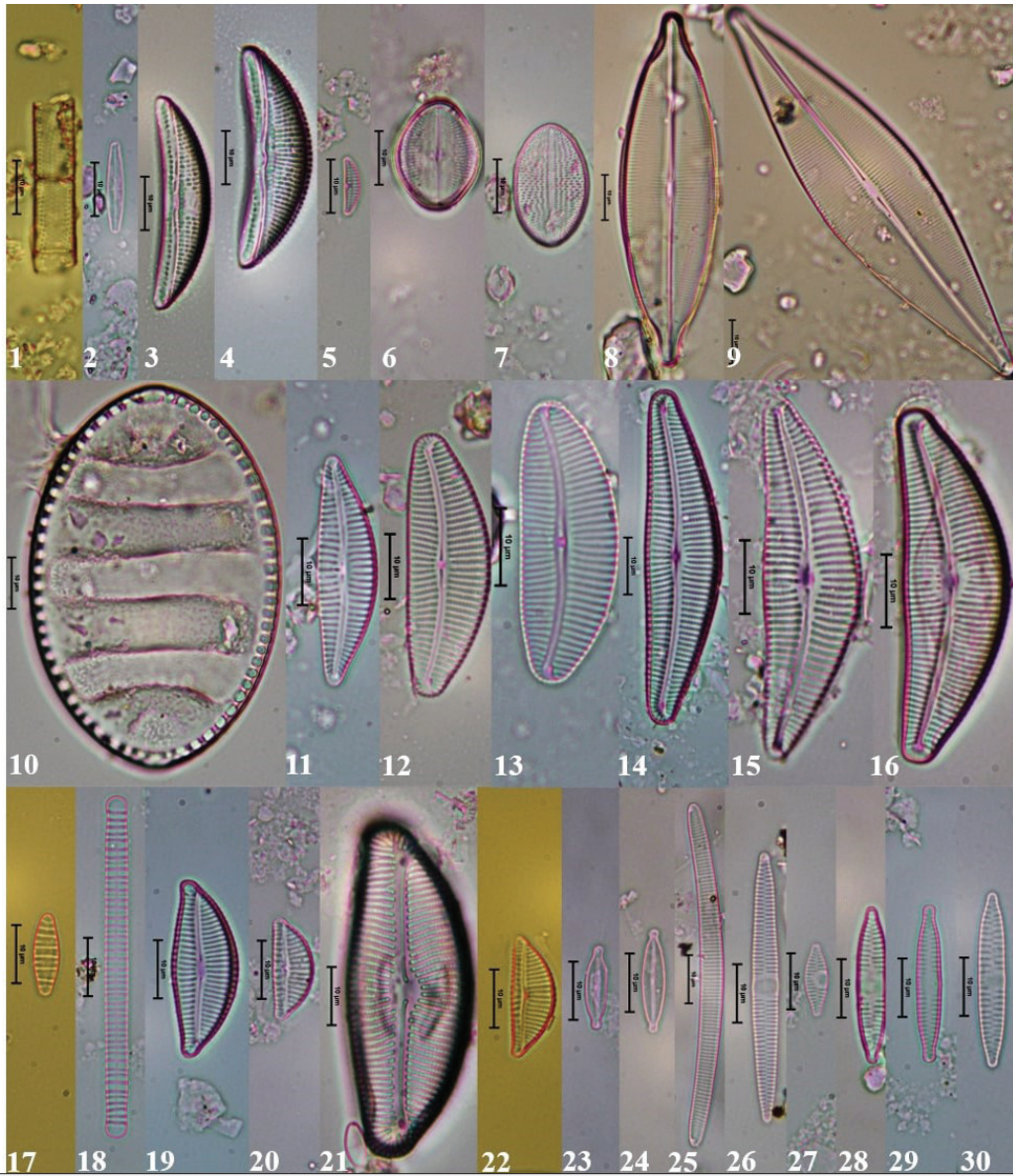
Figure 3. 1) *Aulacoseira granulata*, 2) *Achnanthidium* sp., 3) *Amphora copulata*, 4) *A. ovalis*, 5) *A. pediculus*, 6) *Cocconeis pediculus*, 7) *C. placentula*, 8) *Craticula* cf. *ambigua*, 9) *C. cuspidata*, 10) *Cymatopleura elliptica*, 11) *Cymbella affinis*, 12) *C. cantonatii*, 13) *C. compacta*, 14) *C. lange-bertalotii*, 15) *C. neocistula*, 16) *C. tumida*, 17) *Diatoma mesodon*, 18) *D. tenuis*, 19) *Encyonema auerswaldii*, 20) *E. minutum*, 21) *E. prostratum*, 22) *E. ventricosum*, 23) *Encyonopsis minuta*, 24) *E. subminuta*, 25) *Eunotia bilunaris*, 26) *Fragilaria* cf. *capucina*, 27) *F. perminuta*, 28) *F. vaucheriae*, 29) *Fragilaria* sp.1, 30) *Fragilaria* sp.2.

hungarica were observed only in this season, and their relative abundance is less than 4%.

In the August sampling, the highest number of species was determined at station 5 (27 species), and the least number of species were determined at station 3 (11 species). *Achnanthidium* sp., *Cocconeis placentula*, *Fragilaria perminuta*, and *Navicula reichardtiana* were observed in all stations. In terms of relative abundance, in this period, *C. affinis* (27%) at station 1, *C. placentula* (30%) at station 2, *Achnanthidium* sp. (67%) at station 3, *C. placentula* (82%) at station 4, and *E. auerswaldii* (43%) at station 5 (Figure 6c) were strikingly dominant. *Aulacoseira granulata*, the only member of centric diatom observed in the study in this sampling period, *Amphora copulata*, *Craticula* cf. *ambigua*, *Craticula cuspidata*, *Gomphonema acuminatum*, *G. augur*, *Planothidium lanceolatum*, and *Tryblionella apiculata* from pennate diatoms were found only in this season, and the relative abundance of species other than *P. lanceolatum* (5%) remained below 1%.

In November, no *Phragmites* sp. were encountered. For this reason, sampling was performed only at station 2, and 25
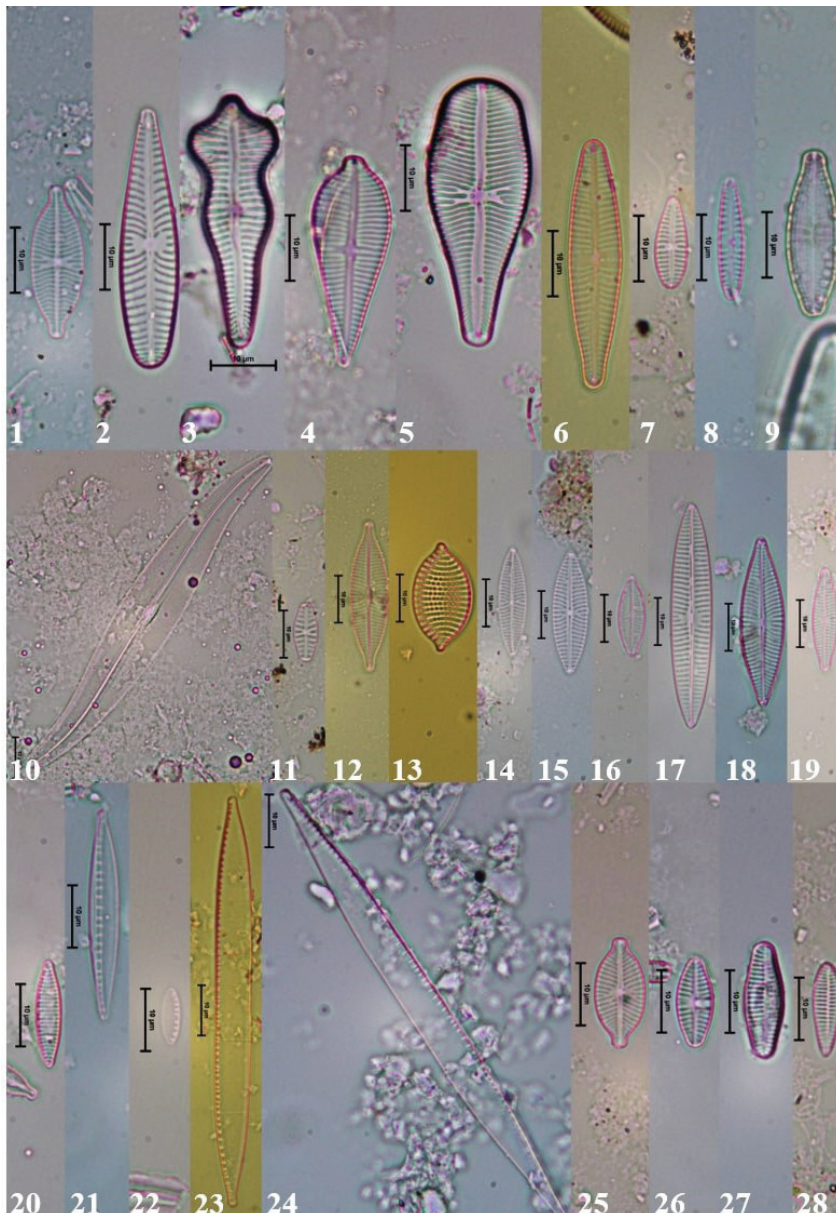
Figure 4. 1) *Geissleria decussis*, 2) *Gomphonella olivacea*, 3) *Gomphonema acuminatum*, 4) *G. augur*, 5) *G. italicum*, 6) *G. micropus*, 7) *G. minuta*, 8) *G. pumilum*, 9) *Gomphonema* sp., 10) *Gyrosigma kuetzingii*, 11) *Hippodonta hungarica*, 12) *Navicula capitoradiata*, 13) *N. compressa*, 14) *N. cryptotenelloides*, 15) *N. novaesiberica*, 16) *N. reichardtiana*, 17) *N. tripunctata*, 18) *N. trivialis*, 19) *N. veneta*, 20) *Nitzschia amphibia*, 21) *N. dissipata*, 22) *N. inconspicua*, 23) *N. intermedia*, 24) *N. recta*, 25) *Placoneis* sp., 26) *Planothidium frequentissimum*, 27) *P. lanceolatum*, 28) *Rhoicosphenia abbreviata*.

epiphytic diatom species were found. *Fragilaria perminuta* (31%) and *Navicula tripunctata* (29%) were identified as the dominant species in this period (Figure 6d). *Navicula compressa*, *Nitzschia inconspicua*, *N. recta*, and *Rhoicosphenia abbreviata* were also found only in this period, and the relative abundance of the species was observed to be below 1%.

Statistical Evaluation of Data

In order to reveal the relationship between the number of species of epiphytic diatoms in the reservoir and environmental parameters, Spearman's rank correlation was performed (Table 2), and it was determined that there was only a positive correlation between the number of epiphytic diatom species and the conductivity ($p < 0.05$).

Ordination analyses were run to reveal the relationship between epiphytic diatom species and ecological variables (Figure 7). In the CCA analysis performed, the results show that environmental factors are effective in the distribution of epiphytic diatom assemblages. The most effective explanatory factors
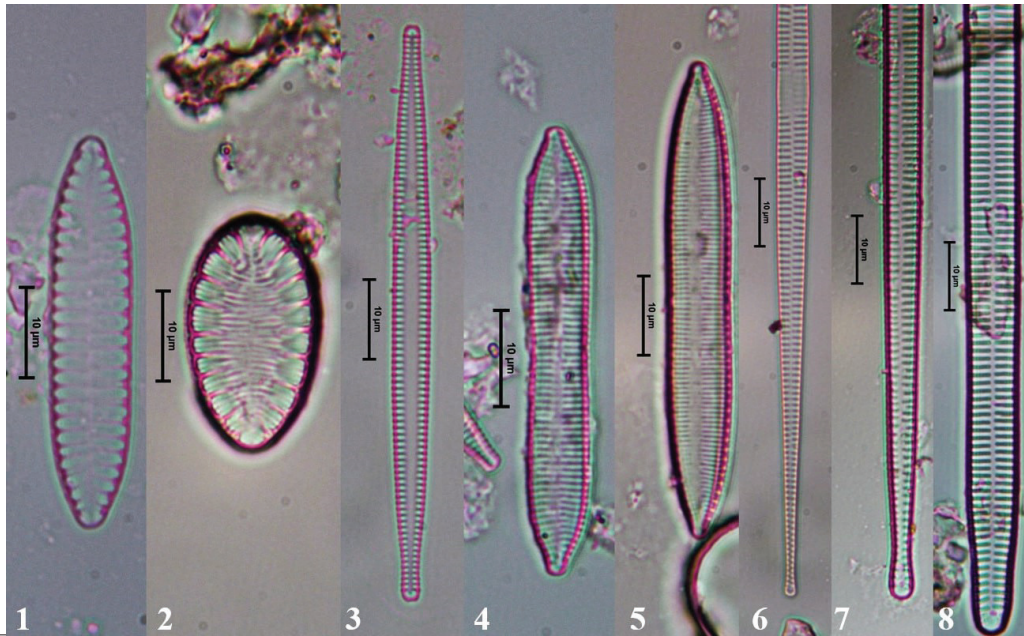
Figure 5. 1) *Surirella angusta*, 2) *S. brebissonii*, 3) *Tabularia fasciculata*, 4) *Tryblionella apiculata*, 5) *T. hungarica*, 6) *Ulnaria acus*, 7) *U. biceps*, 8) *U. ulna.*

Table 1. The list of epiphytic diatoms in the Büyükçekmece Reservoir ("*" shows the new record species in the reservoir).

Taxa	February	May	August	November
Centric diatoms				
Aulacoseira granulata (Ehrenberg) Simonsen, 1979			+	
Pennate diatoms				
Achnanthidium sp.		+	+	+
*Amphora copulata (Kützing) Schoeman&Archibald, 1986			+	
Amphora ovalis (Kützing) Kützing, 1844		+	+	
*Amphora pediculus (Kützing) Grunow, 1875			+	+
*Cocconeis pediculus Ehrenberg, 1838		+	+	+
Cocconeis placentula Ehrenberg, 1838	+	+	+	+
*Craticula cf. *ambigua* (Ehrenberg) Mann, 1990			+	
Craticula cuspidata (Kützing) Mann, 1990			+	
Cymatopleura elliptica (Brébisson) Smith, 1851			+	+
Cymbella affinis Kützing, 1844	+	+	+	+
Cymbella cantonatii Lange-Bertalot, 2002	+			
Cymbella compacta Østrup, 1910		+	+	
*Cymbella lange-bertalotii Krammer, 2002		+	+	
*Cymbella neocistula Krammer, 2002	+		+	
Cymbella tumida (Brébisson) Van Heurck, 1880		+	+	

Table 1 (Continued)				
Taxa	**February**	**May**	**August**	**November**
Pennate diatoms (Continued)				
*Diatoma mesodon (Ehrenberg) Kützing, 1844	+			+
*Diatoma tenuis Agardh, 1812		+		
*Encyonema auerswaldii Rabenhorst, 1853	+	+	+	
*Encyonema minutum (Hilse) Mann, 1990	+	+	+	
Encyonema prostratum (Berkeley) Kützing, 1844			+	
Encyonema ventricosum (Agardh) Grunow, 1875	+	+	+	
*Encyonopsis minuta Krammer&Reichardt, 1997	+	+	+	+
Encyonopsis subminuta Krammer&Reichardt, 1997			+	
*Eunotia bilunaris (Ehrenberg) Schaarschmidt, 1880		+		
*Fragilaria cf. capucina Desmaziéres, 1830		+		+
*Fragilaria perminuta (Grunow) Lange-Bertalot, 2000	+	+	+	+
*Fragilaria vaucheriae (Kützing) Petersen, 1938	+	+	+	+
Fragilaria sp.1	+			
Fragilaria sp.2	+	+	+	
*Geissleria decussis (Østrup) Lange-Bertalot&Metzeltin, 1996		+		
Gomphonella olivacea (Hornemann) Rabenhorst, 1853	+	+	+	+
Gomphonema acuminatum Ehrenberg, 1832			+	
Gomphonema augur Ehrenberg, 1841			+	
*Gomphonema italicum Kützing, 1844		+	+	
*Gomphonema micropus Kützing, 1844	+	+		+
*Gomphonema minuta Fusey, 1953	+	+	+	+
*Gomphonema pumilum (Grunow) Reichardt&Lange-Bertalot, 1991		+	+	+
Gomphonema sp.	+			
*Gyrosigma kuetzingii (Grunow) Cleve, 1894		+	+	
*Hippodonta hungarica (Grunow) Lange-Bertalot, Metzeltin&Witkowski, 1996		+		
*Navicula capitatoradiata Germain in Gasse, 1986	+			
*Navicula compressa (Ehrenberg) De Toni, 1891				+
*Navicula cryptotenelloides Lange-Bertalot, 1993		+	+	+
*Navicula novaesiberica Lange-Bertalot, 1993		+		
*Navicula reichardtiana Lange-Bertalot, 1989	+	+	+	+
Navicula tripunctata (Müller) Bory, 1822	+	+	+	+
Navicula trivialis Lange-Bertalot, 1980	+	+	+	+

Table 1 (Continued)				
Taxa	**February**	**May**	**August**	**November**
Pennate diatoms (Continued)				
Navicula veneta Kützing, 1844		+	+	+
Nitzschia amphibia Grunow, 1862		+	+	
Nitzschia dissipata (Kützing) Rabenhorst, 1860	+	+		+
Nitzschia inconspicua Grunow, 1862				+
Nitzschia intermedia Hantzsch *in* Cleve&Grunow, 1880	+			
Nitzschia recta Hantzsch *in* Rabenhorst, 1862				+
Placoneis sp.			+	
Planothidium frequentissimum (Lange-Bertalot) Lange-Bertalot, 1999			+	
Planothidium lanceolatum (Brébisson *in* Kützing) Lange-Bertalot, 1999			+	
Rhoicosphenia abbreviata (Agardh) Lange-Bertalot, 1980				+
Surirella angusta Kützing, 1844	+			
Surirella brebissonii Krammer&Lange-Bertalot, 1987	+	+	+	
Tabularia fasciculata (Agardh) Williams&Round, 1986	+			
Tryblionella apiculata Gregory, 1857			+	
Tryblionella hungarica (Grunow) Frenguelli, 1942		+		
Ulnaria acus (Kützing) Aboal, 2003		+		
Ulnaria biceps (Kützing) Compère, 2001	+			
Ulnaria ulna (Nitzsch) Compère, 2001	+	+	+	
Total Number of Species in Seasons	**28**	**38**	**43**	**25**
Total Number of Species	**66**			

are temperature and conductivity, respectively, and these variables played an important role in the distribution of the species ($p<0.05$). It was determined that temperature, conductivity, DO, and pH had a strong positive correlation with Axis 1, and salinity had a strong positive correlation with Axis 2 ($p<0.05$). According to CCA, it was revealed that the environmental variables measured in this study did not affect the distribution of *C. affinis* and *C. lange–bertalotii*. It was determined that temperature was positively related with *E. minuta*, *G. kuetzingii*, and *N. veneta* while being negatively related with *N. dissipata* and *U. ulna*. In addition, conductivity had a positive correlation with *E. minuta* and *E. ventricosum* while having a negative correlation with *C. compacta* and *U. ulna*. Furthermore, this analysis shows that *E. minuta*, *N. trivialis*, and *N. veneta* are negatively affected by DO and pH, and *F. vaucheriae*, *G. pumilum*, *N. dissipata*, and *S. brebissonii* by salinity.

In order to reveal the epiphytic diatom species diversity, the Shannon–Weaver (*H'*) diversity index was employed based on

the number of species and individuals in all sampling periods (Figure 8). Due to the low water level in November, only station 2 (*H'*= 3.13) could be sampled, so other stations were not included in the measurement. Considering all the sampling periods, it was determined that the index varied between 1.24 (August) and 3.38 (May).

Clustering analyses were used to determine the similarities of the stations investigated in Büyükçekmece Reservoir. Accordingly, while investigating the similarities of the stations in terms of biotic variables, Bray–Curtis similarity analysis was employed (Figure 9a), and it was determined that the highest similarity was between stations 1 and 2 (69.1%). The lowest similarity rate was observed between stations 2 and 3 (44.5%). It was also noted that station 3 had a low similarity rate with other stations (<54%) and differed from other stations. By using Euclidean distance (ED) to determine the similarity between the stations in terms of ecological variables (Figure 9b), stations 2 and 4 were found to be the closest stations (ED= 4.8), and stations 3 and 5 were found to be
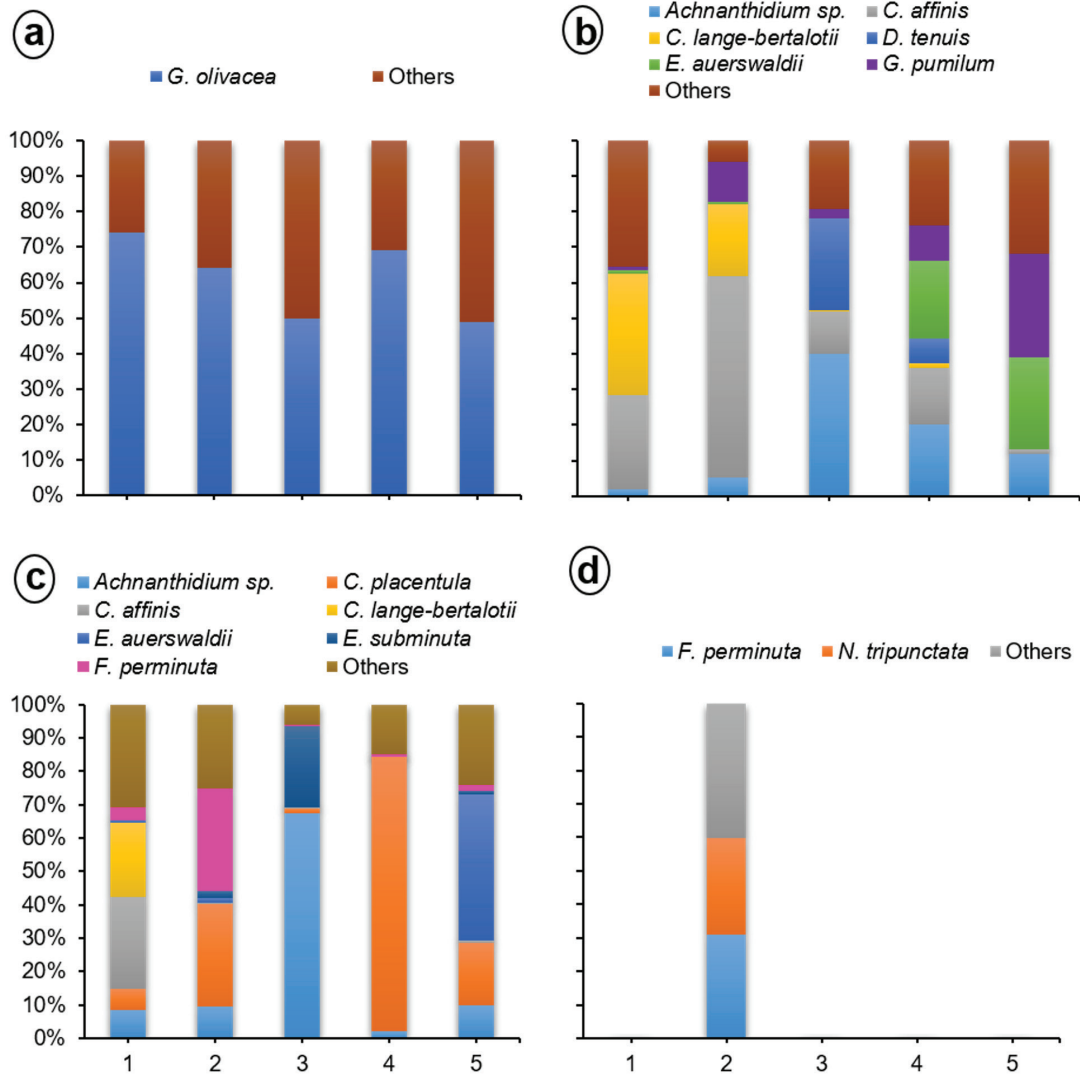
Figure 6. The relative abundance of the dominant epiphytic diatom species (> 20%) in the Büyükçekmece Reservoir (a) February, b) May, c) August and d) November; *Cocconeis placentula*: C. placentula, *Cymbella affinis*: C. affinis, *Cymbella lange–bertalotii*: C. lange-bertalotii, *Diatoma tenuis*: D. tenuis, *Encyonema auerswaldii*: E. auerswaldii, *Encyonopsis subminuta*: E. subminuta, *Fragilaria perminuta*: F. perminuta, *Gomphonella olivacea*: G. olivacea, *Gomphonema pumilum*: G. pumilum, *Navicula tripunctata*: N. tripunctata).

Table 2. Spearman's rank correlation between environmental parameters and epiphytic diatoms (**p<0.01, *p<0.05, *H'*: Shannon–Weaver diversity index).

	Temperature	Salinity	Conductivity	Dissolved oxygen	pH	Epiphytic diatoms
Salinity	-0.236					
Conductivity	0.553*	0.355				
Dissolved oxygen	-0.541*	-0.126	-0.691**			
pH	-0.287	-0.417	-0.651**	0.784**		
Epiphytic diatoms	0.276	-0.051	0.587*	-0.264	-0.169	
H'	0.062	-0.037	0.370	-0.118	-0.168	0,845**
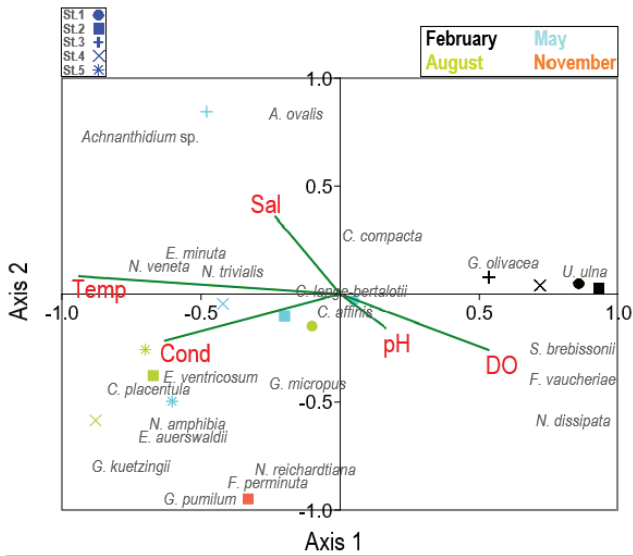
Figure 7. CCA results showing relationships between environmental variables and epiphytic diatom taxa distributions (*p* < 0.05). (Cond: Conductivity, DO: Dissolved oxygen, Sal: Salinity, Temp: Temperature; *Amphora ovalis*: *A. ovalis*, *Cocconeis placentula*: *C. placentula*, *Cymbella affinis*: *C. affinis*, *Cymbella compacta*: *C. compacta*, *Cymbella lange–bertalotii*: *C. lange-bertalotii*, *Encyonema auerswaldii*: *E. auerswaldii*, *Encyonopsis minuta*: *E. minuta*, *Encyonema ventricosum*: *E. ventricosum*, *Fragilaria perminuta*: *F. perminuta*, *Fragilaria vaucheriae*: *F. vaucheriae*, *Gomphonella olivacea*: *G. olivacea*, *Gomphonema micropus*: *G. micropus*, *Gomphonema pumilum*: *G. pumilum*, *Gyrosigma kuetzingii*: *G. kuetzingii*, *Navicula reichardtiana*: *N. reichardtiana*, *Navicula trivialis*: *N. trivialis*, *Navicula veneta*: *N. veneta*, *Nitzschia amphibia*: *N. amphibia*, *Nitzschia dissipata*: *N. dissipata*, *Surirella brebissonii*: *S. brebissonii*, *Ulnaria ulna*: *U. ulna*).

Figure 8. Shannon–Weaver diversity index in the sampling periods.
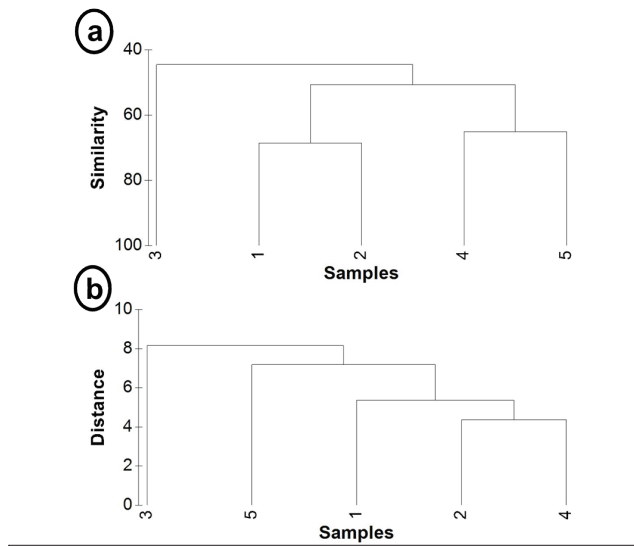
Figure 9. Dendrograms of cluster analysis based on Bray-Curtis similarity index (a) and Euclidean Distance (b) in the Büyükçekmece Reservoir.

the most distant to each other (ED= 8.1). In terms of Euclidean Distance, it was observed that station 3 differed from other stations, similar to the Bray–Curtis similarity analysis.

The Status of Büyükçekmece Reservoir in Terms of Water Quality Parameters

According to the measured DO and conductivity in the study, it was aimed to ascertain the ecological water quality class and trophic level of the reservoir (Table 3). According to the Surface Water Quality Control Regulation (12) considering the conductivity and DO values, the reservoir is of very good (I) and good

Table 3. Ecological water quality status and trophic level of the lake according to conductivity and dissolved oxygen values (*Classification*: "I" Very good, "II" good, "III" Moderate; *Trophic Level*: "O" oligotrophic, "M" mesotrophic, "E" Eutrophic").

Stations	Conductivity				Dissolved Oxygen				Trophic Status (DO)			
	Feb	May	Aug	Nov	Feb	May	Aug	Nov	Feb	May	Aug	Nov
1	I	II	II	II	I	II	I	I	O	O	O	O
2	I	I	II	II	I	I	I	I	O	O	O	O
3	II	II	II	II	I	II	I	I	O	O	O	O
4	I	II	II	II	I	I	I	III	O	O	O	M
5	I	II	II	III	I	I	III	III	O	O	M	E

(II) quality, but in terms of DO values in some seasons and stations (August and November), it is at the moderate (III) class water quality level. At the same time, when the trophic level of the lake was evaluated according to DO, it was determined that oligotrophic conditions prevailed throughout the study, and the eutrophic situation prevailed only at station 5 in the November sampling period. When the reservoir is classified according to *H′* values, stations 1, 2, and 4 were poor, stations 3 and 5 were moderate in February; stations 1, 2, 3, and 5 were moderate, and station 4 was good in May; stations 3 and 4 were poor, stations 2 and 5 were moderate, and station 1 was good in August while station 2 was of good status in November.

DISCUSSION

In this study conducted seasonally on epiphytic diatoms in Büyükçekmece Reservoir, 66 species were identified. 36 of the identified species (54.4%) are new records for the reservoir, and some genera (*Eunotia, Geissleria, Hippodonta*, and *Tabularia*) were first encountered in this study in the reservoir. Also, in addition to these 36 new species records, the species which were reported by Balkis–Ozdelice et al. (24) as new record species for the reservoir (*Cymbella cantonatii, C. compacta, Encyonopsis subminuta, Navicula trivialis*, and *Surirella brebissonii*), were also found in this study.

In Büyükçekmece Reservoir, only one study covering epiphytic diatoms was carried out (18), and 42 species were reported. Of the species acquired by Temel (18), 13 species (13.7%) were common, 29 species (30.5%) were found only in the study of Temel (18), and 53 species (55.8%) were detected only in the present study. According to these two studies, the number of epiphytic diatom species of the reservoir was determined to be 95. In addition to epiphytic algae in the reservoir, epilithic, epipelic, and phytoplanktonic organisms in the water column were also analysed (17–24). The species obtained from all these studies are presented in a list (24). According to Balkis–Ozdelice et al. (24), a total of 333 phytoplankton species were reported in the reservoir, and it was stated that 128 of these species were reported to be composed of diatoms. By adding 36 epiphytic diatom species obtained in this study to the list, this number was updated as 164 for diatoms and 369 for total phytoplankton. When considering the epiphytic diatom studies carried out in lakes and reservoirs in Turkey; 39 epiphytic diatom species from Karkamış and Birecik Reservoirs (46), 31 from Lake Liman (47), 66 from Lake Gala (48), and 61 from Lake Mogan (49) have been reported. Accordingly, it has been determined that Büyükçekmece Reservoir has a similar number of epiphytic diatom species with other lakes and reservoirs.

While Temel (18) noted that *Cocconeis placentula, Navicula tripunctata* (=*N. gracilis*), and *Nitzschia palea* were common and numerous, *C. placentula* and *N. tripunctata* were widely observed in our study whereas *N. palea* was not found. In addition, in the present study, *C. affinis, E. minuta, F. perminuta, F. vaucheriae, G. olivacea, G. minuta, N. reichardtiana, N. tripunctata*, and *N. trivialis* were widely recorded (in all seasons). Additionally, *E.*

minuta and *G. pumilum*, which are reported to be rare species for Turkish freshwater diatom flora (50), are commonly encountered in the reservoir, and *E. subminuta*, another rare species in Turkey, was rarely observed in the Büyükçekmece Reservoir.

In this study, it was observed that pennate diatom members from epiphytic diatoms are dominant, especially *G. olivacea* in the February sampling, *C. affinis* in May, *Achnanthidium* sp. and *C. placentula* in August, and *F. perminuta* in November. The dominance of pennate diatoms in the epiphytic habitat compared to centric diatoms is similar to the previous study in the reservoir (18), as well as with the studies performed in other lakes (51-53). In addition, Round (54) reported that *Fragilaria, Cocconeis, Gyrosigma, Caloneis, Navicula, Amphora, Cymbella*, and *Nitzschia* are very common in calcareous waters while *Pinnularia* and *Neidium* are very common in acidic waters. In addition, Round (55,56) reported that in addition to these genera, *Cymatopleura elliptica* species increased in neutral and slightly alkaline waters, and *Amphora ovalis* increased significantly in alkaline waters. In this study, the prevalence of the common species in calcareous waters and the absence of *Pinnularia* and *Neidium*, representing acidic environments in epiphytic habitats, showed that the environment was calcareous and alkaline. One of the ecological variables, the pH value between 7.49 and 8.28 also supports this finding.

As is known, diatoms are used as indicators of pH, conductivity, salinity, and trophic level (57). Lange-Bertalot et al. (58) stated that *Navicula veneta*, which was also observed in this study, is one of the diatom types that can be used as a pollution indicator, but the relative abundance of this species in the stations analysed in Büyükçekmece Reservoir remained below 1%. Overall in the study, *G. olivacea* is the species that increased its abundance at low temperature and high pH values. Similarly, Koçer and Şen (59) stated in their study in Lake Hazar that this species is dominant under similar ecological conditions. Since the relationship of this species with temperature and pH could not be revealed in the CCA analysis, it was not possible to conclude whether it could be used as an indicator or not. Also, in CCA analysis, it was determined that *N. veneta* had a positive relationship with temperature and *E. ventricosa* had a positive relationship with conductivity ($p < 0.05$). These species can be considered as potential indicators, but further studies are needed to verify their status as indicator species. Also, according to ordination analysis, temperature and conductivity were revealed to be the main factors affecting diatom distribution.

Surirella brebissonii, F. vaucherii, and *N. dissipata*, which are epiphytic diatom species, were negatively correlated with temperature and salinity; *C. compacta* and *U. ulna* were negatively correlated with conductivity; *E. minuta, N. trivialis*, and *N. veneta* were negatively correlated with pH and DO. With the spring period, an increase in temperature and conductivity was observed, and it was determined that *C. affinis* and *C. lange–bertalotii*, which are dominant species in this period, were not affected by the ecological variables measured in the study. However, Kelly et al. (60) reported

65

that *C. affinis* could be specified as a high–quality indicator type for moderately alkaline lakes. In this study, pH varied between 7.91 and 8.05 during the periods when *C. affinis* was dominant. With temperature conditions reaching the optimum level (~25°C) during the summer period, *Achnanthidium* sp. and *C. placentula* became dominant. Among these species, *C. placentula* was found to show a positive correlation with temperature and conductivity. It was noted that this species was not observed under 0.500 mS/cm conductivity value and reached the maximum abundance at station 4 in August when the highest temperature value in the study was determined. Kindt and Small (61) reached similar results with this study and stated that the abundance of *C. placentula* increased with the increase in temperature.

Van Dam et al. (62) stated that the species belonging to the genus *Cymbella* and *Eunotia* were found in regions with high dissolved oxygen concentrations. Similarly, in the Büyükçekmece Reservoir, DO has reached a high concentration (18.4 mg/L) at station 2 in May while the relative abundance of *C. affinis* and *C. lange–bertalotii* at this station reached 76%. In addition, *Eunotia bilunaris* was observed only in the May sampling where the DO concentration was high. Cox (63) reported that *Navicula capitatoradiata* and *N. veneta* were more common in waters with high conductivity. Contrary to this finding, both species were found abundant in February and May samples (compared with other seasons), where the conductivity was low in the Büyükçekmece Reservoir. Reimer et al. (64) stated that *C. placentula* is a cosmopolitan species due to its high tolerance to the change of environmental factors. As similar, *C. placentula* was observed in almost every season in this study.

As it is known, as the temperature increases, the solubility of gases decreases. It was observed that the dissolved oxygen concentration increased with the decrease in temperature in cold periods (February, November) in the Büyükçekmece Reservoir. Similar results were found in a study conducted in Tasmanlı Pond (65). The number of species was also found to be high in May and August, which represent warm periods. However, in a study conducted in Topçu Lake (51), a decrease in the number of species was reported in July and August (in warm periods). This situation reveals that environmental factors may decrease or increase the number of species.

When the evaluation was made on the basis of stations, it was determined that station 3 was represented with fewer species than other stations in terms of the number of diatom species in the reservoir. Bray–Curtis and Euclidean Distance among the cluster analysis were applied in the study, and it was revealed that station 3 was separated from the other stations according to both analyses. Also, according to Spearman's rank correlation, a positive relationship was observed between conductivity and the number of epiphytic diatom species ($p<0.05$). While the highest conductivity values in February and May were reached at station 3, there was no increase observed in terms of the number of species. In fact, it is remarkable that only 8 cells belonging to 5 species were found in the February sample.

Shannon–Weaner diversity index (H'), used for determining the structure of the communities, varied between 1.24 and 3.38 in the study. The lowest values in the study were obtained in August. During this period, *Achnanthidium* sp. (St.3, 67%) and *C. placentula* (St.4, 82%) were dominant species, and this situation caused a decrease in H' values. Also, it was determined that the diversity at station 5, which is located in the north of the reservoir and close to the stream, did not show a significant change seasonally. Molvær et al. (45) classified waters for the ecological quality. According to this classification, Büyükçekmece Reservoir was generally in poor and moderate status, and in some sampling periods, it was found to be in good status (St.4 in May, St.1 in August, and St.2 in November). In addition, it was observed that H' values obtained from studies on epiphytic diatoms in other freshwater resources ranged from 0.867 to 1.427 (47, 48). Accordingly, it was revealed that the diversity of Büyükçekmece Reservoir is at a higher level than the other sources.

CONCLUSION

As a result, this study aimed to determine the epiphytic diatoms and abundance conditions in the reservoir, and newly recorded species for the lake were reported. In the reservoir, it was also reported that according to the conductivity and DO values, the lake is of very good (I) and good (II) quality. Also, in terms of DO values, it was observed that the reservoir was oligotrophic during the February and May sampling periods, station 5 was mesotrophic, other stations were oligotrophic during the August sampling period, stations 1, 2, and 3 were oligotrophic, station 4 was mesotrophic, and station 5 was eutrophic during the November sampling period. Eutrophication conditions have occurred since station 5 is located close to the Karasu Stream, which is the biggest nutrient source of the reservoir and has been reported to carry a significant amount of nutrient load, and the occupancy rate of the reservoir had decreased to 40% during the November sampling period. Balkis–Ozdelice et al. (24) proposed that the phosphorus intake to Büyükçekmece Reservoir be controlled. Also, according to H' classification, Büyükçekmece Reservoir was generally in poor and moderate status. For these reasons, it is necessary to monitor the ecological quality status of the reservoir with monitoring studies.

Conflict of Interest: The authors declare that they have no conflicts of interest.

Author Contributions: Conception/Design of study: T.O.A., N.B.O.; Data Acquisition: T.O.A., N.B.O., T.D.; Data Analysis/Interpretation: : T.O.A., N.B.O., T.D., C.N.S.; Drafting Manuscript: T.O.A., N.B.O., T.D., C.N.S.; Final Approval and Accountability: T.O.A., N.B.O., T.D., C.N.S.

REFERENCES

1. Medlin LK, Kooistra WHCF, Gersonde R, Sims PA, Wellbrock U. Is the origin of diatoms related to the end-Permian mass extinction? Nova Hedwigia 1997; 65: 1-11.

2. Round FE, Crawford RM, Mann DG. Biology of diatoms, the diatoms: Biology and morphology of the genera. Sandgren CD, editor. Cambridge: Cambridge University Press; 1990. 746 p.

3. Ács É, Szabó K, Tóth B, Kiss KT. Investigation of benthic algal communities, especially diatoms of some Hungarian streams in connection with reference conditions of the Water Framework Directives. Acta Bot Hung 2004; 46 (3-4): 255-78.

4. Soininen J, Paavola R, Muotka T. Benthic diatom communities in boreal streams: community structure in relation to environmental and spatial gradients, Ecography 2004; 27(3): 330-42.

5. Cumming BF, Wilson SE, Hall RI, Smol JP. Diatoms from British Columbia (Canada) Lakes and their relationship to salinity, nutrients and other limnological variables. Bibliotecha Diatomalogica 1995. 207 p.

6. Battarbee RW, Charles DF, Dixit SS, Renberg I. Diatoms as indicators of surface water acidity. Stoermer EF, Smol JP, editors. The Diatoms: Applications for the enviromental and earth sciences. Cambridge: Cambridge University Press; 1999. pp. 98-121.

7. John J. Bioassesment on health of aquatic systems by the use of diatoms. Ambasht RS, Ambasht NK, editors. Modern Trends in Applied Aquatic Ecology. New York, USA: Kluwer Academic Publications; 2003. pp. 1-20.

8. Taylor JC, Harding WR, Archibald CGM. An illustrated guide to some common diatom species from South Africa. Gezina, South Africa: Water Research Commission; 2007. Report No: 282/07.

9. Bozarth A, Maier UG, Zauner S. Diatoms in biotechnology: modern tools and applications. Appl Microbiol Biotechnol 2009; 82: 195-201.

10. Official Journal of the European Communities. Directive 2000/60/EC of the European Parliament and of the Council, establishing a framework for community action in the field of water policy. The European Parliament and the Council of the European Union 2000; 327: 1-73.

11. Official Gazette of the Republic of Turkey. Water pollution control regulations. Official Gazette of the Republic of Turkey 2004; No: 25687.

12. Official Gazette of the Republic of Turkey. Surface water quality management regulation. Official Gazette of the Republic of Turkey 2016; No: 29797.

13. Stener-Kovács C, Buczkó K, Hajnal É, Padisák J. Epiphytic, littoral diatoms as bioindicators of shallow lake trophic status: Trophic Diatom Index for Lakes (TDIL) developed in Hungary. Hydrobiologia 2007; 589: 141-54.

14. Dalkıran N, Zünbülgil B, Karacaoğlu D, Dere Ş. Uluabat gölü epifitik diyatomelerinin uzun dönemdeki değişimleri. LimnoFish 2016; 2(3): 153-63.

15. Sanal M, Demir N. Use of the epiphytic diatoms to estimate the ecological status of Lake Mogan. Appl Ecol Environ Sci 2018; 16(3): 3529-43.

16. Solak CN, Çetin T, Karaaslan Y, Kaleli A, Yılmaz E, Duran M, Kıvanç G, Kimençe, T, Aynur-Koyunoğlu, Ş., Çankaya, B.F., Yılmaz-Aşık, D. Common diatoms of phytobenthos in Gediz River Basin. Turkish Journal of Water Science & Management 2019; 3(2): 58-70.

17. Temel M. Büyükçekmece Gölü Bentik Alg Florası, Süleyman Demirel Univ. Eğirdir Su Ürün. Fak. Derg. 1996-1997; 5: 173-90.

18. Temel M. Büyükçekmece Gölü bentik alg florası, Kısım II: Epilitik ve epifitik alg toplulukları. In: X. National Fisheries Symposium, Adana: 22-24 September 1999; 877-86.

19. Temel M. The phytoplankton of Lake Büyükçekmece, İstanbul, Turkey, Pak J Bot 2002; 34(1): 81-92.

20. Aktan-Turan Y, Aykulu G, Albay M, Okgerman H, Akçaalan R, Gürevin C, Dorak Z. Büyükçekmece Gölü'nde aşırı artış gösteren fitoplankterlerin gelişimini kontrol eden faktörlerin araştırılması. TÜBİTAK, Ankara. 2006. Report No: 103Y127.

21. Aktan Y, Gürevin C, Dorak Z. The effect of environmental factors on the growth and size structure of two dominant phytoplankton species in Büyükçekmece Reservoir (İstanbul, Turkey). Turk J Biol 2009; 33: 335-40.

22. Gulecal Y, Temel M. Water quality and phytoplankton diversity in Büyükçekmece Watershed, Turkey. J Water Resource Prot 2014; 6: 55-61.

23. Yilmaz N. Water quality assessment based on the phytoplankton composition of Buyukcekmece Dam Lake and its influent streams (Istanbul), Turkey. Desalin Water Treat 2019; 159: 3-12.

24. Balkis-Ozdelice N, Solak CN, Durmus T. The use of phytoplankton communities to determination of the ecological status of Büyükçekmece Dam-Lake and the investigation of water quality problems. TÜBİTAK, Ankara; 2020. Report No: 118Y347.

25. Demir N, Atay D. Kurtboğazı ve Çamlıdere Baraj Göllerinin Fitoplanktonu. In: X. National Fisheries Symposium, 1999; p. 577-87.

26. Directorate General for State Hydraulic Works (DSİ). Büyükçekmece Barajı ve tesisleri ikmal inşaatı aylık iş durumu. DSİ papers, Istanbul; 1985.

27. İSKİ. "Büyükçekmece Barajı son 14 gün içindeki mevcut su hacimleri" https://www.iski.istanbul/web/tr-TR/baraj-doluluk, Last Accessed Date: 03 May 2021.

28. İSKİ. "Baraj Doluluk Oranları - Mevcut Su Miktarının Barajlara Göre Dağılımı". http://www.iski.istanbul/web/tr-TR/baraj-doluluk, Last Accessed Date: 11 November 2019.

29. Winter JG, Duthie HC. Epilithic diatoms as indicators of stream total N and total P concentration. J North Am Benthol Soc 2000; 19(1): 32-49.

30. Hendey NI. A revised check-list of British marine diatoms. J Mar Biolog Assoc UK 1974; 54(2): 277-300.

31. Battarbee RW, Cameron NG, Golding P, Brooks SJ, Switsur R, Harkness D, McGovern A. Evidence for holocene climate variability from the sediments of a Scottish remote mountain lake. J Quat Sci 2001; 16(4): 339-46.

32. Hustedt F. Heft 10: Bacillariophyta (Diatomeae). Pascher A. editor. Die Süsswasser-Flora Mitteleuropas. Jena, Germany: Verlag von Gustav Fischer; 1930. 466 p.

33. Patrick R, Reimer CW. The diatoms of the United States, Exclusive of Alaska and Hawaii. Philadelphia. Philadelphia, USA: Wiley; 1966. 688 p.

34. Patrick R, Reimer CW. The diatoms of the United States Vol.2, Part 1. Philadelphia, USA: Wiley; 1975.

35. Krammer K, Lange-Bertalot N. Süßwasserflora von Mitteleuropa Bacillariophyceae 3. Teil: Centrales, Fragilariaceae, Eunotiaceae. Stuttgart, Germany: Gustav Fischer Verlag; 1991.

36. Krammer K, Lange-Bertalot N. Süßwasserflora von Mitteleuropa Bacillariophyceae 4. Teil: Achnanthaceae, Kritische Ergänzungen zu Navicula (Lineolatae) und Gomphonema Gesamtliteraturverzeichnis Teil 1-4. Stuttgart, Germany: Gustav Fischer Verlag; 1991.

37. Krammer K, Lange-Bertalot N. Süßwasserflora von Mitteleuropa Bacillariophyceae 1. Teil: Naviculaceae. Berlin, Germany: Gustav Fischer Verlag; 1997.

38. Krammer K, Lange-Bertalot N. Süßwasserflora von Mitteleuropa Bacillariophyceae 2. Teil: Bacillariaceae, Epithemiaceae, Surirellaceae. Berlin, Germany: Gustav Fischer Verlag; 1997.

39. Siegel S. Nonparametric statistics for the behavioral sciences. New York, USA: McGraw-Hill; 1956.

40. Shannon CE, Weaver W. The mathematical theory of communication. Urbana, USA: The University of Illinois Press; 1949.

41. Clarke KR, Warwick RM. Change in marine communities: An approach to statistical analysis and interpretation (2nd edition). Plymouth, England: Primer-E; 2001.

42. Lepš J, Šmilauer P. 2003. Multivariate analysis of ecological data using CANOCO. New York, USA: Cambridge University Press; 2003.

43. McCune B, Mefford MJ. PC-ORD, Multivariate analysis of ecological data (Version 6.22) Oregon, USA: MjM software; 2011.

44. Hammer Ø, Harper DAT, Ryan PD. PAST: Paleontological statistics software package for education and data analysis. Palaeontol Electron 2001; 4(1): 1-9.

45. Molvær J, Magnusson J, Pedersen A, Rygg B. Vanndirektivet: utarbeidelse av system for marin klassifisering. Framdriftsrapport høsten 2008. TA-2465/2009.

46. Morkoyunlu-Yüce A, Ertan ÖO, Yıldırım, MZ. Epiphytic and epilithic diatoms in dam lakes (Euphrates - Turkey). Yunus Araştırma Bülteni 2015; 3: 45-51.

47. Soylu N, Maraşlıoğlu F, Gönülol A. Epiphytic diatom flora o f Liman Lake (Bafra-Samsun). Ekoloji 2011; 20(79): 57-62.

48. Öterler B. Community structure, temporal and spatial changes of epiphytic algae on three different submerged macrophytes in a shallow lake. Pol J Environ Stud 2017; 26(5): 2147-58.

49. Sanal D, Demir, N. Use of the epiphytic diatoms to estimate the ecological status of Lake Mogan. Appl Ecol Environ Res 2018; 16(3): 3529-43.

50. Solak CN, Çetin T, Kaleli A. Distribution of benthic diatom (Phytobenthos) composition in Küçük Menderes River Basin. Turkish Journal of Water Science & Management 2018; 2(1): 1-35.

51. Akköz C, Güler S. The algal flora of Topçu Lake (Yozgat) I: Epilytic and Epiphytic Algler. S Ü Fen Ed Fak Fen Derg 2004; 23: 7-14.

52. Szabo K, Tihamer KK, Taba G, Acs E. Epiphytic diatoms of the Tisza River, Kisköre Reservoir and some oxbows of the Tisza River after the cyanide and heavy metal pollution in 2000. Acta Bot Croat 2005; 64(1): 1-46.

53. Shaawiat AO, Hassan FM. Qualitative and quantitative study of epiphytic diatoms on two macrophytes in a lotic ecosystem, Iraq. Indian J Ecol 2017; 44(3): 504-15.

54. Round FE. An investigation of two benthic algal communities in Malham Tarn, Yorkshire. J Ecol 1953; 41(1): 174-97.

55. Round FE. Studies on bottom living algae in same lakes of English lake district. Part III. The distribution on the sediments of algal group other than the Bacillariophyceae. J Ecol 1957; 45(2): 649-64.

56. Round FE. Studies on bottom living algae in same lakes of English lake district. Part III. The distribution of Bacillariophyceae on the sediments. J Ecol 1957; 45(2): 343-60.

57. Cox EJ. 1991. What is the basis for using diatoms as monitors of river quality? Whitton BA, Rott E, Fredrich G, editors. Use of algae for monitoring rivers. Innsbruck, Austria: Universitat Innsbruck; 1991.

58. Lange-Bertalot H, Hofmann G, Werum M, Cantonati M. Freshwater benthic diatoms of Central Europe: Over 800 common species used in ecological assessment. Koeltz Botanical Books; 2017. 942 p.

59. Koçer MAT, Şen B. The seasonal succession of diatoms in phytoplankton of a soda lake (Lake Hazar, Turkey). Turk J Bot 2012; 36: 738-46.

60. Kelly M, Acs E, Bertrin V, Bennion H, Borics G, Burgess A, Denys L, Ecke F, Kahlert M, Karjalainen SM. et al. Water Framework Directive intercalibration technical report: Lake phytobenthos ecological assessment methods. Publications Office of the European Union; 2014. pp.125,

61. Kindt AC, Small PF. Correlation between temperature, colonization rate, and population density of the diatom *Cocconeis placentula* in freshwater streams. J Freshw Ecol 2002; 17(3): 441-5.

62. Van Dam H, Mertens A, Sinkeldam J. A coded checklist and ecological indicator values of freshwater diatoms from the Netherlands. Neth J Aquat Ecol 1994; 28(1): 117-33.

63. Cox EJ. Studies on the diatom genus *Navicula* Bory. VII. The identity and typification of *Navicula gregaria* Donkin, *N. cryptocephala* Kütz. and related taxa. Diatom Res 1995; 10(1): 91-111.

64. Reimer CW, Henderson MV, Patrick R. Bibliography, addenda, and corrigenda for The Diatoms of the United States. Proc Acad Nat Sci Philadelphia 2001; 151(1): 129-55.

65. Gümüş F, Gönülol A. Epilithic and epiphytic algae of Taşmanlı Pond (Sinop-Turkey). Karadeniz Fen Bilimleri Dergisi 2017; 7(1): 102-16.

A Preliminary Metabarcoding Study of Prokaryotes in Gökçeada Salt Lake Lagoon, Turkey

Sibel Kucukyildirim Celik¹ ⓘD

¹Hacettepe University, Faculty of Science, Department of Biology, Ankara, Turkey

ORCID IDs of the authors: S.K.C. 0000-0003-2241-3060

ABSTRACT

Objective: Microorganisms play an important role in all ecosystem processes and a growing body of molecular and ecological evidence has shown that microbial biodiversity is much more diverse and complex than previously anticipated. This study aimed to determine the prokaryotic microorganisms present in Gökçeada Salt Lake Lagoon.

Materials and Methods: A metabarcoding approach was used to determine the microbial diversity in Gökçeada Salt Lake Lagoon.

Results: 16S rDNA targeted sequencing revealed 5 Archaea and 31 Bacteria species and Archaea represented 63.2%. The most frequent Archaea genus was *Halorubrum*, which belongs to the Euryarchaeota phylum, and the dominant species of Bacteria was *Halomonas sulfidaeris* (Proteobacteria phylum).

Conclusion: This work will contribute to our understanding of the microbial community structure and composition in coastal lagoons. Hovewer, further surveys will improve our knowledge on microbiota in Gökçeada Salt Lake Lagoon.

Keywords: Biodiversity, halophile, 16S rDNA, metabarcoding

INTRODUCTION

Microorganisms are the most abundant taxonomically and metabolically diverse organisms on Earth. It is well established that microbiota plays an important role in ecosystem stability and sustainability (1). However, biodiversity-based research has mainly focused on plants and animals, giving little attention to microorganisms. In environmental samples, the identification of micro-organisms at the species level by conventional techniques is costly, time-consuming, and also continues to be resolved. Recently, many studies have been conducted to provide information about the diversity and distribution patterns of microorganisms, however, it is remarkable that there is still much unknown.

Application of DNA sequence-based methods has led to significant progress in molecular taxonomy and systematics over the last twenty years, revealing re-

markably large diversity even in environments that are relatively well studied. For taxonomic purposes, sequencing of the specific regions (i.e. variable regions of 16S, 5S, or 23S rDNA genes) of isolates has resulted in the development of extensive public DNA sequence databases. Moreover, high-throughput sequencing technologies provide an opportunity to generate large amounts of data in a relatively short time. One of the most important advantages of this method is the ability to identify large numbers of species from environmental samples with different characteristics (2,3).

Until recently, microbial biodiversity studies mainly conducted on extreme environments (such as high or low temperature, high or low pH) were yet little explored and particularly unique. In this work, the sampling area was a coastal lagoon located in the southeast of Gökçeada Island (Turkey), called Gökçeada Salt Lake Lagoon. The maximum depth of the lagoon is 2 meters,

and its total area is approximately 2 km². Coastal lagoons like Gökçeada Salt Lake Lagoon are considered wetlands and have a special hydrological structure formed by a transition zone between fresh and saltwater. Since each wetland ecosystem has its own physicochemical properties, and community structure should be evaluated separately (4).

This study aimed to determine the prokaryotic community structure in Gökçeada Salt Lake Lagoon using a culture-independent approach that includes metabarcoding based on amplicon sequencing. Metabarcoding is mainly used to characterize species-level diversity in the environmental samples and is considered a method that has the potential to identify rare taxa (5). In addition to the identification of microorganisms at the species-level, information about abundance, distributions, and biological functions of these microorganisms can be obtained by the metabarcoding approach. The high sensitivity and specificity of the method provide an advantage, especially in organisms that cannot be cultured in vitro (6-8). Because previous work is only based on conventional methods (4,9), the prokaryotic diversity in Gökçeada Salt Lake Lagoon is likely limited to only identifiable species. Also, another motivation for this study is that no study focusing on prokaryotic microorganisms in Gökçeada Salt Lake Lagoon has previously been included in the literature. In short, the metabarcoding approach used in this study allows us to determine prokaryotes without prior cultivation and provide a deeper analysis of the prokaryotic diversity in Gökçeada Salt Lake Lagoon.

MATERIALS AND METHODS

Sampling and Physicochemical Analysis

To determine the prokaryotic diversity of Gökçeada Salt Lake Lagoon, three water samples (1 Liter of each) were sampled aseptically in September 2019 (40° 7′ 47.2″ N 25° 56′ 52.1″ E) (Figure 1). All samples were stored at 4℃ and immediately transported to the laboratory. The analysis of physicochemical parameters (total salinity, major anion and cation concentrations
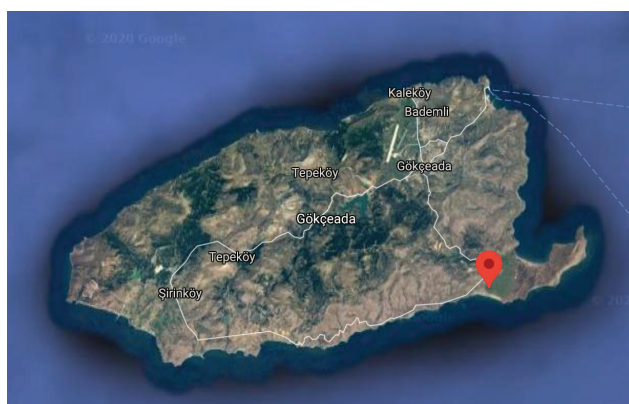

Figure 1. Gökçeada Salt Lake Lagoon in Turkey. The sampling area was shown with a red circle on the map (Satellite imagery: Google/Google Maps (n.d.)).

(pH and Na⁺, K⁺, Ca²⁺, Mg²⁺, Cl⁻, CO₃²⁻, SO₄²⁻ and NO₃⁻) in the samples were performed by Hacettepe University Water Chemistry Laboratory.

DNA Isolation and Sequencing

For DNA isolation, water samples (500 ml each) were filtered through a vacuum filter (0.22 μm filter membrane). Then, filter membranes were cut into small pieces and DNA was isolated using ZymoBIOMICS® DNA Miniprep Kit (Zymo Research, Irvine, CA) according to the manufacturer's instructions. Isolated DNA samples were analyzed on a 1% agarose gel, and DNA quantity was evaluated using Nanodrop 2000 UV-Vis spectrophotometer (Thermo Fisher, USA). Quantified DNA samples were combined based on equal molarity and were stored at −20 ℃ before analysis.

The sample was processed with the BM Labosis (Turkey) Sequencing Service: Targeted Metabarcoding by using the specific primers that targeting the prokaryotic 16S rDNA gene, (515F (5′-GTGYCAGCMGCCGCGGTAA-3′) and 806R (5′-GGACTACNVGGGTWTCTAAT-3′)) (10-12). The sequencing protocol of the Earth Microbiome Project was used and adapted to the Illumina MiSeq instrument (11). After the amplicon library was prepared, the product was quantified with qPCR fluorescence reading. The library was cleaned using Select-a-Size DNA Clean & Concentrator™ (Zymo Research, Irvine, CA). Then, qualitative and quantitative measurement of the library was performed with TapeStation® and Qubit®. The sample was sequenced using the Illumina MiSeq instrument following the manufacturer's recommended protocol.

Data Analysis

Raw data were processed and read quality was controlled by FastQC and QIIME2. DADA2 was used to obtain specific amplicon sequences and chimeric sequences were excluded from the analysis using the same program (13). QIIME2 was used to cluster DNA sequence data with more than 97% similarity as operational taxonomic units (OTUs) (14,15) and chimeric OTUs were extracted from the dataset using USEARCH algorithm (16). Taxonomic assignments of OTUs were performed using the QIIME2 pipeline (15) and SILVA database using a 70% confidence level cutoff for assignment (17). Raw sequencing data were recorded in the NCBI database (PRJNA517326). Figure 2 was prepared using Krona (18).

RESULTS AND DISCUSSION

Physicochemical analyses

During sampling, temperature and pH were measured as 20.9℃ and 6.98, respectively. The physicochemical properties of the samples are shown in Table 1. Sodium (Na⁺) and Chloride (Cl⁻) ions were found to have the highest concentration in the samples. According to the chemical composition of the Lagoon, it can be expected that halophilic organisms dominate in this environment.

After 16S rDNA sequencing, 57,847 high-quality paired-end reads were obtained. The number of identified prokaryotic
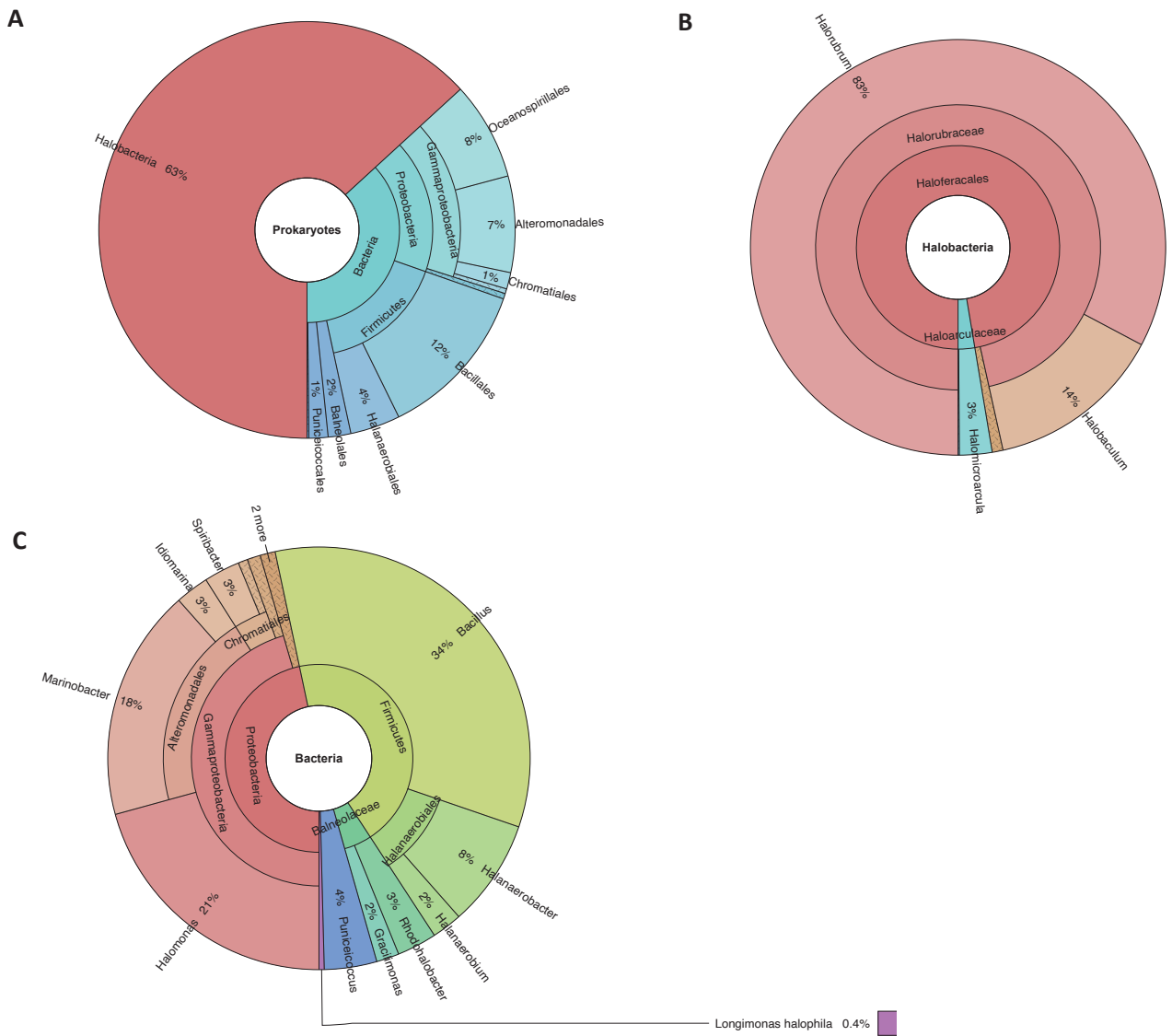
Figure 2. Relative distributions of prokaryotes (A), Archaea (B) and Bacteria (C) as obtained from 16S rDNA metabarcoding data.

Table 1. Physicochemical properties of the samples collected from Gökçeada Salt Lake Lagoon (ion concentrations in g/L).

	Temperature (°C)	pH	Na$^+$	K$^+$	Ca^{2+}	Mg^{2+}	HCO$_3^-$	Cl$^-$
Average	20.9	6.98	111.63	3.47	2.27	16.07	0.24	225.12

species in the sample was found to be 36 by comparison of OTUs with the SILVA database (Table 2). Despite 63.2% of the sample consisting of Archaea members, only 5 archaeal species were determined (Figure 2A). The most abundant genus of Archaea was *Halorubrum* (82.7%), and the others were *Halobaculum* (13.7%), *Halomicroarcula* (2.5%), *Halobellum* (0.8%), and Halosimplex (0.1%) (Figure 2B). Metagenomic

and metabarcoding approaches were previously used to investigate microbial compositions of different hypersaline environments (6, 19, 20), and the Archaea was previously described as the dominant group in these environments (21,22). As observed in this study, *Halorubrum* was previously reported among dominant archaeal genera in salt lakes and salterns (23,24).

Table 2. Species detected in this study via metabarcoding approach

Organism			No. of reads	%
Prokaryotes	Archaea	*Halorubrum sp.*	3922	52.30
Prokaryotes	Archaea	*Halobaculum sp.*	652	8.69
Prokaryotes	Bacteria	*Halomonas sulfidaeris*	462	6.16
Prokaryotes	Bacteria	*Bacillus persicus*	420	5.60
Prokaryotes	Bacteria	*Bacillus litoralis*	350	4.67
Prokaryotes	Bacteria	*Marinobacter aquaticus*	261	3.48
Prokaryotes	Bacteria	*Marinobacter flavimaris*	168	2.24
Prokaryotes	Archaea	*Halomicroarcula sp.*	120	1.60
Prokaryotes	Bacteria	*Puniceicoccus vermicola*	111	1.48
Prokaryotes	Bacteria	*Halanaerobacter lacunarum*	100	1.33
Prokaryotes	Bacteria	*Halomonas fontilapidosi*	91	1.21
Prokaryotes	Bacteria	*Rhodohalobacter halophilus*	84	1.12
Prokaryotes	Bacteria	*Halanaerobacter salinarius*	78	1.04
Prokaryotes	Bacteria	*Spiribacter aquaticus*	76	1.01
Prokaryotes	Bacteria	*Idiomarina atlantica*	71	0.95
Prokaryotes	Bacteria	*Bacillus pseudofirmus*	49	0.65
Prokaryotes	Bacteria	*Halanaerobacter jeridensis*	49	0.65
Prokaryotes	Bacteria	*Halanaerobium praevalens*	47	0.63
Prokaryotes	Bacteria	*Marinobacter persicus*	47	0.63
Prokaryotes	Bacteria	*Bacillus mesophilus*	41	0.55
Prokaryotes	Archaea	*Halobellus sp.*	40	0.53
Prokaryotes	Bacteria	*Bacillus thioparans*	37	0.49
Prokaryotes	Bacteria	*Gracilimonas halophila*	34	0.45
Prokaryotes	Bacteria	*Bacillus hemicellulosilyticus*	30	0.40
Prokaryotes	Bacteria	*Hydrogenovibrio halophilus*	28	0.37
Prokaryotes	Bacteria	*Guyparkeria hydrothermalis*	20	0.27
Prokaryotes	Bacteria	*Arcobacter group*	18	0.24
Prokaryotes	Bacteria	*Halanaerobium saccharolyticum*	17	0.23
Prokaryotes	Bacteria	*Gracilimonas tropica*	14	0.19
Prokaryotes	Bacteria	*Marinobacter salinus*	13	0.17
Prokaryotes	Bacteria	unknown	11	0.15
Prokaryotes	Bacteria	*Halomonas glaciei*	11	0.15
Prokaryotes	Bacteria	*Ruegeria intermedia*	8	0.11
Prokaryotes	Bacteria	*Halomonas zhaodongensis*	8	0.11
Prokaryotes	Bacteria	*Desulfohalobium sp.*	6	0.08
Prokaryotes	Archaea	*Halosimplex sp.*	5	0.07
Total			**7499**	

A total of 31 bacterial species were identified (Table 2). Proteobacteria were the dominant bacterial phylum (47% of bacteria) and followed by Firmicutes (44% of bacteria). *Bacillus* (33.6%), *Halomonas* (20.7%), *Marinobacter* (17.7%), *Halanaerobacter* (8.2%) were the most common and most abundant bacterial genera in the sample analyzed (Figure 2C). Considering the chemical composition of the Lagoon, the presence of halophilic bacterial genera such as *Salinibacter* could be expected (25). However, our analysis did not find any OTU related to *Salinibacter*, which may be a result of the abundance of some haloarchaeal species (e.g. *Halorubrum*), which can inhibit *Salinibacter* growth as previously suggested by Anton et al. (26).

In conclusion, in this study, the prokaryotic diversity of Gökçeada Salt Lake Lagoon was evaluated, and Euryarchaeota, Proteobacteria, and Firmicutes members were found to be essential components of its prokaryotic community. This study allows us to improve our knowledge of the prokaryotic community structure in the sampling area. But a more comprehensive microbiome analysis can be obtained with future metabarcoding/metagenomic analyses by focusing on both prokaryotic and eukaryotic microbes. In addition, although OTUs that cannot be associated with any taxa are relatively few in this study, OTUs still have the potential to contribute to the identification of new organisms. In future studies, it is planned to collect samples from different depths and locations of the lake and elaborate the analyses to enlighten complete microbial diversity and microbial community structure.

Peer-review: Externally peer-reviewed.

Conflict of Interest: The author declare that she has no conflicts of interest to disclose.

Financial Disclosure: There are no funders to report for this submission.

REFERENCES

1. Wardle DA. Communities and ecosystems: Linking the aboveground and below-ground components. Princeton, NJ: Princeton University Press; 2002.

2. Leininger S, Urich T, Schloter M, Schwark L, Qi JW, Nicol G, et al. Archaea predominate among ammonia-oxidizing prokaryotes in soils. Nature 2006; 442: 806-9.

3. Sogin ML, Morrison HG, Huber JA, Welch DM, Huse SM, Neal PR, et al. Microbial diversity in the deep sea and the underexplored "rare biosphere". PNAS 2006; 103: 12115-20.

4. Aslan H, Gonulal O, Can-Yilmaz E, Elipek B, Baytut O, Tosunoglu M, et al. Species diversity in lentic, lotic, marine and terrestrial biotopes of Gokceada Salt Lake Wetland (Canakkale, Turkey). Fresenius Environ Bull 2018; 5: 2853-66.

5. Taberlet P, Coissac E, Pompanon F, Brochmann C, Willerslev E. Towards next-generation biodiversity assessment using DNA metabarcoding. Mol Ecol 2012; 21: 2045-50.

6. Fouts DE, Szpakowski S, Purushe J, Torralba M, Waterman RC, et al. Next generation sequencing to define prokaryotic and fungal diversity in the bovine rumen. PLoS One 2012; 7: e48289.

7. Pavan-Kumar A, Gireesh-Babu P and Lakra WS. DNA Metabarcoding: A new approach for rapid biodiversity assessment. J Cell Sci Mol Biol 2015; 2: 111.

8. Abdelfattah A, Malacrinò A, Wisniewski M, Cacciola SO, Schena L. Metabarcoding: a powerful tool to investigate microbial communities and shape future plant protection strategies. Biol Control 2017; 120: 1-10.

9. Bassler-Veit B, Barut IF, Merc E, Avsar N, Nazik A, Kapan-Yesilyurt S, et al. Distribution of microflora, meiofauna, and macrofauna assemblages in the hypersaline environment of northeastern Aegean Sea coasts. J Coast Res 2013; 29: 883-98.

10. Amaral-Zettler LA, McCliment EA, Ducklow HW, and Huse SM. A method for studying protistan diversity using massively parallel sequencing of V9 hypervariable regions of small-subunit ribosomal RNA Genes. PLoS One 2009; 4: e6372.

11. Caporaso JG, Lauber CL, Walters WA, Berg-Lyons D, Huntley J, Fierer N, et al. Ultra-high-throughput microbial community analysis on the Illumina HiSeq and MiSeq platforms. ISME J 2012; 6: 1621-4.

12. Walters W, Hyde ER, Berg-Lyons D, Ackermann G, Humphrey G, Parada A, et al. Improved bacterial 16S rRNA gene (V4 and V4-5) and fungal internal transcribed spacer marker gene primers for microbial community surveys. mSystems 2016; 1: e00009-15.

13. Callahan BJ, McMurdie PJ, Rosen MJ, Han AW, Johnson AJA, Holmes S. DADA2: High resolution sample inference from Illumina amplicon data. Nat Methods 2016; 13: 581-3.

14. Caporaso JG, Kuczynski J, Stombaugh J, Bittinger K, Bushman FD, et al. QIIME allows analysis of high throughput community sequencing data. Nat Methods 2010; 7: 335-6.

15. Bolyen E, Rideout JR, Dillon MR, et al. Reproducible, interactive, scalable and extensible microbiome data science using QIIME 2. Nat Biotechnol 2019; 37: 852-7.

16. Edgar RC. UPARSE: Highly accurate OTU sequences from microbial amplicon reads. Nature Methods 2013; 10: 996-8.

17. Yilmaz P, Parfrey LW, Yarza P, Gerken J, Pruesse E, Quast C, et al. The SILVA and "All-species Living Tree Project (LTP)" taxonomic frameworks. Nucleic Acids Res 2014; 42: 643-8.

18. Ondov BD, Bergman NH, Phillippy AM. Interactive metagenomic visualization in a Web browser. BMC Bioinform 2011; 12: 385.

19. Ghai R, Pašić L, Fernández AB, Martin-Cuadrado AB, Mizuno CM, McMahon KD, et al. New abundant microbial groups in aquatic hypersaline environments. Sci Rep 2011; 1: 135.

20. Fernandez AB, Ghai R, Martin-Cuadrado AB, Sanchez-Porro C, Rodriguez-Valera F, Ventosa A. Prokaryotic taxonomic and metabolic diversity of an intermediate salinity hypersaline habitat assessed by metagenomics. FEMS Microbiol Ecol 2014; 88: 623-35.

21. Oren A. Life at high salt concentrations. In: Dworkin M, Falkow S, Rosenberg E, Schleifer K-H, Stackebrandt E, editors. The prokaryotes. A handbook on the biology of bacteria: ecophysiology and biochemistry, vol 2. New York: Springer; 2011. p. 263-82.

22. Simachew A, Lanzén A, Gessesse A, Øvreås L. Prokaryotic community diversity along an increasing salt gradient in a soda ash concentration pond. Microb Ecol 2016; 71: 326-38.

23. Mutlu MB, Martinez-Garcia M, Santos F, Pena A, Guven K, Anton J. Prokaryotic diversity in Tuz Lake, a hypersaline environment in inland Turkey. FEMS Microbiol Ecol 2008; 65: 474-83.

24. Mutlu MB, Guven K. Bacterial diversity in Çamaltı Saltern, Turkey. Pol J Microbiol 2015; 64: 37-45.

25. Elevi Bardavid R, Ionescu D, Oren A, Rainey FA, Hollen BJ, Bagaley DR, et al. Selective enrichment, isolation and molecular detection of *Salinibacter* and related extremely halophilic Bacteria from hypersaline environments. Hydrobiologica 2007; 576: 3-13.

26. Anton J, Pena A, Santos F, Martinez-Garcia M, Schmitt-Kopplin P, Rossello-Mora R. Distribution, abundance and diversity of the extremely halophilic bacterium *Salinibacter ruber*. Saline Syst. 2008; 4: 15.